

**AN EXPERIMENTAL INVESTIGATION OF THE CONVERSION OF NO TO NO₂
IN A SIMULATED GAS TURBINE ENVIRONMENT**

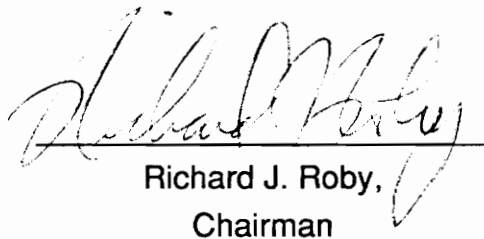
by

James W. Hunderup

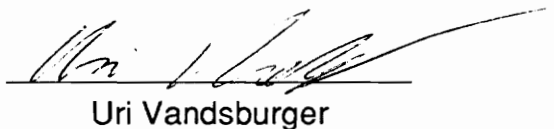
Thesis submitted to the Faculty of Virginia Polytechnic Institute and State
University in partial fulfillment of the requirements for the degree of

MASTER OF SCIENCE
in
Mechanical Engineering

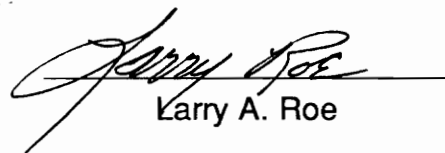
APPROVED:



Richard J. Roby,
Chairman



Uri Vandsburger



Larry A. Roe

October 1993
Blacksburg, Virginia

C.2

LD
5655
V855
1993
H 862
C.2

AN EXPERIMENTAL INVESTIGATION OF THE CONVERSION OF NO TO NO₂ IN A SIMULATED GAS TURBINE ENVIRONMENT

by

James W. Hunderup

Committee Chairman: Richard J. Roby
Mechanical Engineering

(ABSTRACT)

Unexpectedly high concentrations of NO₂ have been noted in stack emissions from industrial gas turbines. NO₂ formation appears to occur through the so called "HO₂ mechanism" in which NO combines with HO₂ to produce NO₂ and OH. In this study, the formation of NO₂ was investigated through computer modeling and experimental testing. Computer modeling utilized the CHEMKIN chemical kinetics program and a subset of a previously published C-H-O-N system mechanism. Experimental work was conducted using a high pressure flow reactor designed and built in the course of the study. The effects of pressure, temperature, and the presence of a NO₂ promoting hydrocarbon, methane, were investigated. It was discovered that as pressure increased from 1 atm. to 8.5 atm., the rate and amount of NO converted to NO₂ also increased. There also appeared to be a temperature "window" between approximately 800 and 1000 K in which NO to NO₂ conversion readily occurred. The presence of methane was seen to enhance NO conversion to NO₂, and a ratio of [CH₄]/[NO] was found to be a useful parameter in predicting NO₂ formation. Significant NO conversion to NO₂ was noted for [CH₄]/[NO] > 1 at the hydrocarbon injection point. Experimental results validated those trends obtained from modeling with a modified C-H-O-N mechanism.

ACKNOWLEDGEMENTS

There are many people to whom I owe my gratitude for making my M.S. degree a reality. Foremost, I would like to express my gratitude to my thesis advisor, Dr. Rick Roby. I would not be where I am today without his guidance and friendship. He afforded me the opportunity and gave me the confidence to pursue and achieve my goals.

I would like to thank the other members of my committee, Dr. Uri Vandsburger and Dr. Larry Roe. I have valued your knowledge and suggestions. I thank my entire committee for their patience and understanding.

I thank General Electric and, in particular, Dr. Yoshi Kuwata for their sponsorship and support of this project. I have enjoyed my contact with those at G.E. and hope that they will find the results of this study enlightening.

Ted Roth, J.C.S., and Chip Zimlik spent many hours helping me collect data and run the computer model. I owe you my thanks for your time and efforts. You both have contributed a great deal to the sometimes tedious "dirty work" which was necessary to complete this study.

Throughout my years at Virginia Tech my family - Mom, Dad, Pete, and Kathleen - have continually and unconditionally supported me. For this, I am grateful.

My gratitude goes to all the Roby students: James Reaney, Dan Gottuk, Doug Wirth, and especially Linda Blevins and Michelle Peatross. Your advice and friendship have been invaluable. I miss the lively conversations of Friday afternoon seminars.

Throughout the years I have spent at Tech I have made friends I will always remember. You offered me support, advice, and encouragement, and at times kept me sane. I thank you all, especially Linda Blevins, Michelle Peatross, Ted Roth, Anita Roth, Adam Berger, Eric Albright, and Linda Hoover.

TABLE OF CONTENTS

	Page
ABSTRACT	ii
ACKNOWLEDGEMENTS.....	iii
TABLE OF CONTENTS	iv
LIST OF FIGURES.....	vii
LIST OF TABLES.....	x
1 INTRODUCTION	1
1.1 BACKGROUND AND MOTIVATION	1
1.2 SCOPE OF STUDY.....	5
2 COMPUTER MODELING.....	6
2.1 CHEMKIN	6
2.2 COMBUSTOR MODEL.....	7
2.3 THE REACTION MECHANISM.....	10
2.4 MODELING RESULTS.....	11
2.4.1 The Effect of Temperature	13
2.4.2 The Effect of Pressure	16
2.4.3 The Effect of Methane.....	22
2.4.4 The Effect of Carbon Monoxide	25
2.4.5 The Effect of Water.....	25

2.4.6 The Effect of $[\text{NO}]_0$	31
2.4.7 Kinetic Rate Constants Considerations	31
3 EXPERIMENTAL APPARATUS AND PROCEDURE.....	38
3.1 APPARATUS.....	38
3.1.1 The Pressure Vessel.....	38
3.1.2 The Burner and Related Components.....	45
3.1.3 Instrumentation and Control	49
3.2 FLOW REACTOR FACILITY OPERATION	57
3.3 EXPERIMENTAL PROCEDURE.....	58
4 EXPERIMENTAL RESULTS	65
4.1 NO_x PROFILES.....	65
4.2 TEMPERATURE	69
4.3 PRESSURE	69
4.4 UNBURNED HYDROCARBONS	75
4.5 FLOW RATE CONSIDERATIONS.....	78
4.6 SUMMARY.....	78
5 DISCUSSION	80
5.1 MIXING CONSIDERATIONS.....	85
5.1.1 Mixing and NO_x Profiles	86
5.1.2 Mixing and NO_2/NO_x Profiles	95
5.2 PROBE EFFECTS.....	98
5.3 IMPORTANT VARIABLES REGARDING $\text{NO}-\text{NO}_2$ CONVERSION	101
5.3.1 Temperature	101
5.3.2 Pressure.....	105

5.3.3 Unburned Hydrocarbons.....	109
5.3.4 Comparison of Promoting Factors	112
5.4 APPLICATION TO THE INDUSTRIAL GAS TURBINE.....	113
6 SUMMARY, CONCLUSIONS, AND RECOMMENDATIONS.....	116
6.1 SUMMARY & CONCLUSIONS.....	116
6.2 RECOMMENDATIONS	118
REFERENCES	121
APPENDIX A: Reaction Mechanism	124
APPENDIX B: Thermodynamic Data Base	131
APPENDIX C: CHEMKIN .grf File Manipulation Program	139
APPENDIX D: Shop Drawings.....	146
APPENDIX E: Rotameter Calibration Curves.....	151
APPENDIX F: Experimental Data Processing Program.....	158
APPENDIX G: Uncertainty Analysis	164
VITA	170

LIST OF FIGURES

Figure	Page
2.1 Computer model system schematic	8
2.2 NO _x profiles for base cases	12
2.3 NO ₂ /NO _x profiles for base cases	14
2.4 NO ₂ /NO _x profiles for base cases and lower temperature cases.....	15
2.5 NO ₂ /NO _x profiles for various pressures.....	17
2.6 Maximum NO ₂ /NO _x as a function of pressure.....	18
2.7 The effect of an instantaneous pressure and temperature drop on NO ₂ formation	20
2.8 The effect of an instantaneous pressure and/or temperature drop on NO ₂ formation	21
2.9 A gradual pressure drop in step-wise fashion from 10 atm., 1100 K to 6 atm., 950 K. [CH ₄] ₀ = 1010 ppm. (Modified Miller & Bowman Mechanism)	23
2.10 The effect of varying [CH ₄] ₀ on NO ₂ /NO _x	24
2.11 The effect of methane and carbon monoxide on the formation of NO ₂	26
2.12 The effects of water addition on NO ₂ formation. (34.0% air dilution case, 10 atm.)	27
2.13 The effects of water addition on NO ₂ formation. (53.4% air dilution case, 10 atm.)	28
2.14 The effects of water addition on NO ₂ formation. (66.3% air dilution case, 10 atm.)	29
2.15 The effect of [NO] ₀ on NO ₂ formation.....	32

2.16	The effect of varying $[\text{CH}_4]_0/[\text{NO}]_0$ on the formation of NO_2	33
2.17	The effect of kinetic parameters on predicted conversion of NO to NO_2 . $P = 10 \text{ atm.}$, $T = 1100 \text{ K}$, and $[\text{CH}_4]_0 = 1010 \text{ ppm.}$	35
2.18	Comparison of Miller & Bowman Mechanism to the Modified Miller & Bowman Mechanism for the air dilution base cases.....	37
3.1	High pressure flow reactor schematic.....	39
3.2	Experimental system schematic	40
3.3	Pressure vessel schematic (1/8 scale)	41
3.4	Schematic of pressure vessel end flanges	43
3.5	Water trap assembly schematic	44
3.6	Schematic showing the relative positions of the injector, liner, and burner.....	47
3.7	Sampling probe schematic	52
3.8(a)	Thermo Environmental Chemiluminescent NO_x Analyzer Schematic (Original configuration).....	53
3.8(b)	Thermo Environmental Chemiluminescent NO_x Analyzer Schematic (Modified configuration for low pressure sampling)	54
3.9	Typical real time NO/NO_x output from the CLA.....	62
4.1	Oxides of nitrogen profiles	66
4.2	NO_x profiles for various conditions.....	67
4.3	NO_x profiles for various pressures	68
4.4	The effect of temperature on NO_2 formation.....	70
4.5	NO_2/NO_x temperature profiles for experimental results at several residence times	71
4.6	The effect of pressure on NO_2/NO_x . No methane injection cases.....	73

4.7	The effect of pressure on NO ₂ formation. T = 847-882 K, [CH ₄] _{inj} = 836-1474 ppm, [NO] _{inj} = 132-183 ppm.....	74
4.8	The effect of pressure on NO ₂ formation	76
4.9	The effect of hydrocarbon promotion on the conversion of NO to NO ₂	77
4.10	The effect of flow rate on NO ₂ /NO _x profiles. P = .96-1.2 atm., T = 862-891 K, and [CH ₄] _o /[NO] _o = O(10)	79
5.1	The effect of kinetic parameters on predicted conversion of NO to NO ₂ . P = 10 atm., T = 1100K, and [CH ₄] _o = 1010 ppm	81
5.2	Selected species profiles	83
5.3`	NO _x profile similarities at a given pressure	87
5.4	Schematic showing the relative positions of the injector, liner, and burner.....	89
5.5	Comparison of NO _x profiles at 1.2 atm. for CH ₄ injection and no CH ₄ injection cases.....	91
5.6	Real time NO/NO _x output from CLA for Re = 664 and for Re = 1868	94
5.7	Comparison of NO _x profiles with dissimilar Reynolds numbers	96
5.8	Comparison of NO ₂ /NO _x profiles with and without methane injection	97
5.9	NO ₂ /NO _x profiles at 5 atm. and similar temperature and injection conditions...	100
5.10	Temperature effect on NO ₂ formation.....	103
5.11	Comparison of NO ₂ /NO _x temperature profile for modeling and experimental results. Experimental points taken at 28 ms. Modeling points taken at 10 ms. P = 5 atm., [CH ₄] _o ≅ 1000 ppm	104
5.12	The effect of pressure on NO ₂ formation. T = 1100 K, [CH ₄] _o ≅ 1000 ppm	107
5.13	The effect of pressure on NO ₂ formation. T = 847-891 K, [CH ₄] _o = 1000 ppm	108
5.14	The effect of hydrocarbon promotion on the conversion of NO to NO ₂	111

LIST OF TABLES

Table		Page
1	Experimental Run Conditions	60
2	Comparison of HO_2/OH and NO_2/NO_x at 150 ms as predicted by the computer model	84
3	Reynolds Numbers for Experimental Runs	93

CHAPTER 1 - INTRODUCTION

1.1 BACKGROUND AND MOTIVATION

The past decade has seen a marked increase in public concern for the environment. After many years of neglect, industry was forced to confront the issues of air borne emissions from the burning of fossil fuels with the passage of the Clean Air Act of 1970. Since that time, the production of major air borne pollutants - NO_x , SO_x , CO, unburned hydrocarbons (UHC's), and particulate matter - from combustion sources has decreased significantly. The 1980's saw increased environmental awareness. Environmental concerns are now not only a scientific issue, but also have become social, political, and economic issues. The recent Amendments to the Clean Air Act, enacted in 1990, stipulate further reduction in combustion source emissions. After two decades of significant reduction in air borne pollutants, the 1990's will prove to be a challenging period in further reduction of emission levels. In order to achieve further reductions from combustion generated pollutants, the mechanisms of pollution formation must be well understood on both thermodynamic and chemical kinetic levels.

The formation of oxides of nitrogen is of particular interest due to the role it plays in the formation of photochemical smog and acid rain. Of the two main constituents of NO_x ($\text{NO} + \text{NO}_2$), NO_2 is more toxic. It is also a gas which becomes visible (brown color) at relatively low concentrations. NO is colorless. In many practical combustion systems, NO_2 remains a small fraction of NO_x . However, it has been noticed in some systems that the ratio of NO_2/NO_x increases to a significant level, particularly as total NO_x emissions decrease. Since NO_2 becomes visible at relatively low concentrations, a

small increase can lead to visible concentrations. For power producing plants as well as other industries, visible emissions from the stack are undesirable from a public relations point of view. These factors show NO₂ formation to be an area worthy of examination.

Although unexpectedly high levels of NO₂ have been reported in gas turbine emissions since the mid-seventies, study of the mechanisms of NO₂ formation has been largely neglected until recently. Much research has been conducted in the past two decades on the subject of NO_x formation in combustion systems. However, a very small portion of this research has been devoted to the investigation of NO₂ formation. The majority of the work has been directed toward formation of nitric oxide (NO), which usually appears in much greater concentrations than NO₂. As a consequence, the mechanisms of NO formation are relatively well understood in comparison to those of NO₂ formation.

In nearly all investigations of NO₂ formation, concentrations of NO₂ have been determined through analyses of combustion gas samples. Hot combustion gases are typically sampled via a quartz or stainless steel probe. During the seventies, combustion gas samples were generally obtained through water cooled probes at relatively high pressures. Hot gases were rapidly quenched as they passed through the probe. The samples were usually found to contain high levels of NO₂. In 1975, J.D. Allen [1] questioned the reliability of "conventional probe sampling techniques." He suggested that NO₂ is formed in the probe during sampling, and, therefore, post-sampling measurements would not reflect actual combustion system concentrations. Johnson *et al.* [2] showed through laser induced fluorescence that NO₂ levels measured after probe sampling do not, in fact, represent levels found in the actual combustion system. The

samples contained a much higher level of NO_2 . These important research findings make suspect much of the work done in the 70's in which probe effects were neglected.

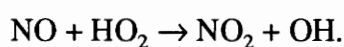
Probe effects remain an unavoidable obstacle in combustion gas sampling but can be minimized. Conditions in the probe which have been found conducive to NO_2 formation are rapid quenching of the sample, high pressure, and the presence of unburned fuel species [2-6]. It is believed that much of the NO_2 is produced by the catalytic conversion of NO at the probe walls where the temperature gradient is greatest. Keeping these points in mind, probe effects can be minimized by a slow sampling rate at low pressure in an uncooled probe.

Conditions conducive to NO_2 formation in the probe can also be extended to the combustion system. It has been observed that NO_2 is produced in areas of large temperature gradients in the flame. Hargraves *et al.* [7] found that little or no NO_2 is formed in the main combustion region but that the NO_2/NO_x ratio is greatest along the periphery of the flame where the hot combustion gases mix with cool surrounding air. Sano [8] confirmed this through a numerical study of NO_2 production in mixing regions. Temperature is therefore an important variable in NO_2 formation. Bromly *et al.* [9], Hori *et al.* [10], and Marinov and Steele *et al.* [11] have all recently noted very distinct temperature limits above and/or below which little NO is converted to NO_2 . Nearly complete NO conversion only appears to occur in the relatively low temperature region below 1200 K.

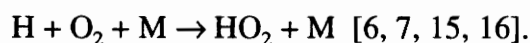
The presence of unburned fuel and/or other oxidizable species, similar to the probe case, also increases the amount of NO_2 produced [7, 9-14]. In separate research projects, Hori *et al.*, Marinov *et al.*, and Bromly *et al.* have investigated the effect of the presence of hydrocarbons on the promotion of NO- NO_2 conversion. Hori and Marinov observed

that higher order hydrocarbons are more effective in promoting NO-NO₂ conversion [10, 11]. They also noted that the type of hydrocarbon has an effect on the temperature region in which NO-NO₂ conversion is nearly complete. Bromly observed that trace amounts of n-butane greatly enhanced NO₂ formation in a similar temperature region [9].

It is widely believed that the majority of NO₂ is produced from the conversion of NO by the HO₂ radical:



Increased concentrations of HO₂ would then result in increased conversion of NO to NO₂. One important pathway that has been suggested for HO₂ formation is



Because this is a 3-body reaction, it would be particularly sensitive to pressure. It is also a reaction that is favored at relatively low temperatures. In turn, the formation of NO₂ would then also be pressure and temperature sensitive. This has been seen in probe and combustion system studies. In probes, it has been observed that relatively high sampling pressures and rapid quenching have a substantial effect on NO₂ formation. Although research on combustion systems has shown that temperature and the presence of unburned hydrocarbons has an important effect on NO₂ formation, no studies prior to this one have investigated the effect of pressure on NO₂ formation.

Few studies have examined NO₂ formation in gas turbines specifically. Johnson and Smith [17] suggest two possible mechanisms for NO₂ formation in industrial gas turbines. The first involves catalytic oxidation of NO, while the second takes into account the HO₂ mechanism. However, these are merely hypotheses and have not been supported by experimental studies. Although NO₂ is still found at times in significant amounts in gas turbine emissions, its presence is still not fully understood.

1.2 SCOPE OF STUDY

The goal of this study was to determine under what conditions NO may be converted to NO₂ in a high pressure environment similar to that of an industrial gas turbine combustor. In achieving this, the effect of pressure on the NO-NO₂ conversion was of particular interest. The objective was achieved through computer modeling and experimental work. The modeling offered a basis of comparison for those results achieved through experimental study. Modeling may also prove to be a useful tool in the "field" for predicting incidences of high NO-NO₂ conversion.

By quantifying under what conditions NO-NO₂ conversion is significant, those conditions which seem to promote the conversion of NO to NO₂ can perhaps be avoided or minimized. This knowledge can also be applied toward a better understanding of the kinetic nature of the process of NO₂ formation.

CHAPTER 2 - COMPUTER MODELING

As a preliminary step to experimental work, computer modeling of the system was undertaken. This modeling served various purposes. It offered insight into the problem of NO-NO₂ conversion. It showed which parameters appeared to be important in NO₂ formation and gave a general idea of the kinetics involved in the process. This affected the design of the high pressure flow reactor used in experimental work. It also offered support for much previous research as well as indicating which areas should be explored in experimental work.

2.1 CHEMKIN

The majority of modeling was conducted using the CHEMKIN chemical kinetics code on the Virginia Tech ME-AMDF VAX system. Some modeling was also done using CHEMKIN II, a PC version of CHEMKIN. CHEMKIN is a chemical kinetics code that was developed at Sandia National Laboratories [18]. It utilizes a driver program [19] and partial differential equation solver and draws from a library of subroutines and a thermodynamic data base in order to solve for species concentrations at points in time as a reaction progresses.

A reaction mechanism, thermodynamic data base, and the input or starting conditions of the reacting flow are provided by the user. The reaction mechanism and the thermodynamic data base used in this study can be found in Appendices A and B respectively. CHEMKIN treats the system as a one dimensional reacting flow. Those

conditions specified in the input file are initial molar concentrations, flow rate, distance over which calculations are made, temperature profile, and a step size. CHEMKIN outputs flow velocity, temperature, and species molar concentrations at each step. Since velocity and distance are known, a time profile of concentrations can be calculated. CHEMKIN output files were downloaded to a personal computer. A FORTRAN program (App. C) was then used to generate data for graphing.

CHEMKIN II for the personal computer was configured slightly differently than CHEMKIN. Instead of a flow rate and distance being entered, starting and ending times were entered with a step size, Δt . The program outputs files containing the species concentration at each step in time. These files were in turn manipulated using a FORTRAN program to create data files for plotting. Species profiles were plotted using the Proplot computer graphics program [20] on a PC.

2.2 COMBUSTOR MODEL

For computer modeling purposes, a simple model of the gas turbine combustor was chosen. The combustor was modeled as a plug flow reactor. This was divided into two sections - a flame zone and a post flame zone (Fig 2.1). The flame zone was considered to be a constant temperature reaction zone at the adiabatic flame temperature. The reactants entering the flame zone were methane, air, and nitric oxide. It was assumed that air entered the combustor at a pressure of 10 atm. and a temperature of 580 K. This pressure approximated conditions in a gas turbine combustor. The inlet temperature was then determined by an isentropic compression from a starting temperature of 298 K. The methane-air flame was at an equivalence ratio of 0.75. At these conditions, the adiabatic

CHEMKIN COMPUTER MODEL

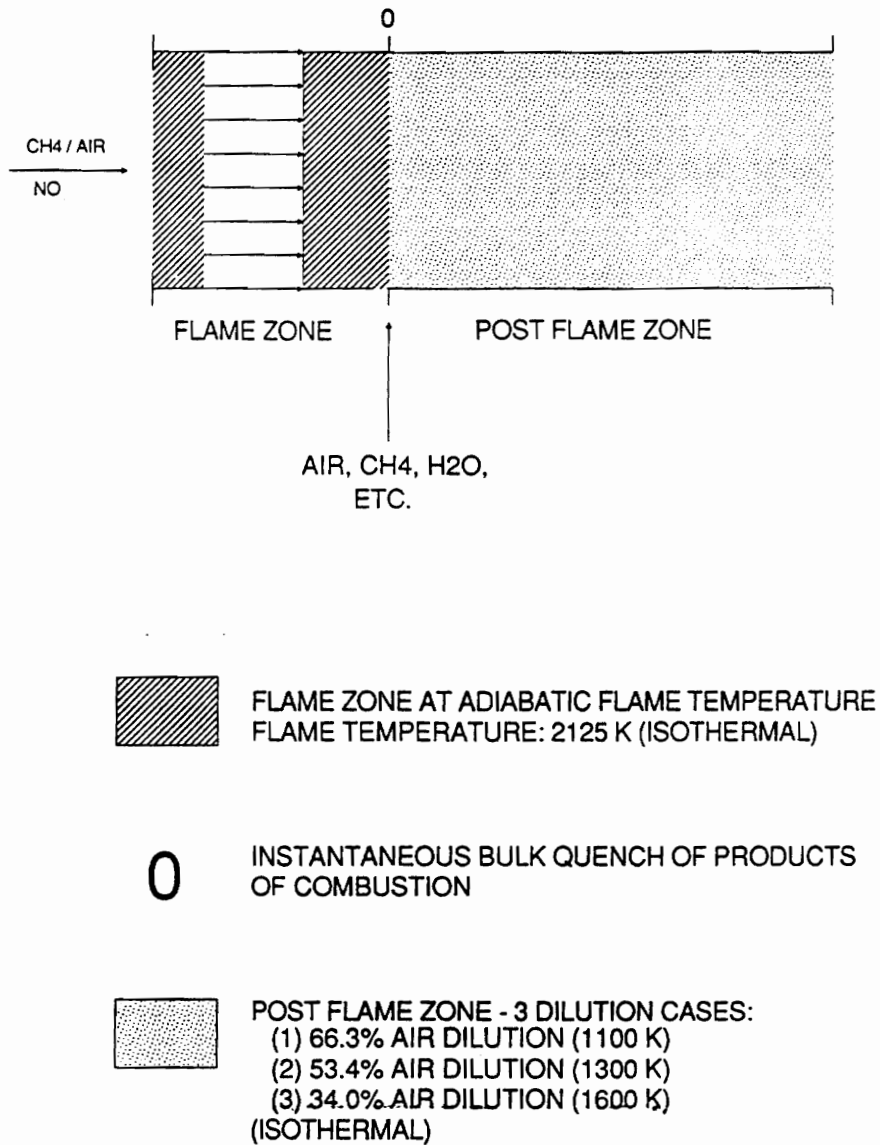


Figure 2.1. Computer model system schematic.

flame temperature is approximately 2125 K. Nitric oxide entered the flame at a concentration of 200 ppm. The NO exited the flame zone at a slightly higher concentration, as there was a net increase in NO concentration as the injected NO passed through the flame zone.

The significant species (those with a concentration greater than or equal to 0.1 ppm) at the end of the flame zone were then used as reactants (input) for the post flame zone. At this point, relatively cool air (580 K) was added to simulate the dilution air in an actual combustor. Thermodynamically, this was modeled as an instantaneous bulk quench of the post flame gases. Temperature was therefore dependent on the percent dilution. The following dilution levels and their corresponding post flame gas temperatures were modeled as base cases:

34.0% air dilution $T = 1600 \text{ K}$

53.4% air dilution $T = 1300 \text{ K}$

66.3% air dilution $T = 1100 \text{ K}$

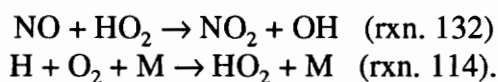
Past investigations of NO_2 formation suggest that the presence of unburned hydrocarbons is a key element in the production of NO_2 [7, 9-14]. At the exit of the flame zone in the computer model, the concentration of CH_4 was very small. For this reason, CH_4 concentration was boosted to O(1000) ppm in order to simulate the presence of unburned hydrocarbons. NO at this point was O(100) ppm. The post flame gases were allowed to react isothermally, and the production of NO_2 was studied as a function of time.

2.3 THE REACTION MECHANISM

The reaction mechanism that was used in the computer model (App. A) of the Miller & Bowman mechanism [16]. The mechanism includes 46 different species and 219 reactions. At the temperatures and pressures that were investigated, the carbon-hydrogen chemistry dominates over the carbon-nitrogen chemistry. However, most of the carbon-nitrogen chemistry of the Miller & Bowman mechanism was retained. This was done in order to verify that it is not important and to keep the model as complete as possible. The species excluded in the model - HCCOH , H_2CN , HCNO , and HOCN - were not believed to be important in the overall scheme. They caused some problems while running the code, including very lengthy run times and run time errors due to extremely small concentrations. For these reasons they were excluded.

An *erratum* [21] to the Miller and Bowman mechanism was published a short period after the original journal article. The reaction affected is reaction 9 of Appendix A. The *erratum* states that "the A-factor for reaction [9] should be $2.05 \times 10^{18} \text{ cm}^3/\text{mole-sec}$, rather than $2.05 \times 10^{19} \text{ cm}^3/\text{mole-sec}$." This was not taken into account for the modeling done for this study. Miller and Bowman state that "this reaction has no effect on the nitrogen chemistry." Nevertheless, several of the base cases were run with the corrected constant. It was confirmed that changing the constant had negligible effect on the modeling results for NO conversion to NO_2 .

The reactions thought to be the most important in the NO- NO_2 conversion mechanism are reactions 132 and 114 (App. A):



The Miller & Bowman mechanism showed the conversion to be an extremely fast process. Under some conditions their mechanism predicted nearly complete conversion within a millisecond. Based on the conditions under which the rate constants were determined and the extraordinarily fast process which they seemed to indicate, it was hypothesized that one or both were in reality too high. To investigate this, a good portion of the modeling was run with the "A" constant for reaction 132 lowered an order of magnitude. In the following section, results presented are those arrived at with the Miller & Bowman mechanism unless otherwise noted. The mechanism containing the reduced "A" constant for reaction 132 will be referred to as the modified Miller & Bowman mechanism. The effect of the rate constants will be examined in detail in section 2.4.7.

2.4 MODELING RESULTS

Computer modeling has confirmed an important finding of past investigations. Total NO_x (NO_x in this thesis shall be defined as $\text{NO} + \text{NO}_2$) is always conserved in the post flame zone to within 0.1 ppm (Fig. 2.2). This indicates that nitrous oxide (N_2O) does not play a role in NO_2 formation. Therefore, the only pathway to NO_2 formation appears to be through NO. The problem then seems to be a question of the causes of high NO to NO_2 conversion resulting in high NO_2/NO_x ratios.

Because NO- NO_2 conversion appears to be a post flame phenomenon, the point of origin for all plotted results is the beginning of this zone. Species concentrations at this point are denoted by a subscripted "o" (for example, $[\text{CH}_4]_o$). By changing the conditions of the post flame zone, the effects of the following parameters on the

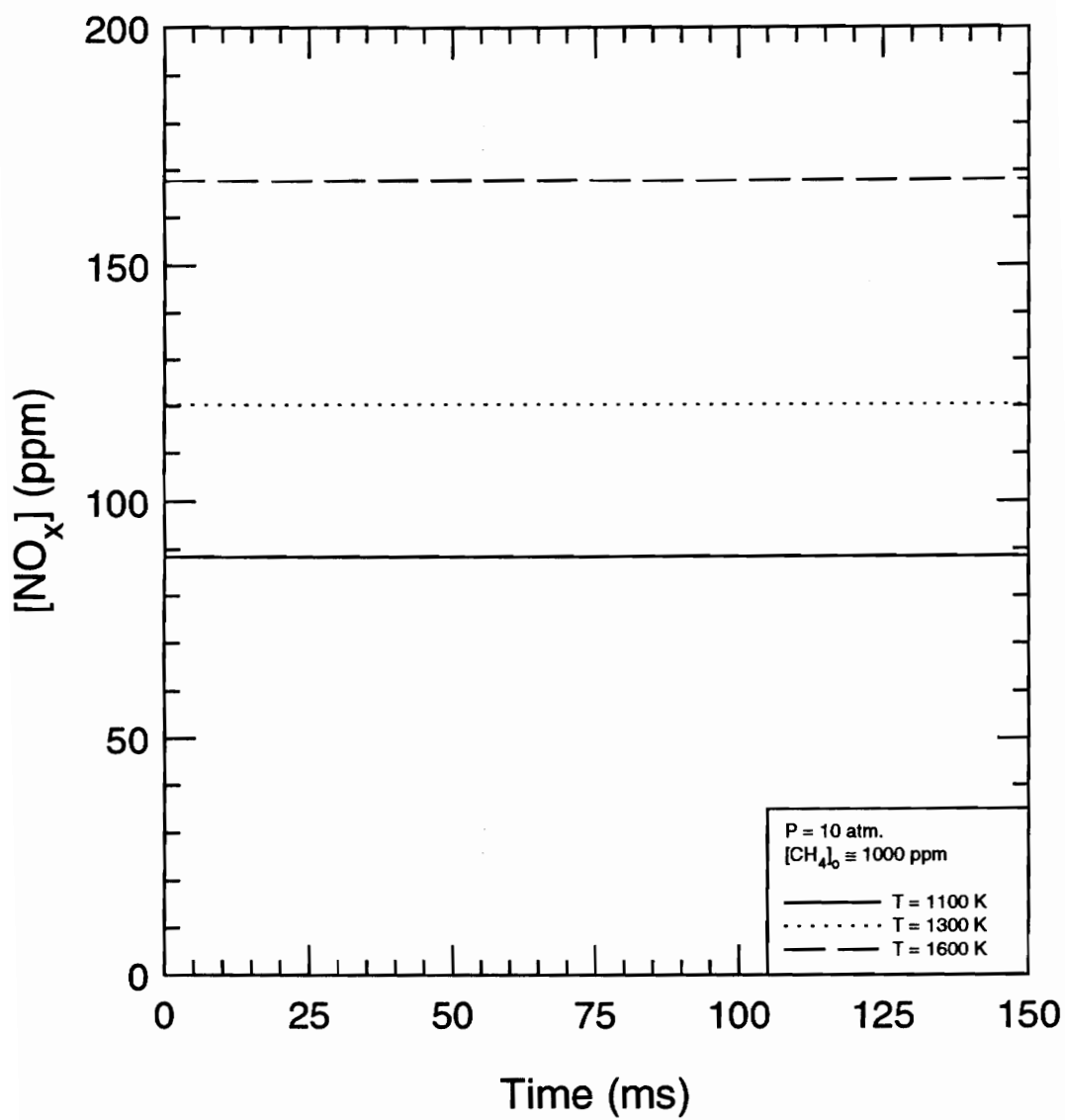


Figure 2.2. NO_x profiles for base cases.

formation of NO_2 were investigated: (1) temperature; (2) pressure; (3) the presence of CH_4 ; (4) the presence of CO ; (5) the presence of H_2O ; (6) $[\text{NO}]_0$; and (7) the rate constants of important reactions.

2.4.1 The Effect of Temperature

Past research has shown temperature to be an important variable in NO - NO_2 conversion. Although NO_x chemistry has frozen out (i.e., total NO_x is neither created nor destroyed) at temperature levels in the post flame gases, NO to NO_2 conversion does occur. In this thesis, "post flame gases" or "post flame zone" shall be defined as the region in which products from the flame have mixed with cool bypass air to reduce the temperature below 1600 K. Post flame gas temperature was altered by air and water dilution at the beginning of the post flame zone. Although water does appear to have a slight chemical effect, its main contribution is thermal in nature. The chemical effect of H_2O addition and its relative importance shall be considered in section 2.4.5.

Figure 2.3 shows a plot of NO_2/NO_x as a function of time for the three air dilution "base" cases. It shows the effect of temperature on NO - NO_2 to be quite dramatic. As temperature decreases the ratio of NO_2 to NO_x increases.

Water addition to post flame gases provided more data on the effect of temperature on NO_2 formation. Water addition modeling suggested that as temperature decreased below 1100 K, NO - NO_2 conversion was increasingly promoted. This was investigated further by lowering the temperature of the post flame gases for the 66.3% air dilution case. The results are shown in Figure 2.4. This figure includes the three base case profiles as well as the others run out to 150 ms. It appears that there is a general trend in

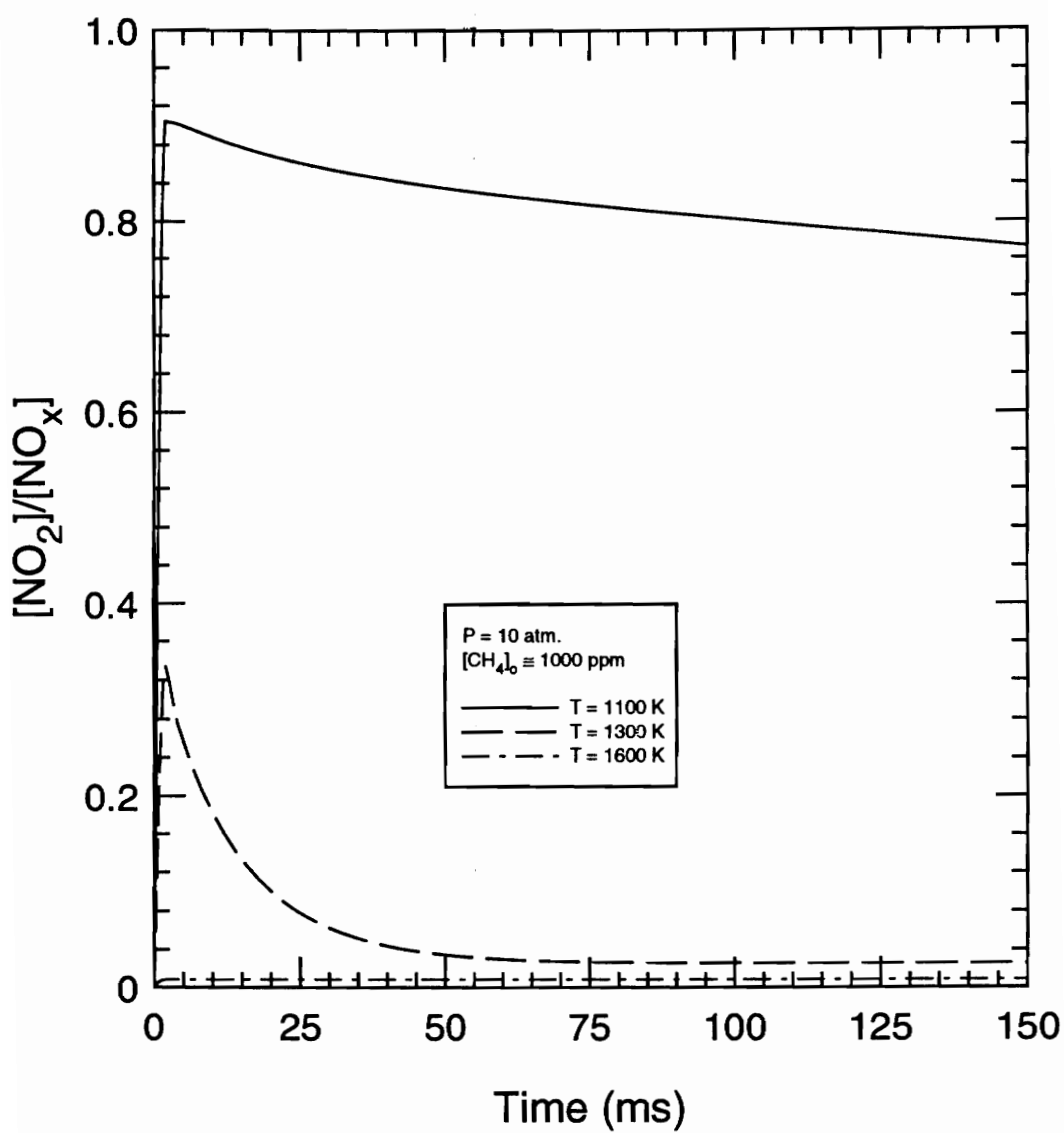


Figure 2.3. NO_2/NO_x profiles for base cases.

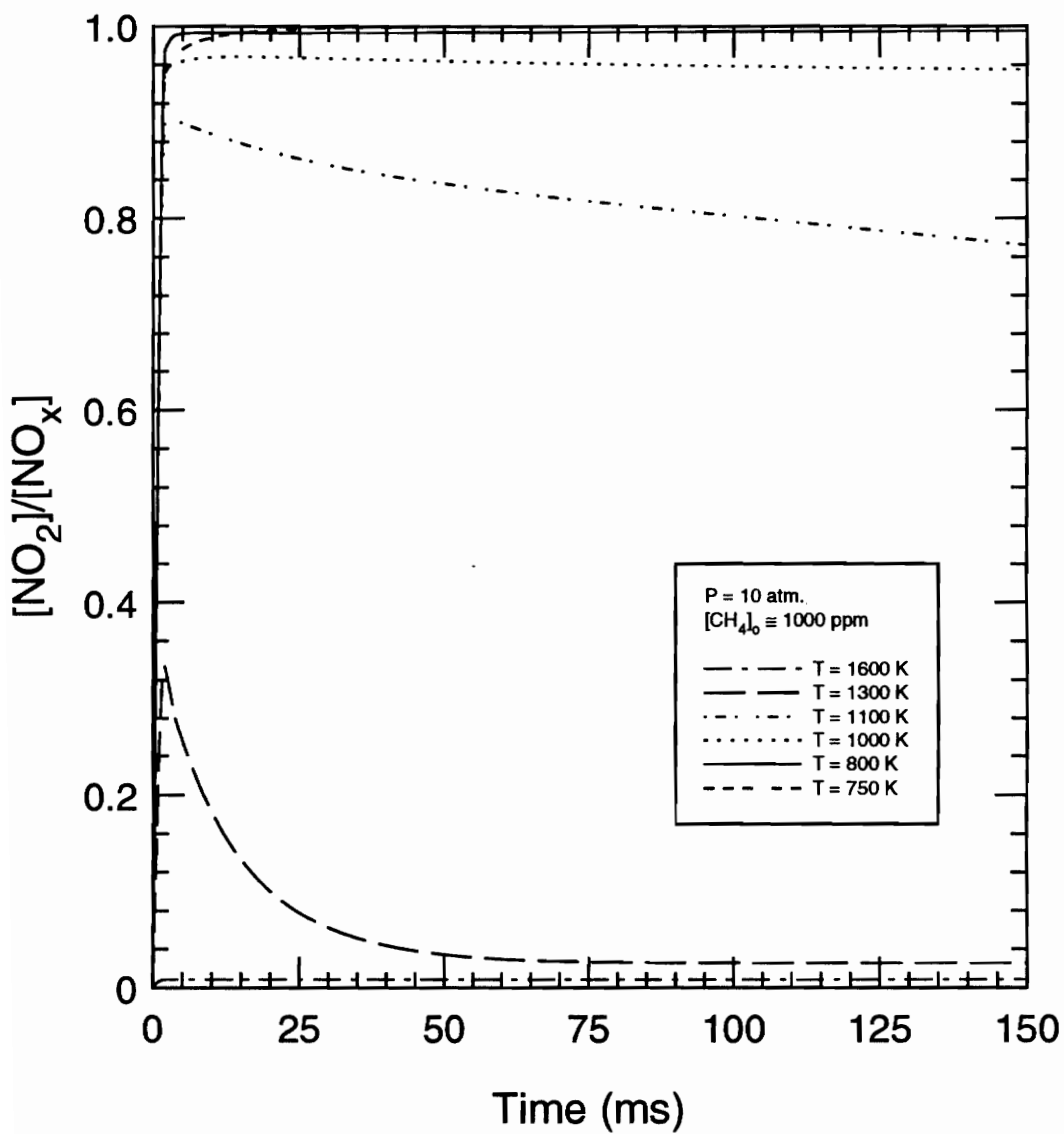


Figure 2.4. NO_2/NO_x profiles for base cases and lower temperature cases.

NO_2/NO_x production at the various temperatures. The profiles are similar in that NO_2/NO_x increases to a maximum and then begins to drop off. The maximum value of NO_2/NO_x and the time at which this point is reached are dependent, however, on the temperature. In all cases, the initial increase in NO_2/NO_x is extremely fast. For the lower temperature cases (700 K and 850 K), NO_2/NO_x approaches 1.00 asymptotically after an initial rapid increase in NO_2/NO_x . These lower temperature cases do not reach a maximum in the time period plotted, but they do reach a "pseudo steady state" of approximately 0.99. These results suggest that as temperature decreases, NO_2/NO_x increases to the point at which virtually all NO is converted to NO_2 . It can also be seen that between 1100 K and 1300 K, NO_2/NO_x ratio decreases dramatically as temperature increases. At higher temperatures NO conversion effectively does not take place. Within a few hundred degrees, NO conversion, for all practical purposes, goes from all to none.

2.4.2 The Effect of Pressure

Pressure of the three base cases was varied in order to study its effect on NO_2 formation. Figure 2.5 shows NO_2/NO_x profiles as a function of time for the 66.3% dilution case. As would be expected if the 3-body HO_2 formation reaction (rxn. 114) is a critical reaction, increasing pressure increases the rate at which NO is converted to NO_2 . It also appears to affect the amount of NO converted to NO_2 . This can clearly be seen in Figure 2.6 which shows $(\text{NO}_2/\text{NO}_x)_{\text{max}}$ as a function of pressure. NO conversion increases dramatically between 1 and 5 atm. before leveling off as the ratio approaches 1.0.

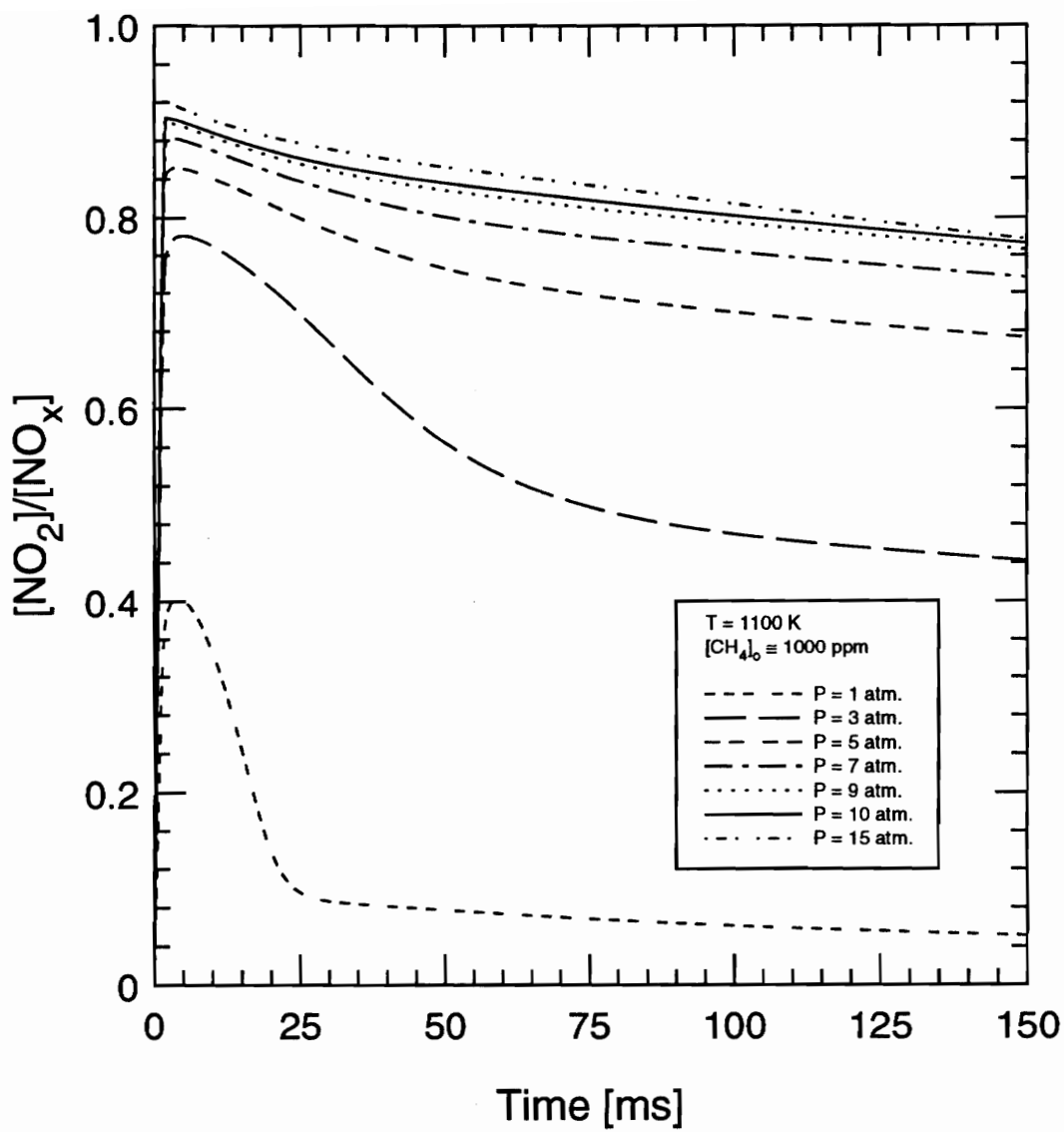


Figure 2.5 NO_2/NO_x profiles for various pressures.

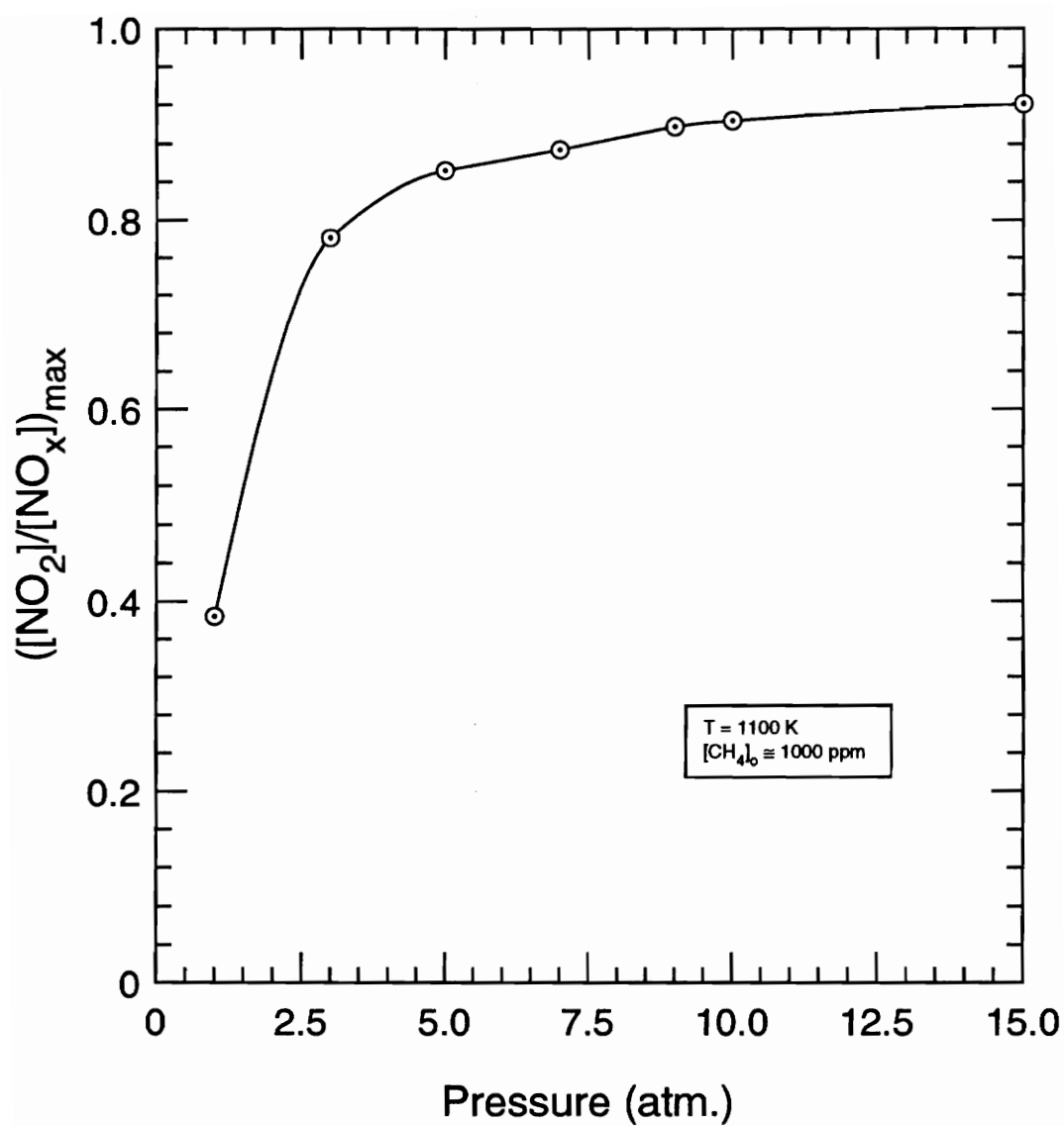


Figure 2.6. Maximum NO₂/NO_x as a function of pressure.

Both sudden and gradual pressure drops were also modeled. A sudden pressure drop from 10 atm. to 1 atm. was modeled to simulate the sudden pressure drop of a test rig. Temperature was estimated by an isentropic expansion assuming the working fluid to be air. The results for the 53.4% air dilution case are shown in Fig. 2.7. The plot shows the effect of the sudden pressure drop at approximately 2 ms and 10 ms. The results at both points are similar. The decrease in NO_2 production is halted and a gradual increase in NO_2 formation then occurs.

This "freeze out" effect of a sudden pressure drop seems to be the result of conflicting effects of temperature and pressure. Modeling has indicated that lower pressures decrease NO_2 formation while lower temperatures promote significant NO_2 production. The final concentration of NO_2 is the result of a trade-off between these two effects. Figure 2.8(a) illustrates this for the 53.4% base case. The plot shows the results of a sudden pressure drop with accompanying temperature drop, a sudden pressure drop neglecting the accompanying temperature drop, and a sudden temperature drop with no accompanying pressure drop. Similar results are obtained for the 66.3% air dilution case. The results, though similar, are much more dramatic for the 34.0% base case (Fig. 2.8(b)). The post flame gases in this case contain much less NO_2 than the other dilution cases due to the high temperature at which they react (1600 K). When pressure is suddenly decreased, but not temperature, a slight decrease in NO_2 concentration occurs. When the temperature is decreased to 829 K a dramatic increase in NO_2 concentration occurs. NO_2/NO_x ratio jumps from under 1% to more than 10% (NO_x is always conserved). The reason for such an increase in NO_2 formation is that the temperature is suddenly decreased to the temperature region which modeling has indicated is conducive to NO_2 formation. In this case, the temperature effect dominates the pressure effect, and the result is a more dramatic increase in NO_2/NO_x than the other base cases.

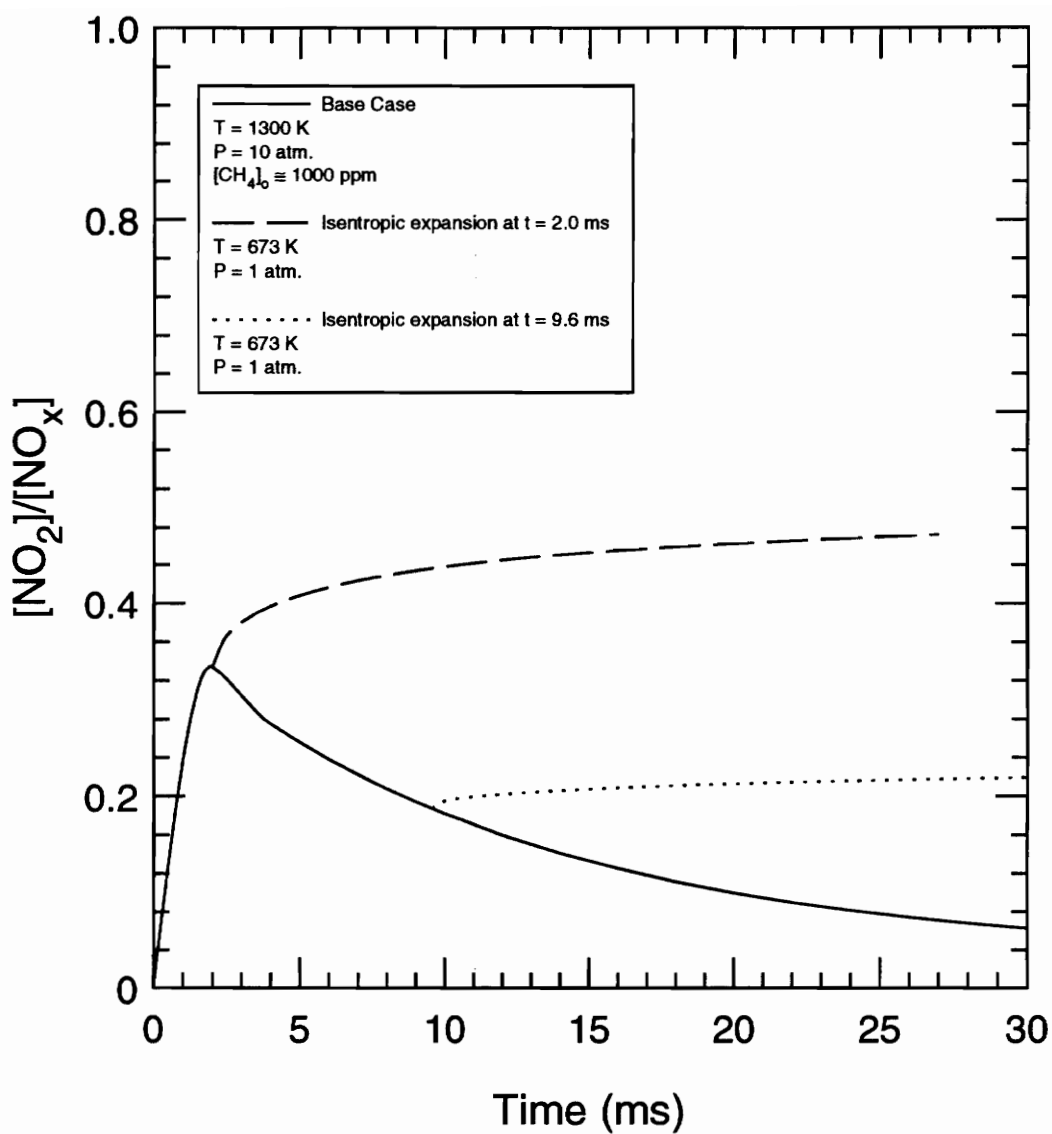


Figure 2.7 The effect of an instantaneous pressure and temperature drop on NO_2 formation.

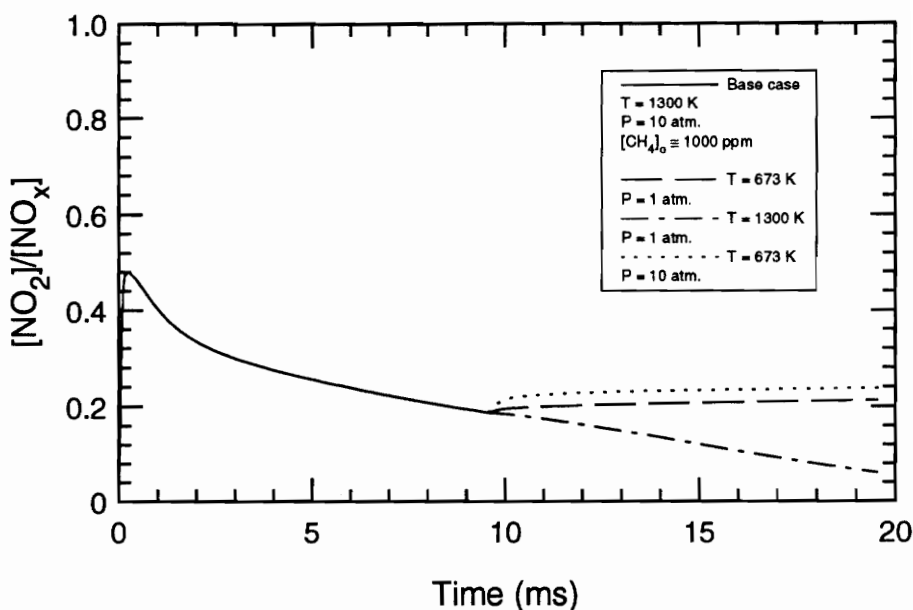


Figure 2.8(a). Instantaneous pressure and/or temperature drop for the 53.4% air dilution base case.

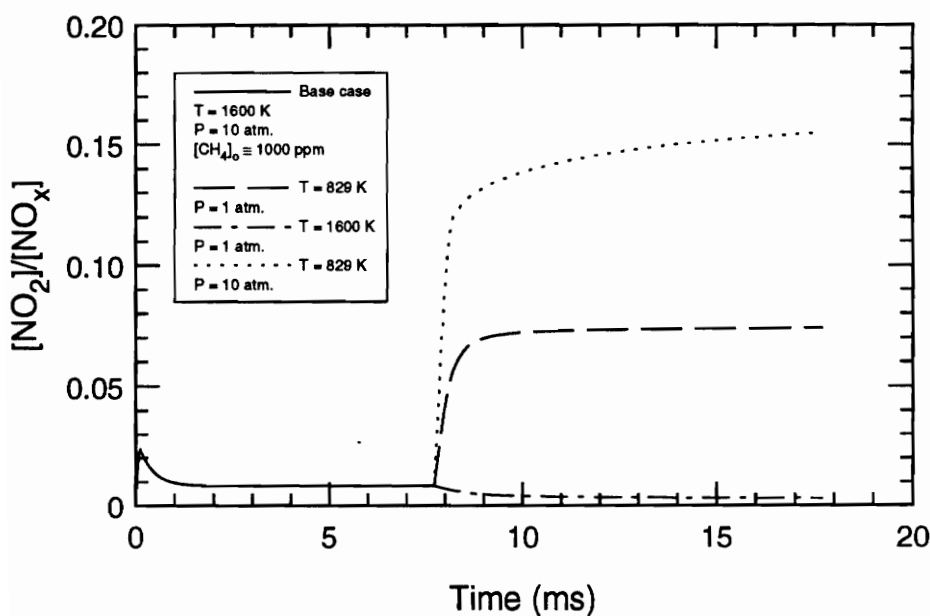


Figure 2.8(b). Instantaneous pressure and/or temperature drop for the 34.0% air dilution base case.

Figure 2.8. The effect of an instantaneous pressure and/or temperature drop on NO_2 formation.

A more gradual expansion was also modeled in a step-wise fashion. The expansion takes place in steps of 1 atmosphere. It was assumed to be an isentropic process. Using this assumption, temperature at each step was calculated assuming the working fluid to be air. Temperature is constant throughout each step. Figure 2.9 shows the results from 10 atm. to 6 atm. for two base cases. A gradual pressure drop shows a slight decrease in NO_2/NO_x , then a gradual increase. Again there appears to be a trade-off between conflicting temperature and pressure effects. It should be mentioned that this process was modeled using the modified Miller & Bowman mechanism. For this case, a similar trend would be expected from the Miller & Bowman mechanism.

2.4.3. The Effect of Methane

It has been noted in combustion systems in both research and real world applications that the presence of hydrocarbons promotes the formation of NO_2 . Much of the most recent NO_2 research has concentrated on the effect of hydrocarbons on NO to NO_2 conversion. In this study, methane was the hydrocarbon selected to seed the post flame gases. This hydrocarbon was chosen because it is the major constituent of natural gas, a common gas turbine fuel. NO_2 formation is not greatly changed by varying levels of $[\text{CH}_4]_0$ until $[\text{CH}_4]_0$ is reduced below 100 ppm. The modeling results indicate that the presence of even relatively small amounts of CH_4 greatly promotes NO_2 formation and that it is not until $[\text{CH}_4]_0$ approaches 0 that there is a significant decrease in NO- NO_2 conversion. Figure 2.10 illustrates this for the 66.3% base case which has a NO concentration of 88 ppm at the beginning of the flame zone.

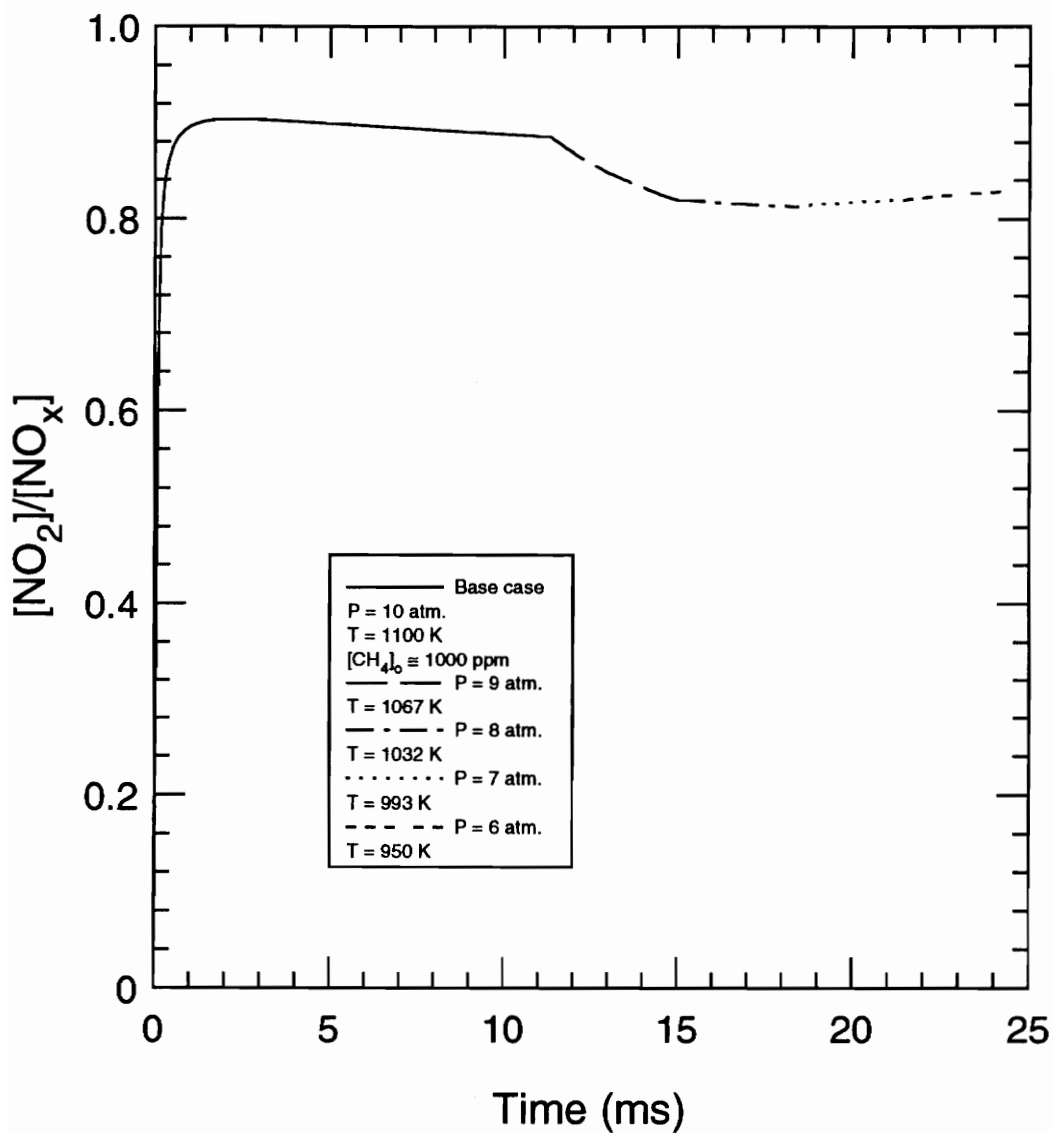


Figure 2.9 A gradual pressure drop in step-wise fashion from 10 atm., 1100 K to 6 atm., 950 K. $[\text{CH}_4]_0 = 1010 \text{ ppm}$. (Modified Miller & Bowman Mechanism)

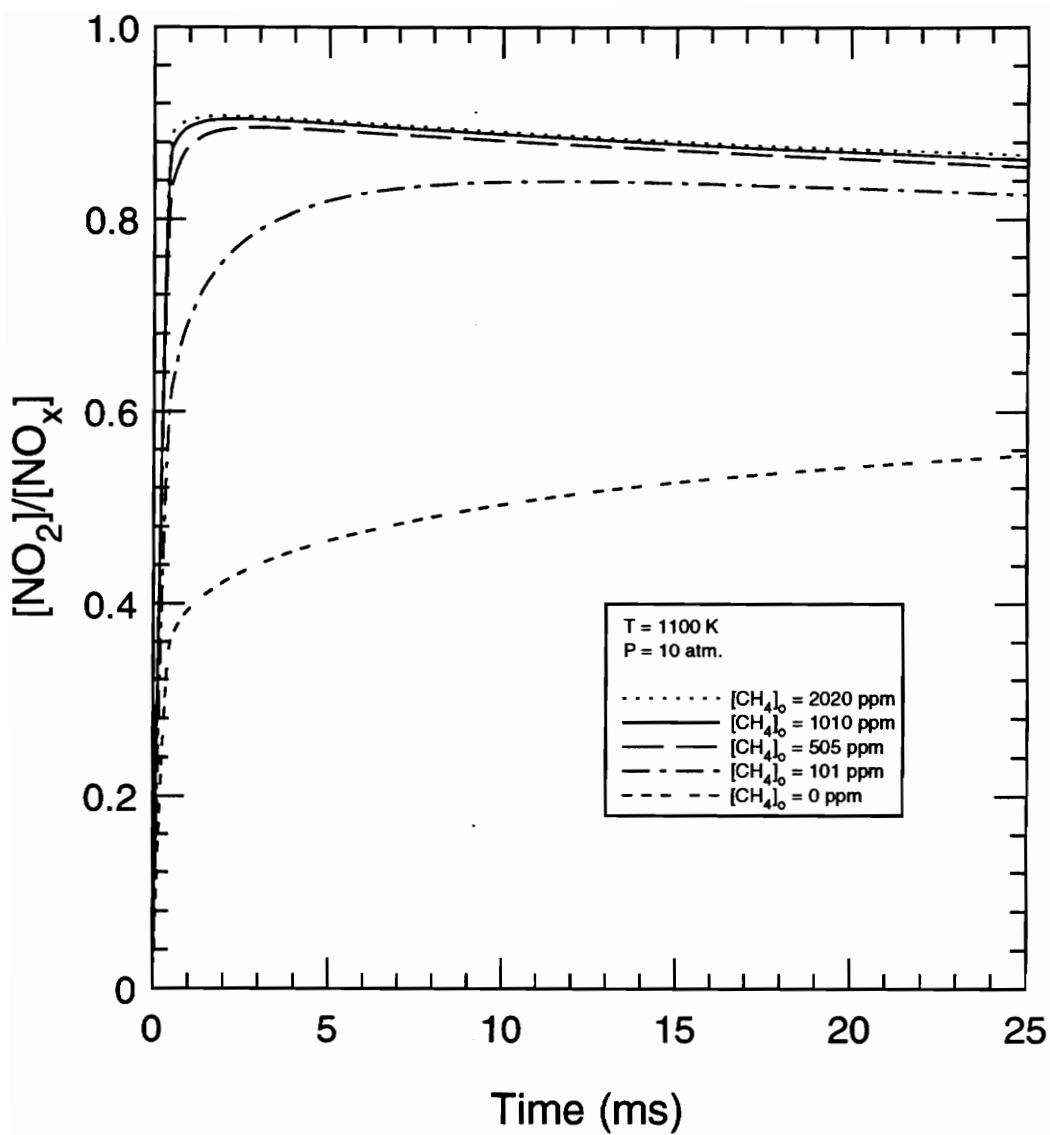


Figure 2.10 The effect of varying $[\text{CH}_4]_0$ on NO_2/NO_x .

2.4.4. The Effect of Carbon Monoxide

Some past research has suggested that the presence of unburned species other than hydrocarbons also promotes the formation of NO_2 . The addition of carbon monoxide to post flame gases was modeled and compared to methane addition. It was seen that carbon monoxide addition has a similar effect to methane addition. The effect, however, is not as dramatic as it is with methane addition. Figure 2.11 shows several plots which compare the effects of various combinations of CH_4 and CO concentrations. In the presence of significant CH_4 ($>0(100)$), CO has little effect. However, if concentrations of CH_4 are negligible, the presence of CO can be seen to increase the production of NO_2 .

2.4.5. The Effect of H_2O

Water concentration at the end of the flame zone before the addition of dilution air was 14.5%. Water was added as a liquid at this point with the dilution air, such that $[\text{H}_2\text{O}]_0$ (i.e., the concentration of water in the beginning of the post flame zone) remained 14.5% in one case and was increased to 20.0% in a second case. Temperature change due to the water addition was neglected. The model was then run isothermally at the temperature of the base case (no water addition). The results for water addition to the three air dilution cases (34.0%, 53.4%, and 66.3%) are plotted with the base cases in Figures 2.12(a), 2.13(a), and 2.14(a), respectively.

These cases were then run taking into account the change in temperature due to the water addition. The temperature of the post flame gases was calculated assuming an adiabatic system and instantaneous bulk quench of the gases at the beginning of the post

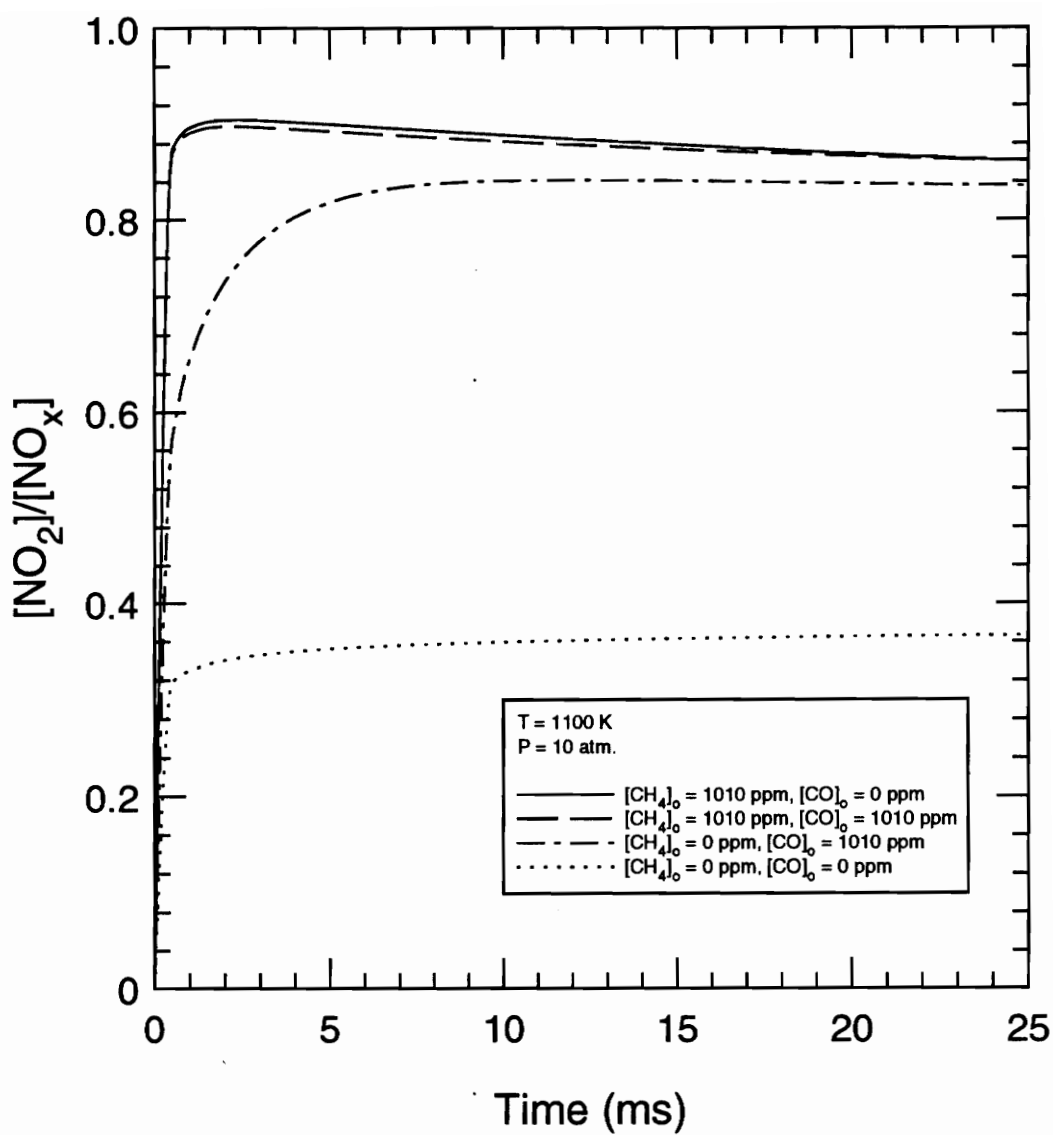


Figure 2.11 The effect of methane and carbon monoxide on the formation of NO_2 .

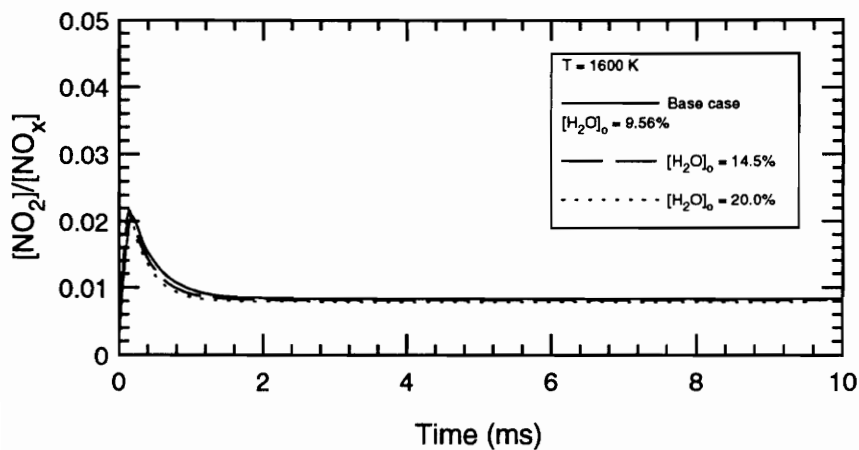


Figure 2.12 (a). The effect of water addition on NO_2 formation. (Temperature effect neglected)

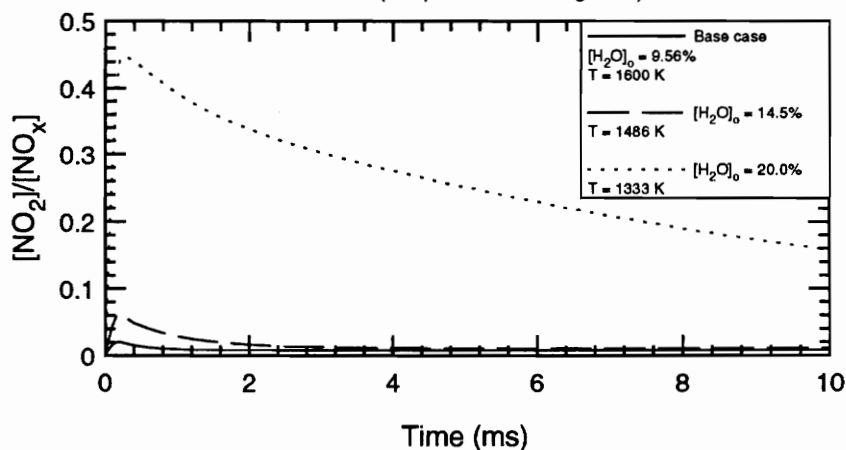


Figure 2.12 (b). The effect of water addition on NO_2 formation. (Temperature effect included)

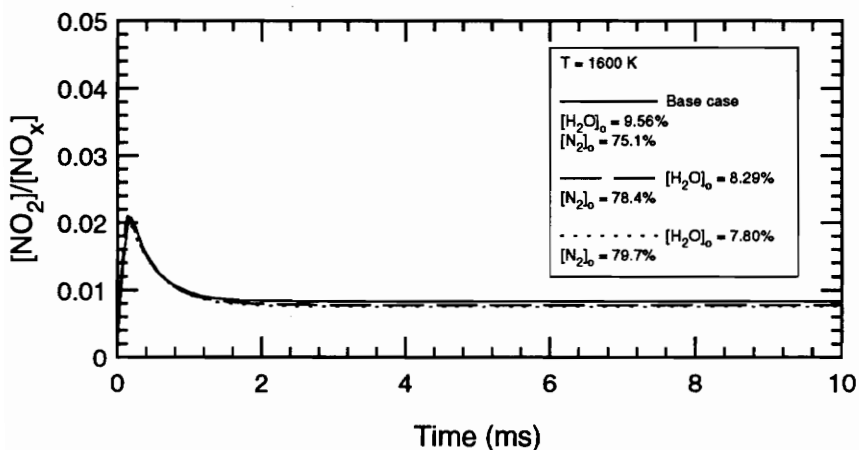


Figure 2.12 (c). The effect of a diluent (N_2) on NO_2 formation. (Temperature effect neglected)

Figure 2.12. The effects of water addition on NO_2 formation. (34.0% air dilution case, 10 atm.)

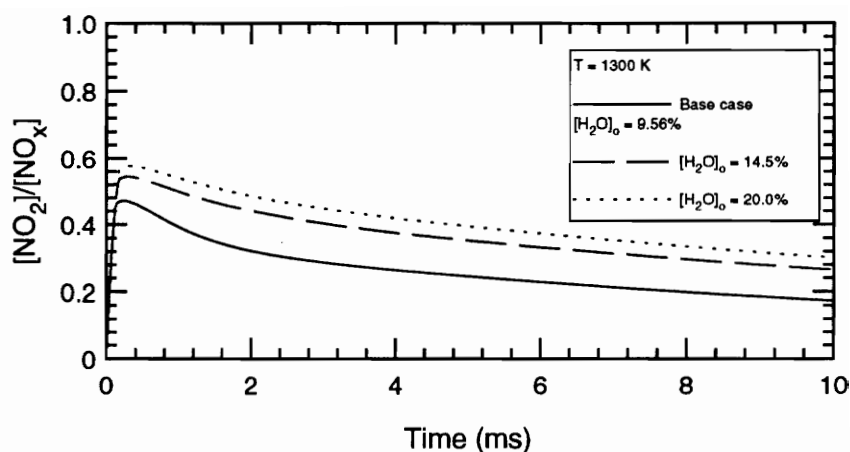


Figure 2.13 (a). The effect of water addition on NO_2 formation. (Temperature effect neglected)

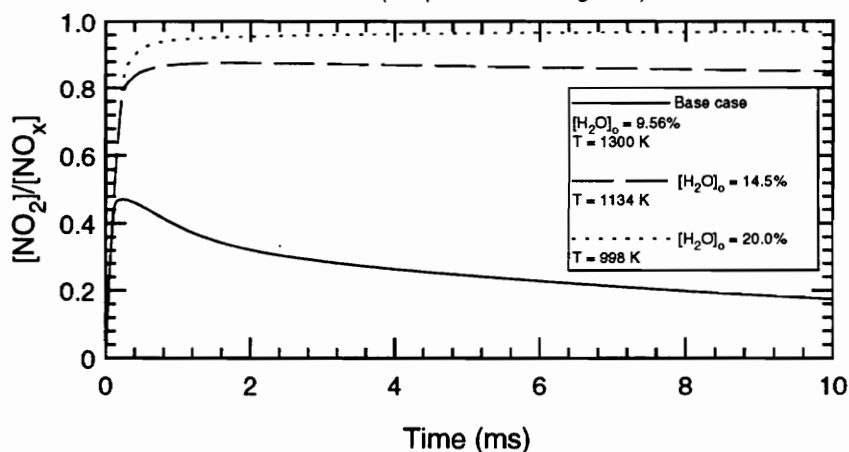


Figure 2.13 (b). The effect of water addition on NO_2 formation. (Temperature effect included)

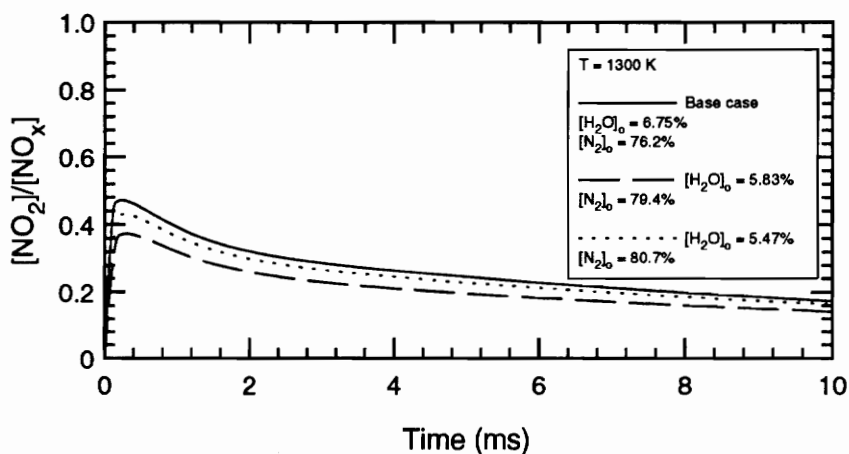


Figure 2.13 (c). The effect of a diluent (N_2) on NO_2 formation. (Temperature effect neglected)

Figure 2.13. The effects of water addition on NO_2 formation. (53.4% air dilution case, 10 atm.)

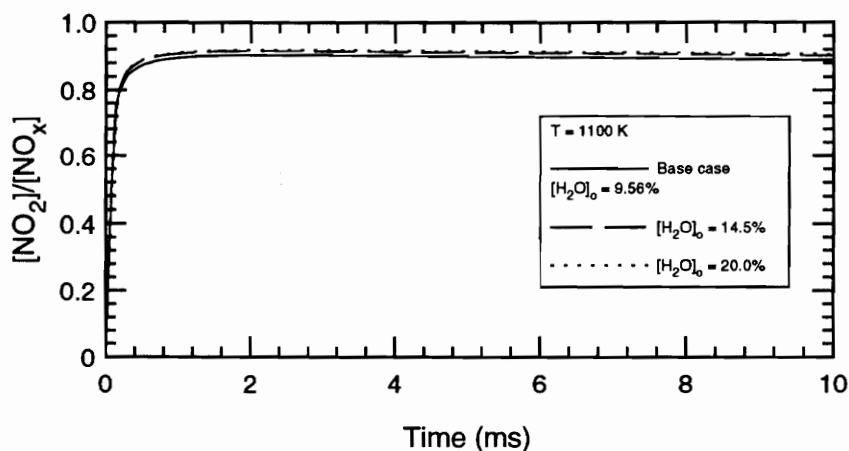


Figure 2.14 (a). The effect of water addition on NO_2 formation. (Temperature effect neglected)

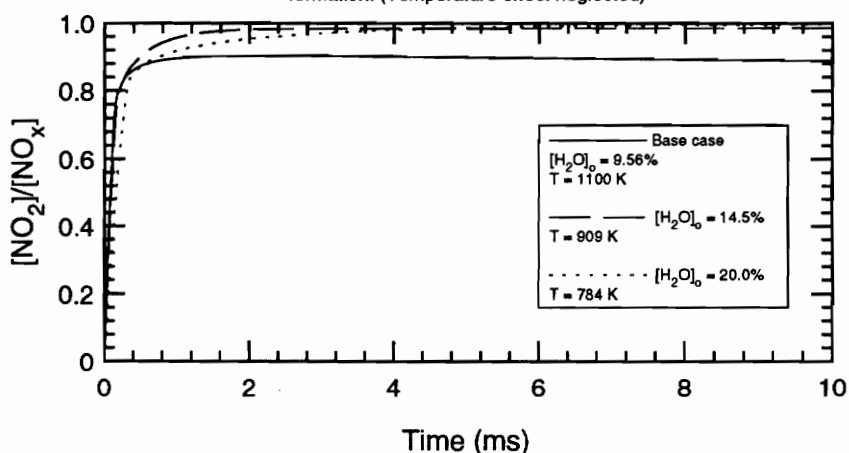


Figure 2.14 (b). The effect of water addition on NO_2 formation. (Temperature effect included)

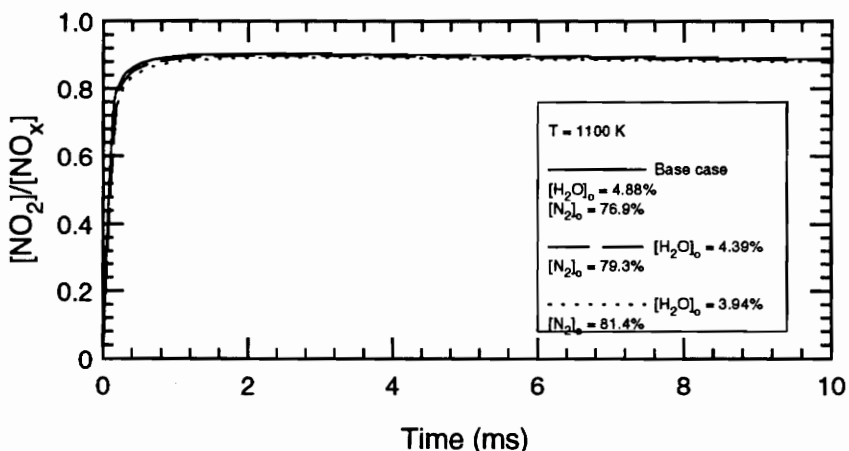


Figure 2.14 (c). The effect of a diluent (N_2) on NO_2 formation. (Temperature effect neglected)

Figure 2.14. The effects of water addition on NO_2 formation. (66.3% air dilution case, 10 atm.)

flame zone. The results are plotted with the base cases in Figures 2.12(b), 2.13(b), and 2.14(b), respectively.

To examine any dilution effect of the water addition, a third set of runs was considered. In this set, the water addition at the beginning of the post flame zone was replaced by nitrogen. The temperature change due to the nitrogen addition was ignored. At the injection point there was already an excess of nitrogen in the main flow, and for the temperatures modeled nitrogen does not react chemically. Therefore, nitrogen played the sole role of a diluent. The results are displayed in Figures 2.12(c), 2.13(c), and 2.14(c), respectively.

From the plots, it appears that the dilution effect of the water addition is negligible. There is a chemical effect of the water addition which is particularly apparent in the 53.4% air dilution case. The temperature effect, however, appears to dominate any other effect in all cases. Figure 2.12 shows the 34.0% air dilution case. For $[H_2O]_0 = 14.5\%$, the resulting temperature of the post flame gases is 1486 K. A NO_2/NO_x profile very similar to the base case is produced at this temperature. The steady-state level of NO_2/NO_x is slightly greater than the base case, but in both cases NO_2 concentrations are relatively small. When $[H_2O]_0$ is increased to 20.0%, the resulting temperature of the post flame gases is 1333 K, and NO_2/NO_x peaks approximately 10 times higher than the base case. This provides more evidence that the mechanism for NO_2 formation is very temperature sensitive and is not active at higher temperatures.

2.4.6. The Effect of $[\text{NO}]_0$

Figure 2.15 shows the effect of $[\text{NO}]_0$, that is, the concentration of NO at the beginning of the post flame gas zone. The rate at which NO_2 is produced is dependent on the initial concentration of NO. At higher $[\text{NO}]_0$ levels, conversion is slower and occurs to a lesser extent. At concentrations above $[\text{NO}]_0 = \text{O}(100)$, this effect seems to be significant. If one also considers the effect of initial CH_4 concentration on the conversion of NO to NO_2 , an important ratio to consider may be $[\text{CH}_4]_0/[\text{NO}]_0$. Figure 2.16 shows the effect of varying this ratio. It would be expected that for a given ratio, the NO_2/NO_x profile would remain the same as $[\text{NO}]_0$ and $[\text{CH}_4]_0$ are varied. This appears to not be the case as can be seen in Figure 2.16. The results are a little ambiguous, but they seem to suggest that $[\text{CH}_4]_0$ has a disproportionate effect on the conversion of NO to NO_2 when compared to $[\text{NO}]_0$. For a given methane or nitric oxide concentration, however, the ratio could prove quite useful.

2.4.7. Kinetic Rate Constants Considerations

The results obtained with the Miller & Bowman mechanism indicate that NO to NO_2 conversion is an extremely rapid process. In some cases, nearly complete conversion is seen in less than 1 millisecond. Does this reasonably model that which occurs in the conversion process in real gas turbine combustors? To answer this question both the reaction mechanism and experimental results must be examined.

Many of the rate constants in the mechanism are well known and have been proven to be accurate in modeling and research efforts. However, there are also reactions whose rate constants are not well known. Some, in fact, are "best guesses" based on the

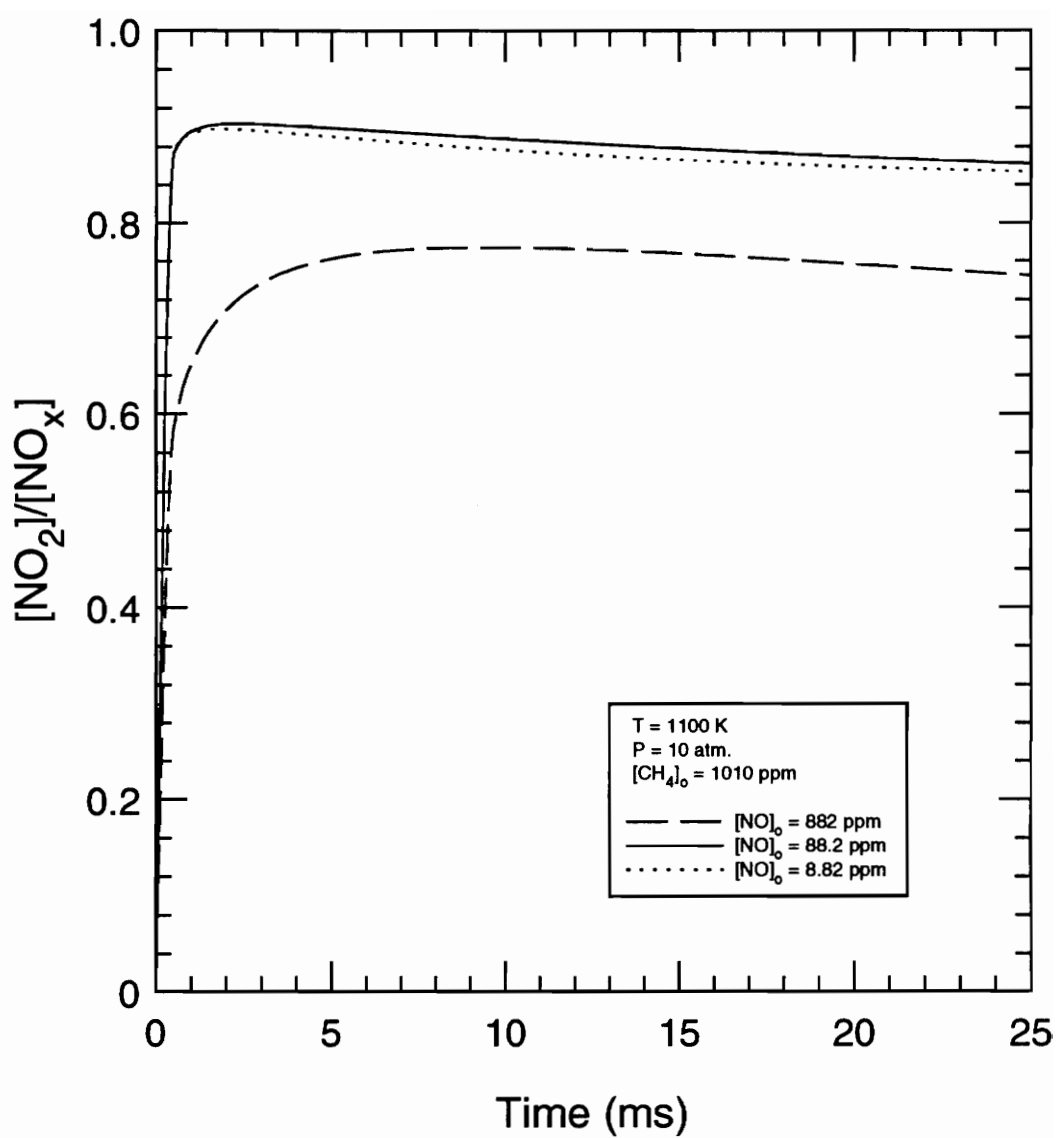


Figure 2.15. The effect of $[\text{NO}]_0$ on NO_2 formation.

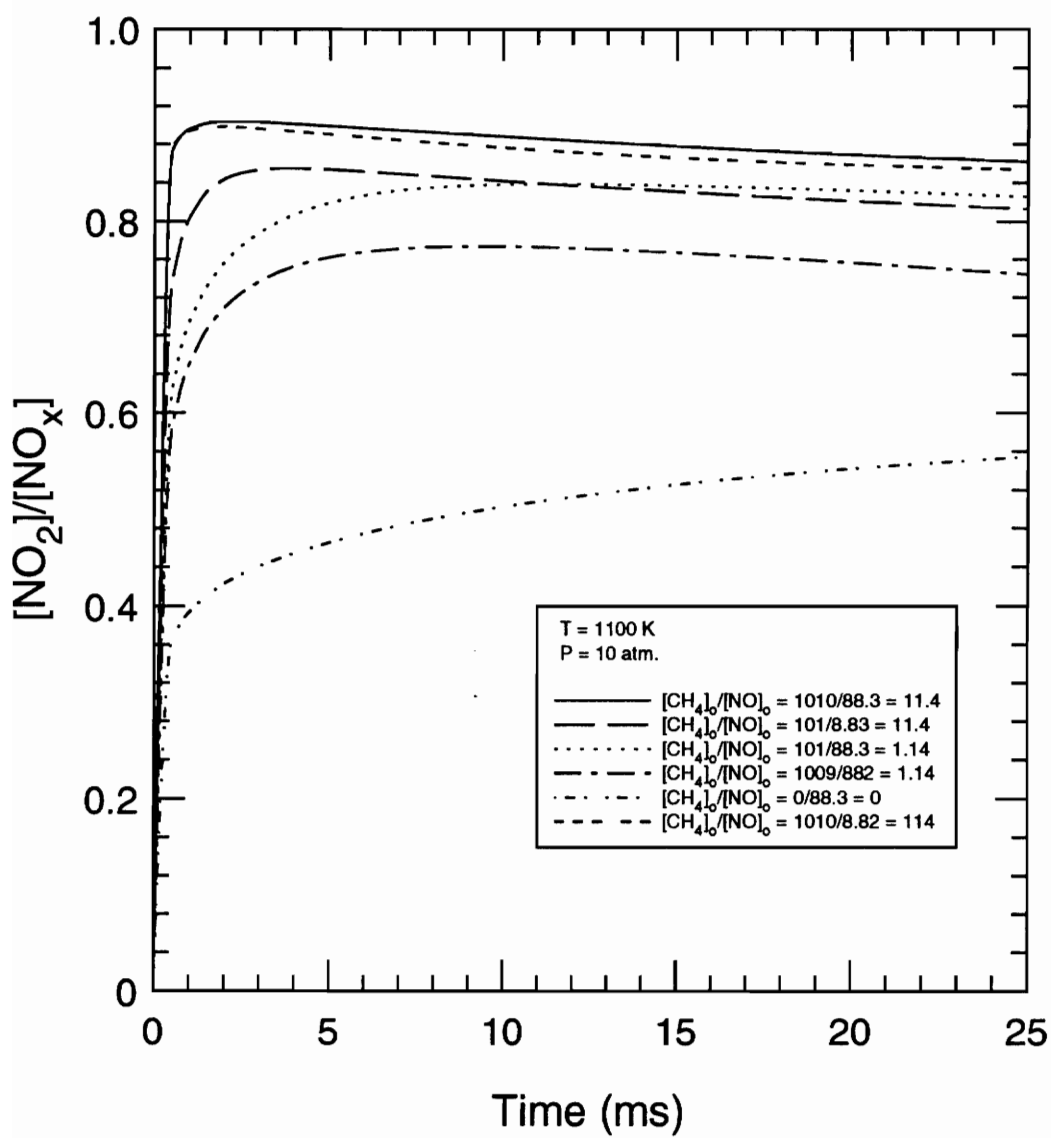
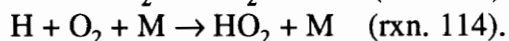
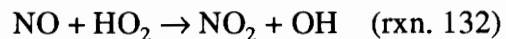


Figure 2.16 The effect of varying $[\text{CH}_4]_0/[\text{NO}]_0$ on the formation of NO_2 .

available research. The two reactions believed to be of greatest importance in the NO-NO₂ conversion mechanism are



There has not been an abundance of experimental research supporting the kinetic parameters for these reactions. Miller and Bowman estimate the constants for reaction 132 to be accurate to $\pm 30\%$ at the conditions at which they were determined [16]. The kinetic parameters for reaction 114 are even less certain. "Perhaps the largest kinetic uncertainty is introduced through uncertainties in the third body efficiencies for reaction [114], particularly for collision partners such as CH₄ and H₂O." [16] Generally, kinetic rate constants are determined at atmospheric or subatmospheric conditions. They may in fact be different at superatmospheric conditions. It is possible that some may be off by as much as an order of magnitude. It is for this reason, that it was decided to investigate the results of modeling with one or both of the "A" constants decreased an order of magnitude.

In general, decreasing the constants resulted in slower formation of NO₂ and lower peak values of NO₂. Figure 2.17 shows the effect of decreasing the constants of the above reactions for the 66.3% air dilution base case. These results show that these two reactions are in fact very important in the NO to NO₂ conversion mechanism. Changing them has a great effect on predicted NO₂ formation. It appears that reaction 132 most greatly affects the rate at which NO is converted to NO₂. Reaction 114 has a greater effect on the peak value of NO₂/NO_x.

Because it is believed that the NO-NO₂ conversion process actually occurs more slowly than the Miller & Bowman mechanism suggests, much of the modeling was run

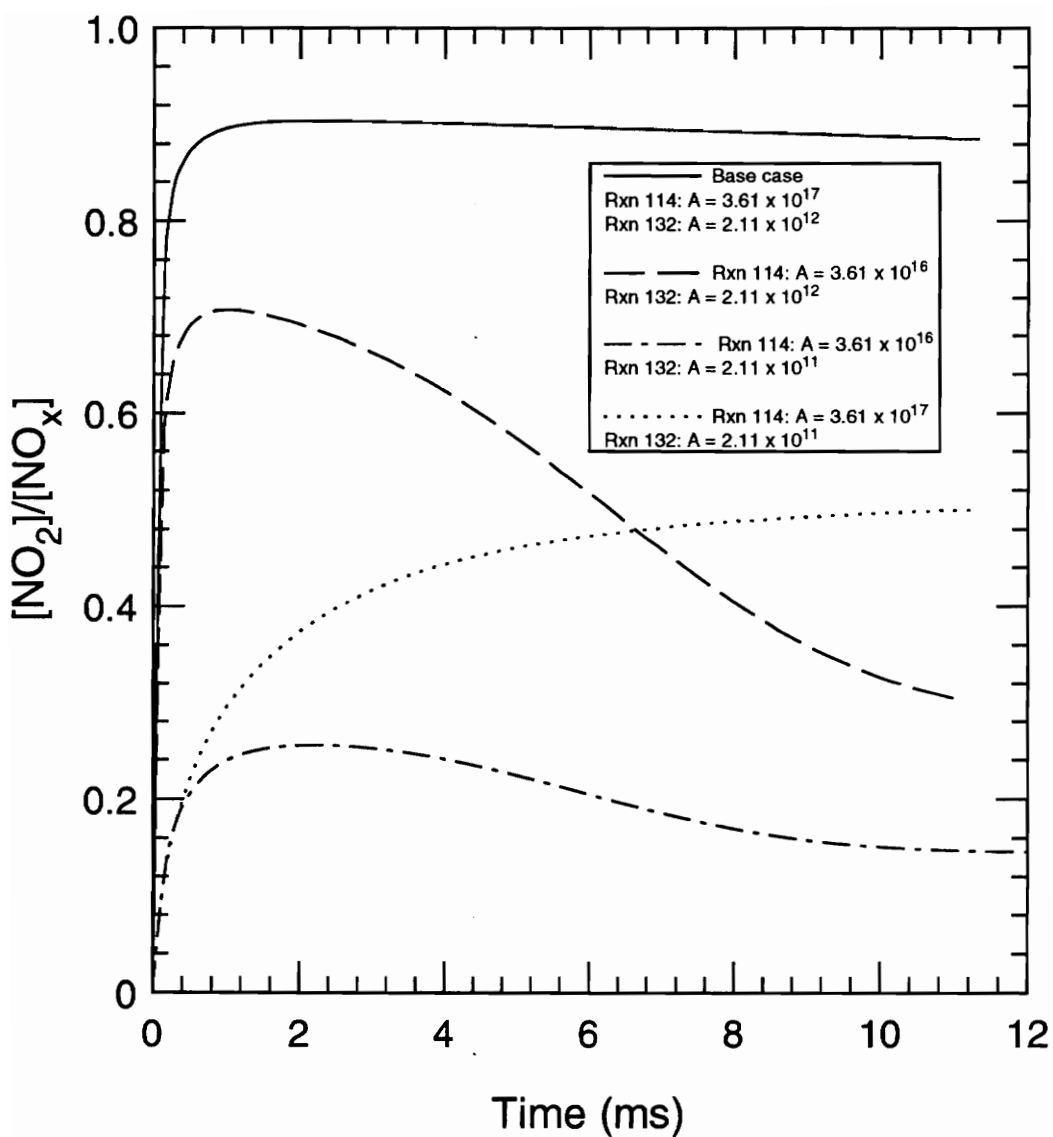


Figure 2.17. The effect of kinetic parameters on predicted conversion of NO to NO_2 . $P = 10 \text{ atm.}$, $T = 1100 \text{ K}$, and $[\text{CH}_4]_0 = 1010 \text{ ppm.}$

with $A = 2.11 \times 10^{11}$ for reaction 132. This value of the "A" constant is an order of magnitude less than that of Miller & Bowman. The constants of reaction 114 were not changed because the model then would not predict the high levels of NO_2 noted in previous research. The reaction mechanism with $A_{132} = 2.11 \times 10^{11}$ will be referred to as the "modified Miller & Bowman mechanism". Results of computer model runs using the modified Miller & Bowman mechanism were similar to those noted above. They generally showed a slower rate of NO_2 formation as well as lower peak values. General trends, however, tended to remain the same. In comparing air dilution cases, the modified mechanism indicates a slightly lower temperature for the upper limit to NO- NO_2 conversion. As a result, less NO is converted to NO_2 for the 1100 K base case than is predicted by the Miller & Bowman mechanism (Fig. 2.18). It also shows a much slower rate of NO_2 formation for the lower temperature range (< 800 K) which suggest that there may be a lower temperature limit for the conversion (Fig. 2.18). It follows that there could be a relatively well defined temperature window outside of which NO is not readily converted to NO_2 .

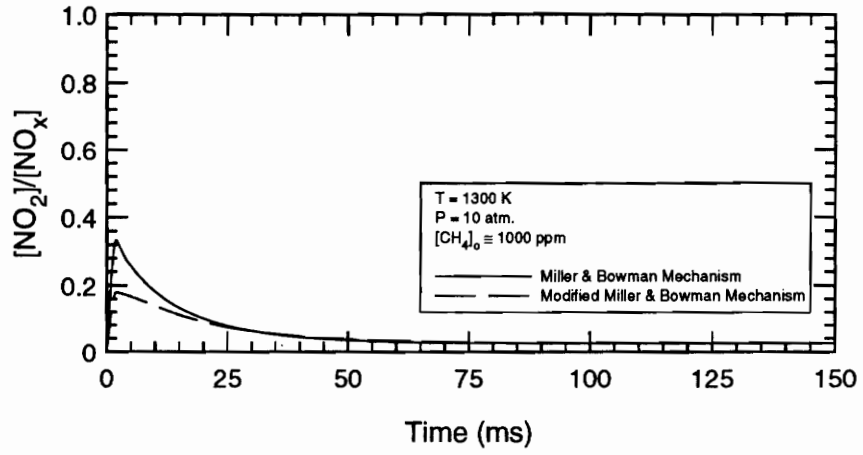


Figure 2.18(a). Base case at 1300 K.

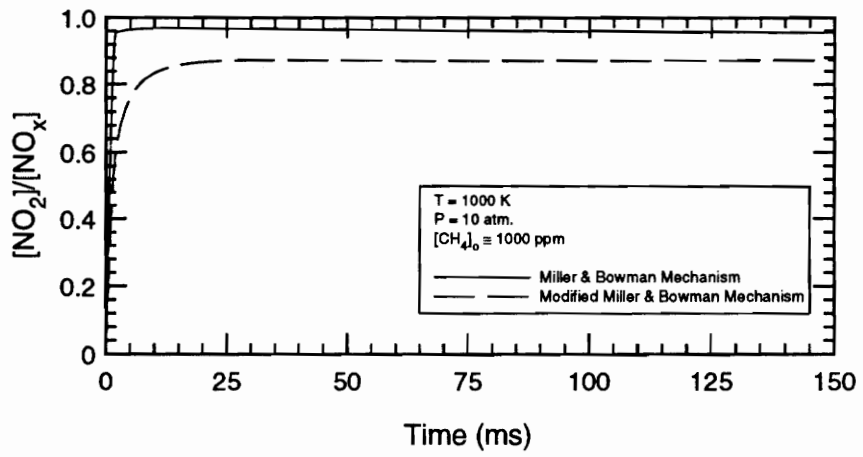


Figure 2.18(b). Base case at 1000 K.

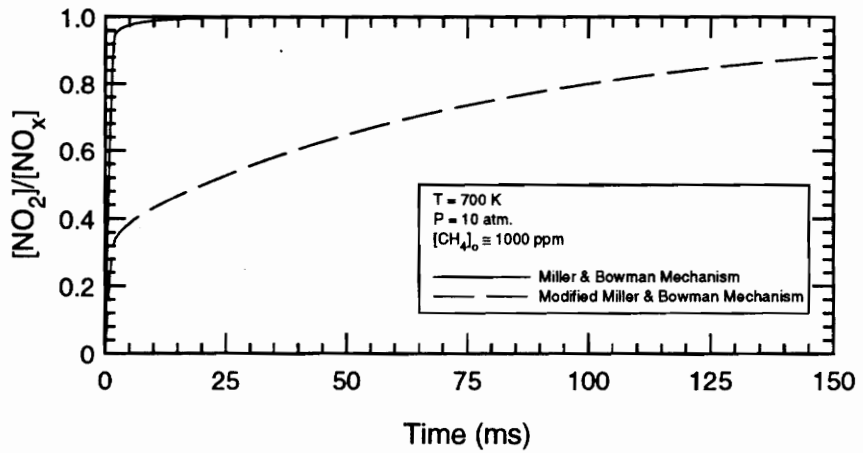


Figure 2.18(c). Base case at 700 K.

Figure 2.18. Comparison of Miller & Bowman Mechanism to the Modified Miller & Bowman Mechanism for the air dilution base cases.

CHAPTER 3 - EXPERIMENTAL APPARATUS AND PROCEDURE

3.1 APPARATUS

The proposed hypothesis, the results of computer modeling, and the results of past investigations all contributed to and influenced the design of the high pressure flow reactor with which the experimental tests in this study were conducted. A schematic of the reactor facility is shown in Figure 3.1. Figure 3.2 shows a system schematic of the experimental facility. The high pressure flow reactor design can be divided into several areas: (1) the pressure vessel, (2) the burner and related components, and (3) instrumentation and control. These will each be discussed below.

3.1.1 The Pressure Vessel

The vessel is based on a similar design developed by Carter, Laurendeau, and King at Purdue University [22]. In order to simulate the environment of a gas turbine combustor, the pressure vessel was designed to withstand working pressures up to 10 atm. (1.013 MPa gauge).

Figure 3.3 is a schematic of the pressure vessel. Shop drawings for the pressure vessel as well as other components of the flow reactor can be found in Appendix D. All components of the pressure vessel were constructed from AISI 316L stainless steel. The components of the vessel were built from three different standard pipe sizes with appropriate flanges. The main body of the vessel has an inside diameter of 20.27 cm (8" nominal, schedule 40s standard pipe). At the ends of the main body, ANSI class 300

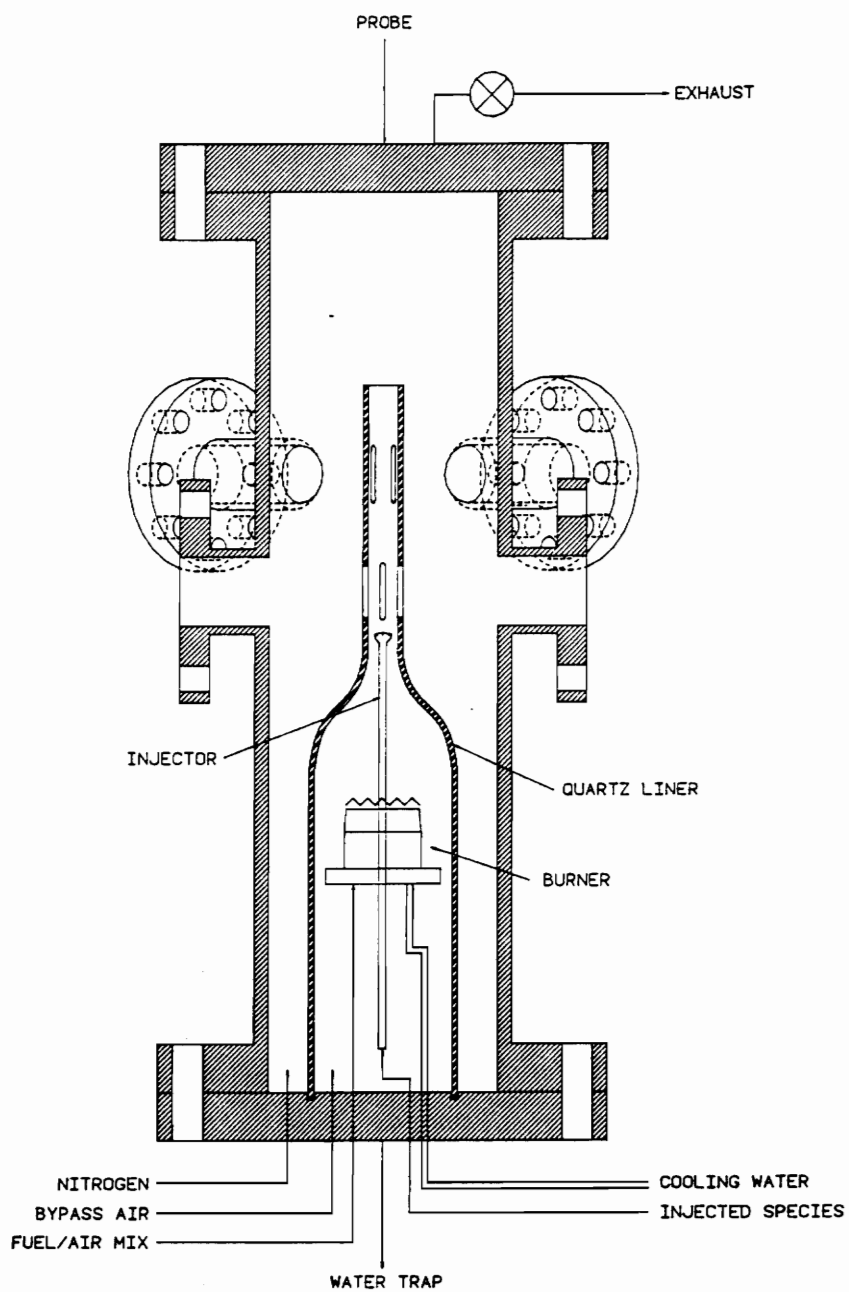


Figure 3.1. High pressure flow reactor schematic.

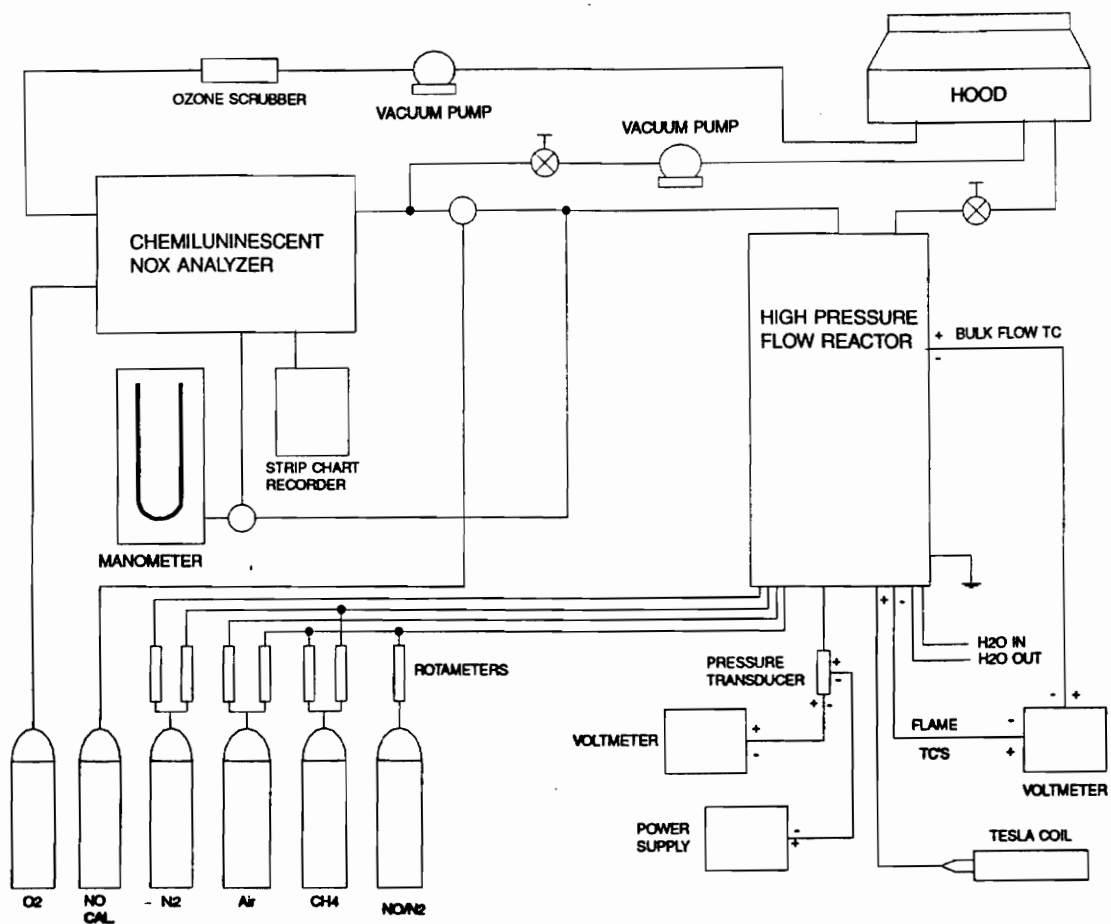


Figure 3.2. Experimental system schematic.

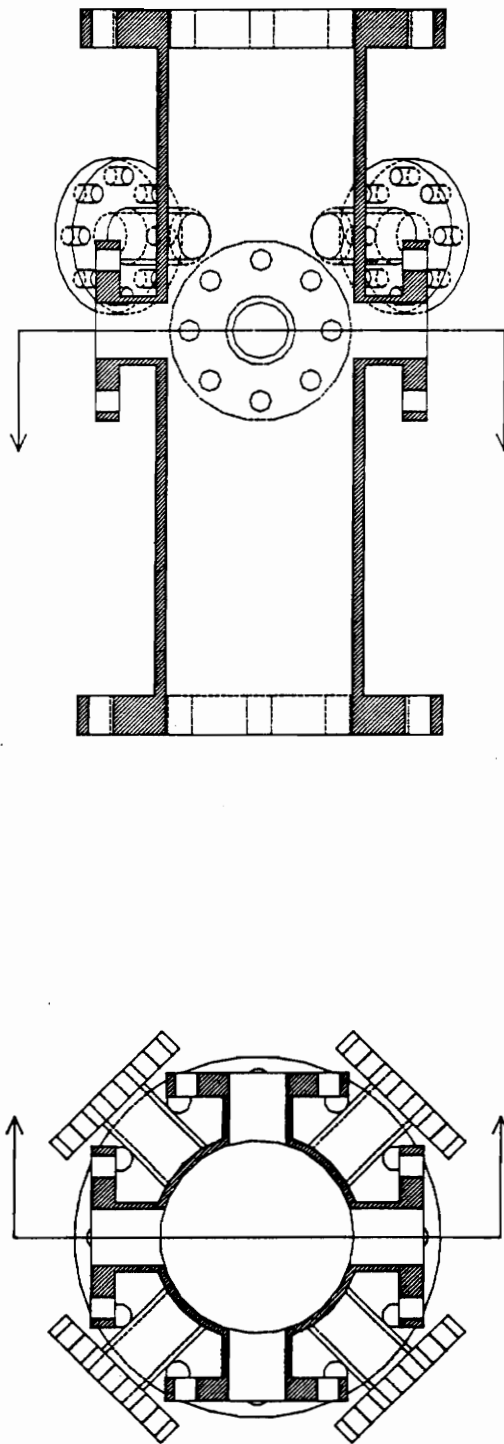


Figure 3.3. Pressure vessel schematic (1/8 scale).

slip-on flanges were welded. Also welded to the main body are eight ports. The bottom four ports were constructed from standard pipe with an inside diameter of 5.900 cm (2-1/2" nominal, schedule 80s). The flanges on these ports are also ANSI class 300 slip-on flanges. The ports are spaced 90° from one another. The top set of ports are offset from the bottom set by 45°. The bottom ports are constructed from standard pipe with an inside diameter of 4.925 cm (2" nominal, schedule 80s).

Blind flanges were machined for access to the interior of the vessel. Figure 3.4 shows schematics of the two large end flanges. The bottom flange contains all inlet ports as well as a water trap assembly and electrical/instrumentation feed-throughs. Polypropylene tubing is sealed with Swagelok fittings at the inlets for air, nitrogen, fuel/air mixture, and the injected species. Inside the vessel, polypropylene tubing conducts the air/fuel mixture to the burner. Tygon tubing provides passage to the injector inlet. The injector does not extend below the bottom flange. The water trap is constructed from AISI 304 1.27 cm stainless steel tubing with a 1.651 mm wall thickness. It is attached to the center of the bottom flange with a Swagelok fitting. Extending off the water trap tube is a relief valve and pressure transducer (Fig. 3.5).

The top flange is of somewhat simpler design than the lower flange. A Cajon Ultra-Torr fitting (bored through) is located at the center of the flange. This functions as a feed-through for a sampling probe. The probe is held in place by set screws located on a Velmex translation stage. This apparatus is secured to the top flange and provides for accurate positioning of the probe tip within the sealed vessel. Offset slightly from center is the exhaust port. Gases are exhausted through 1.27 cm stainless steel tubing (AISI 304). The top flange also houses a Fike rupture disk fitting.

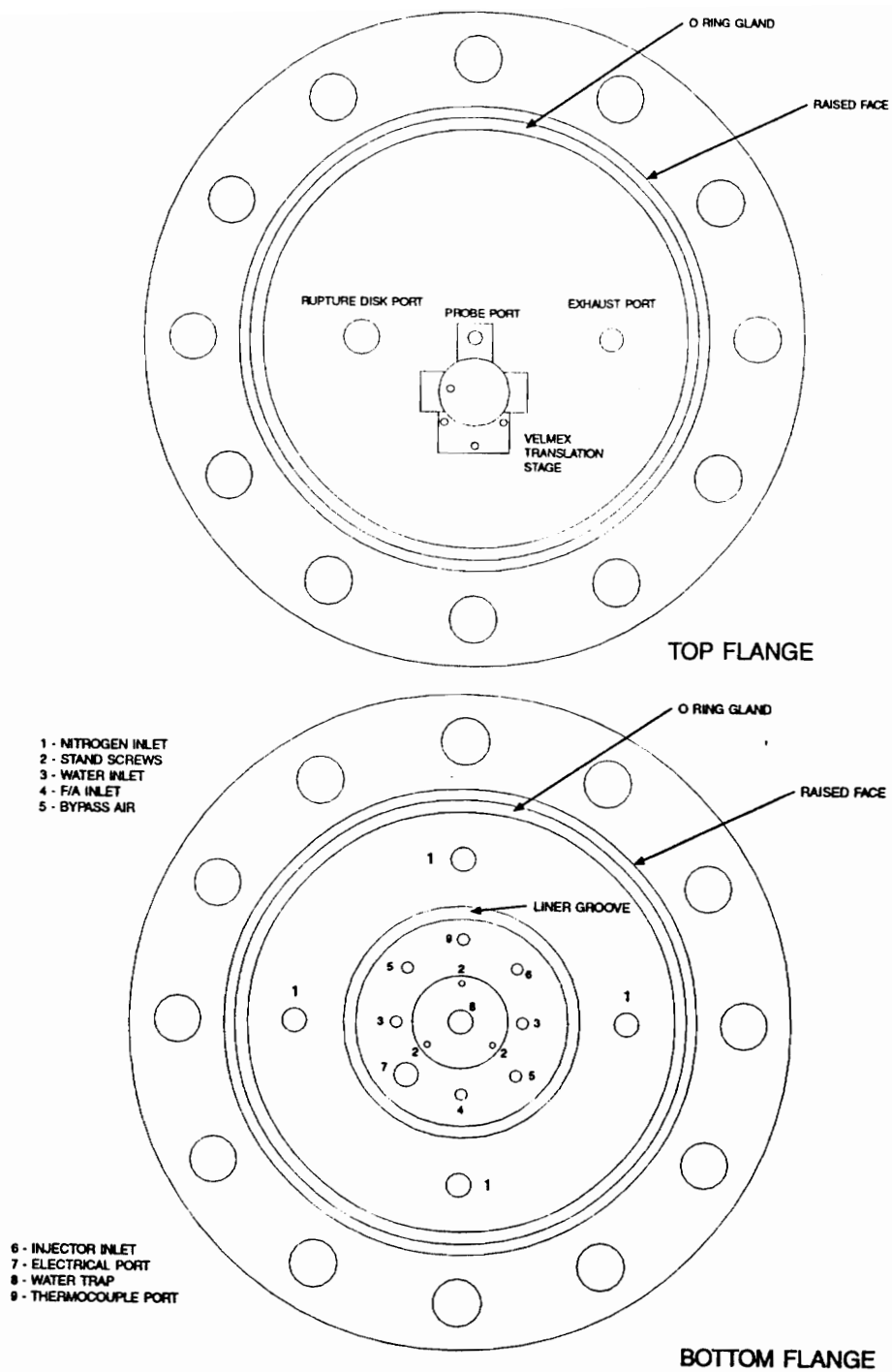


Figure 3.4. Schematic of pressure vessel end flanges.

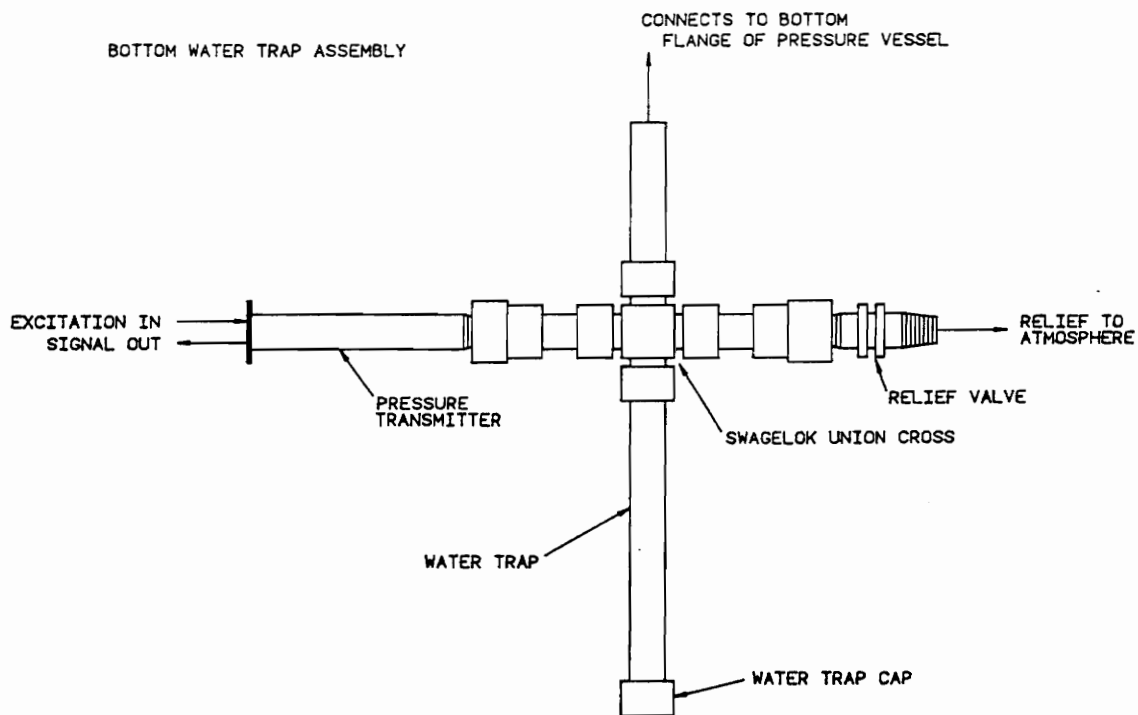


Figure 3.5. Water trap assembly schematic.

It was originally intended that the side ports would provide access for optical measurement of species concentrations. It was decided, however, that probe sampling measurement techniques would be used in this study. The side ports were therefore fitted with appropriate blind flanges. These blind flanges can be machined to fit windows if the need arises in future studies utilizing this facility. A 1/8" NPT port was machined into one of the top side flanges. This port provided access for thermocouple placement in measuring post flame gas temperature.

All flanges were sealed with Parker silicone O-rings. Silicone was selected as the material due to its durability in both a relatively high temperature and corrosive environment. Three different size O-rings were selected for the ports. They are standard sizes 2-448, 2-239, and 2-235.

The pressure vessel was hydrostatically tested to 18.3 atm. (1.86 MPa). The vessel integrity remained intact. The vessel is very similar to the design of Carter *et al.* which was successfully tested hydrostatically to 60 atm. (6.08 MPa) [22]. Although this vessel was only tested to 18.3 atm. (1.86 MPa), it is believed that it could withstand much greater pressures without compromising integrity of the welds and seals. It was not tested to a higher pressure at this time because maximum working pressures were significantly lower than 18.3 atm. (1.86 MPa).

3.1.2 The Burner and Related Components

The phenomenon of NO-NO₂ conversion appears to be a post flame event due to the relatively low temperatures required for it to occur. For the scope of this study, the burner was solely a source of post flame gases. The burner used was a McKenna sintered

bronze, flat flame burner that had been specially modified to allow injection into the post flame gases. A 6.35 mm hole had been bored through the center of the burner. This allowed passage of a quartz injector.

Flame ignition was initiated by throwing an arc between a nichrome wire electrode and the burner head. The nichrome wire electrode was connected to a Tesla coil located outside the pressure vessel. It fed through the bottom flange via a Ceramaseal copper feed-through. In order to insulate the copper electrode, it was necessary to fill the void between the fitting and electrode with Sauereisen (Electrotemp Cement) No. 8. This created a path of greater resistance and helped to prevent an arc from being thrown to the fitting and grounding through the vessel. The nichrome wire electrode was connected to the copper feed-through electrode inside the vessel below the burner. This was then fed through a ceramic insulator to a point just above the burner head. This ignition arrangement could be improved. The gap between the burner head and nichrome electrode was critical. If it was too large the coil current tended to ground through another part of the vessel (most likely through the feed-through fitting), and no arc was thrown to the burner head. If the gap was too small, ignition was difficult at best. In short, the ignition system was not always reliable. The gap distance had to be adjusted at times. This procedure involved dropping the bottom flange - a lengthy process. A two electrode arrangement with a ground electrode taking the place of the burner head was also tried without much success.

The injector and liner were designed to enhance mixing (Fig. 3.6). Modeling suggested that NO-NO₂ conversion is an extremely fast process. It was therefore desirable that mixing occur as thoroughly and quickly as possible. This was achieved with the injector-liner design by converging the liner and creating a throat between the

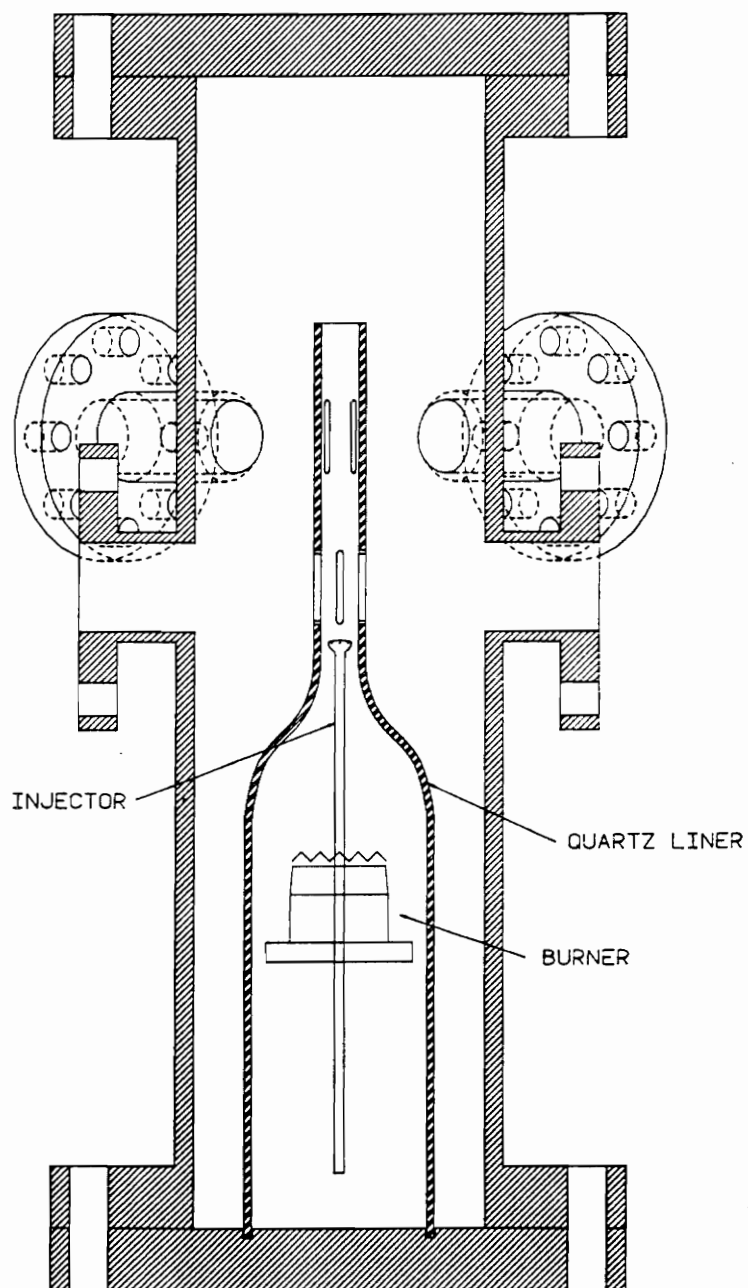


Figure 3.6. Schematic showing the relative positions of the injector, liner, and burner.

liner and the injector. It is at this point that CH_4 was injected into the post flame flow. Bypass air flowed around the burner and mixed with the flame products in order to control temperature of the post flame gases. Convergence of the liner past the burner promoted shear layer mixing of the flame products and bypass air by accelerating the flow through a 94% reduction in flow area. Methane was injected into the flow at the throat created between the bulb of the injector and the wall of the liner. Injection occurred through six, 0.508 mm orifices. The injection jets were spaced 60° apart and flowed normal to the main flow.

The liner served several other purposes. It decreased the flow area so that reasonable flow rates could be used to achieve a desired flow velocity. It was designed for a flow velocity of 1 m/s in the top section of the liner at ten atmospheres. This would have allowed sampling at residence times as short as 1 ms after injection at 10 atm. Unfortunately, the liner was not fabricated to the design specifications. It was intended that the inside diameter of the upper portion of the liner have a diameter of 2.54 cm. It was actually constructed with quartz tubing with a 2.94 cm inside diameter. This resulted in poorer mixing due to decreased turbulence as a result of the larger flow area at the injection point. It also made it difficult to achieve the desired flow velocities for which the liner was designed.

The liner created an annulus between its outside wall and the inside wall of the pressure vessel. Nitrogen was passed through this annulus in order to cool the walls of the pressure vessel. The liner was constructed entirely of quartz. Eight slots were cut into the side of the top portion. These slots coincided with the side ports of the pressure vessel and were intended to provide optical access for infrared measurement techniques in future work. They also provided access to the post flame gas flow for instrumentation

that was found to be necessary or desirable in the course of experimental work with the facility. In this study, a slot provided access for a thermocouple probe used to measure temperature of post flame gases.

After some experimental testing, it was found that significant cooling nitrogen was being entrained into the main flow through the slots in the liner. This caused a significant temperature gradient in the direction of the flow and made it impossible to determine mass flow inside the liner. To eliminate entrainment, the slots were filled with Sauereisen (Electrotemp Cement) No. 8. A small opening was left in one of the top slots for thermocouple access. Any entrainment through this small space was neglected.

The injector, like the liner, was constructed from quartz. This material was selected in order to withstand elevated temperatures at the point at which the injector passes through the flame. The bulb of the injector sat slightly below the level of the first four side ports (approximately 10 cm above the burner).

3.1.3 Instrumentation and Control

Pressure inside the vessel was controlled with a stainless steel Whitey forged body regulating valve. This valve was located downstream from the exhaust port. The pressure inside the vessel was monitored via an Ashcroft Model K1 pressure transmitter which was attached to the bottom flange water trap. A Robertshaw pressure gauge was used in place of the transmitter for a short time while the transmitter was being repaired. To prevent over pressurization, a Nupro relief valve was installed off the water trap. This was adjusted to open at 1.38 MPa. This valve was backed up with a Fike rupture disk mounted on the top flange. The rupture disk was designed to rupture at 2.071 MPa.

Temperature inside the vessel was monitored with Type S Pt/Pt-10%Rh thermocouples. A double thermocouple probe fed through a NPT port in the bottom flange. One thermocouple sat in the flame front. The other was positioned approximately 2.5 cm above the flame. They were used to monitor flame extinction. The third thermocouple fed through a port in a top side flange. This thermocouple probe extended through an opening in the liner to the post flame gas flow. It was used to monitor bulk temperature of the post flame gases. It was assumed that temperature of the post flame gases was relatively isothermal as it passed through the upper section of the liner at steady state. Experimental testing showed this to be a valid assumption. Both thermocouple feed through probes were made by Nanmac Corp. Temperature of the post flame gases was controlled by the amount of air allowed to bypass the burner.

Flow into the facility was metered with various Matheson rotameters. The rotameters were calibrated using dry gas meters or bubble meters depending on tube size. Working pressure for the rotameters was 1.38 MPa gauge (200 psig). All calibrations were completed at this pressure. Calibration curves used in this study are contained in Appendix E. Figure 3.2 contains a schematic of the flow system. Methane was the burner fuel as well as the injected hydrocarbon. Methane was selected as a fuel because it is the major constituent of natural gas - a common industrial gas turbine fuel. Methane was mixed upstream of the burner with both air and a NO/N₂ mixture. A mixture of 0.99% NO in a balance of nitrogen was used to seed the flame. Bypass air entered the pressure vessel at the bottom flange. This bypass air was used to control bulk flow temperature of post flame gases. It also provided cooling for plumbing located under the burner. Cooling nitrogen flowed between the liner and pressure vessel walls. The nitrogen was also plumbed in such a manner as to allow it to flow through the injector.

Before initiating and after terminating CH_4 injection, the injector was purged with nitrogen.

All NO_x concentrations were determined using a Thermo Environmental Corporation Model 10 chemiluminescent analyzer (CLA). As past research has shown, probe conditions are extremely important in avoiding the formation of NO_2 in the probe. Sampling at low pressures in an uncooled probe minimizes probe formed NO_2 . Figure 3.7 shows a drawing of the quartz probe used in these experiments. It is of simple design. It was constructed from 6.350 mm and 3.175 mm quartz tubing. The orifice is approximately 0.178 mm in diameter. The flow chokes through this orifice and the pressure drops from the working pressure to a fraction of an atmosphere. Probe sampling pressures varied from 49 to 117 torr. In order to sample at such low pressures, the CLA had to be modified. It was modified in a manner very similar to the modifications made by Mark Kimball-Linne in his NH_4/NO reaction kinetics research [23]. A schematic of the original configuration of the CLA and its modified configuration are shown in Figure 3.8 [24].

In its original configuration, a sample is drawn through the system by a single vacuum pump. The sample flow chokes through a 20 mil capillary tube. Much of the flow then bypasses the reaction chamber. A small portion is drawn off through a 5 mil capillary tube and flows on to the reaction chamber. The pressure drop through the capillary tubes results in a reaction chamber pressure less than 25 torr. In the reaction chamber, the sample mixes with ozone. The ozone reacts with nitric oxide to form nitrogen dioxide. During the reaction process a photon of light is emitted as excited NO_2 returns to its ground state (chemiluminescent effect). These photons are detected by a photo multiplier tube (PMT). The PMT outputs a voltage directly proportional to the

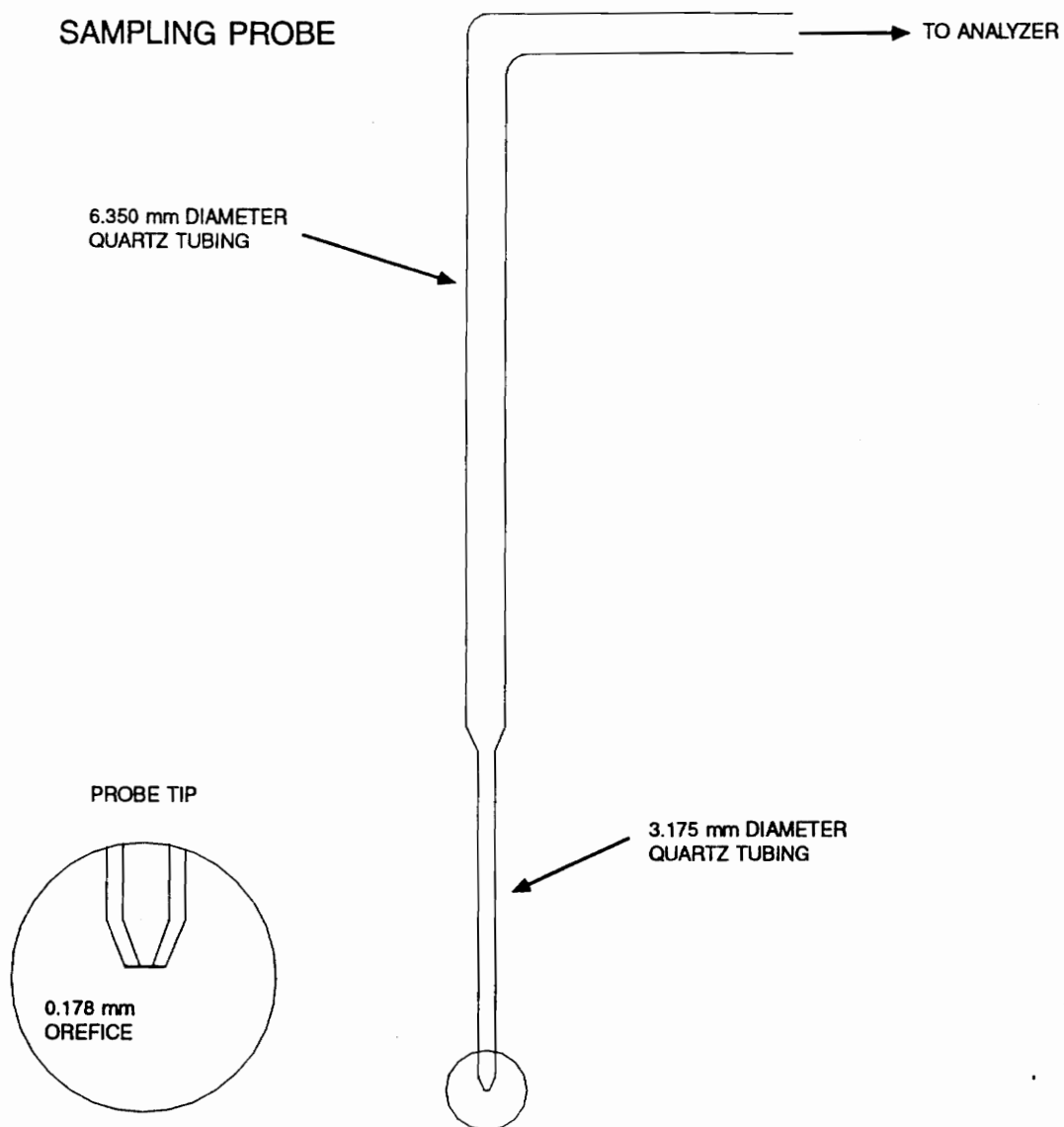


Figure 3.7. Sampling probe schematic.

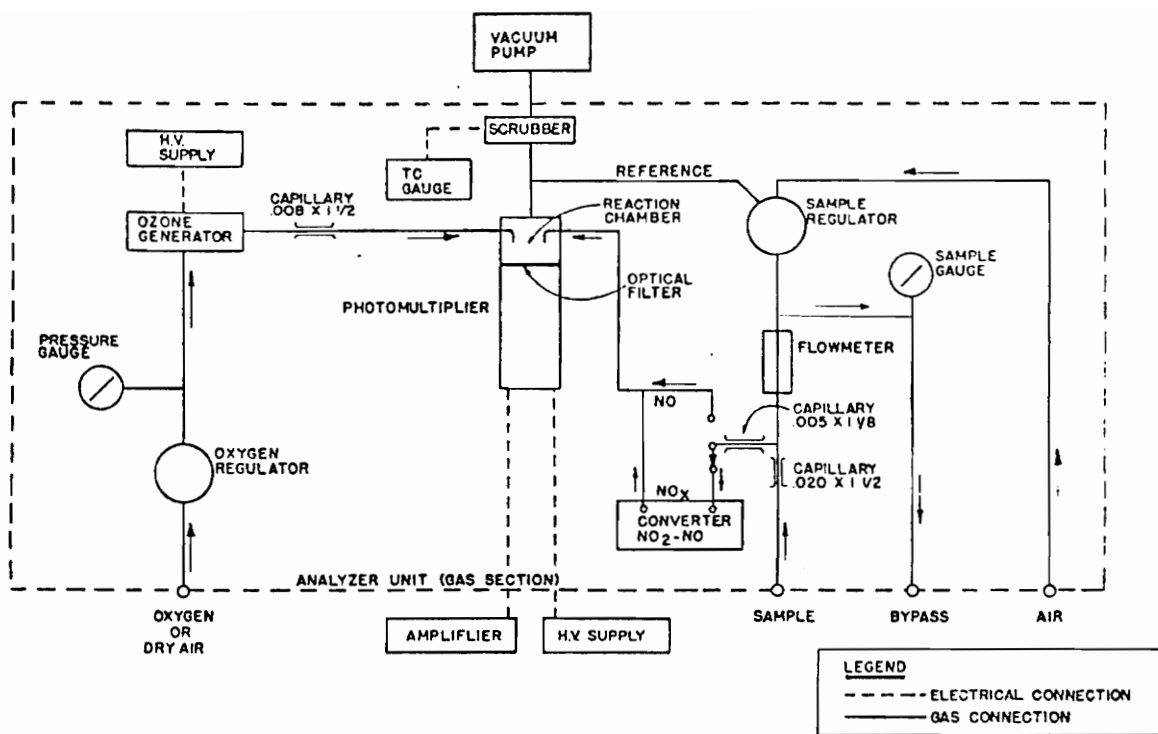


Figure 3.8(a). Thermo Environmental Chemiluminescent NO_x Analyzer (Original configuration) [24].

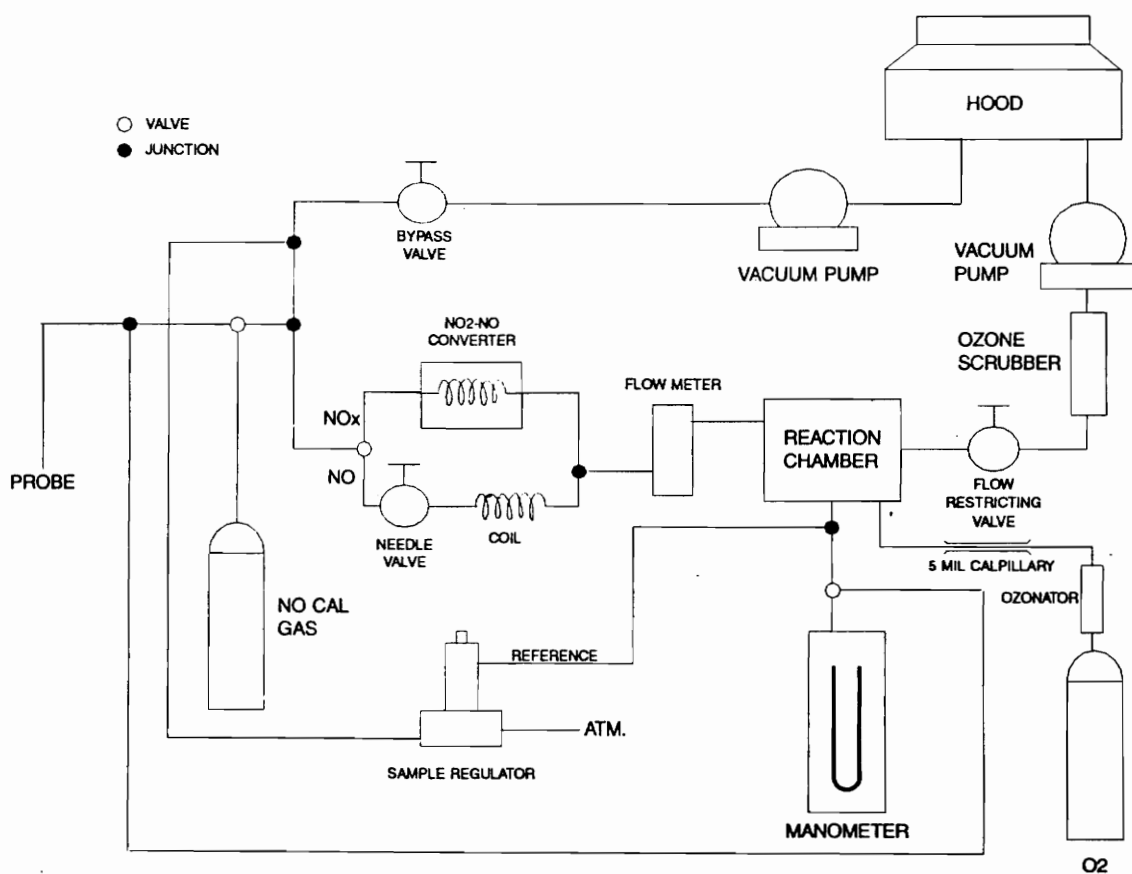


Figure 3.8(b). Thermo Environmental Chemiluminescent NO_x Analyzer (Modified configuration for low pressure sampling).

concentration of NO. If total NO_x is to be measured, the flow is diverted through a NO_2 to NO converter unit. The converter is composed of a coiled length of tubing heated to a temperature of 616 K. As the flow passes through the converter, the stainless steel acts as a catalyst in converting NO_2 to NO. The flow then passes into the reaction chamber and NO reacts with O_3 producing NO_2 and a photon which is detected by the PMT. The result is a measure of total NO_x .

In this study, it was desired that the sampling pressure be reduced significantly in order to minimize probe formed NO_2 . In order to sample at low pressures, it was necessary to make the following modifications to the original configuration of the CLA.

- The 20 mil capillary tube was essentially replaced by the probe orifice. This allowed the entire system to be kept at low pressure.
- The sample pressure regulator was replaced by a vacuum pump with a regulating valve to control the amount of flow bypassed.
- A regulating valve was installed downstream of the reaction chamber. This valve was closed down to a small orifice in order to restrict the flow.
- A manometer was plumbed into the reaction chamber at what was the reference tap. Using a three way valve, the manometer was also plumbed into the sample line before the point at which the bypass flow was diverted from the sample flow. This allowed monitoring of pressure inside the probe.
- The bypass rotameter was connected in series with the reaction chamber in order to monitor flow rate into the reaction chamber.

- The 8 mil ozone capillary was replaced by a 5 mil capillary in order to reduce the flow of ozone into the reaction chamber.

The above modifications are in essence those used by Kimball-Linne in his study. He, however, only measured NO. Passing the flow through the NO₂-NO converter with his configuration resulted in a highly unsteady flow into the reaction chamber at a different pressure than the NO sampling pathway. This made it impossible to calibrate the machine to measure both NO and NO_x. Further modifications were made which reduced flow oscillations and matched flow conditions in both the NO and NO_x sampling pathways. The sample pressure regulator was plumbed into the bypass line upstream from the bypass valve (Fig. 3.8(b)). The reference tap for the regulator was then plumbed into the manometer line from the reaction chamber. This allowed pressure in the reaction chamber and probe lines to be "finely tuned". It also reduced some of the unsteadiness seen in the NO_x sampling pathway.

It appeared that there was a pressure drop through the NO₂-NO converter that was not present in the NO pathway. The coil from an old converter unit was therefore plumbed into the NO pathway in an attempt to physically match flow conditions. This worked when the converter unit was cool; however, when the unit was at working temperatures, there was an increase in pressure drop. Therefore, a valve was installed upstream from the NO coil. This valve was closed down to the point at which flow conditions between the two pathways were equivalent. This was judged by the flow rate measured by the rotameter placed upstream from the reaction chamber. Although matching the pressure drop across the pathways could have been achieved with the valve alone, the NO pathway coil was left in the system because it tended to reduce flow unsteadiness.

Before calibrating the analyzer, the NO_2 -NO converter was allowed to warm up, and the system was allowed to out-gas. NO and NO_x sampling pathway flows were then matched by adjusting the valve in the NO sampling pathway. The sample regulator and various regulating valves were adjusted to the point at which probe and reaction chamber pressures were minimized without resulting in flow unsteadiness. It is possible that flow oscillations were caused by the vacuum pumps. If this is the case, surge tanks plumbed in just upstream of the pumps could prove beneficial.

After adjusting the analyzer to the "edge of unsteadiness" as described above, the CLA was calibrated as per instructions in its manual. Room air was used as a zero gas. The calibration gas used was 240 ppm NO in a balance of nitrogen.

NO_2 concentrations were determined by recording NO and NO_x concentrations at a point and then calculating the NO_2 present. NO and NO_x levels were recorded using a strip chart recorder. No corrections for quenching effectiveness were made for other gases besides nitrogen in the NO_x samples.

3.2 FLOW REACTOR FACILITY OPERATION

The following procedure was followed in igniting a flame in the high pressure flow reactor. A side flange was left open during the ignition procedure for safety purposes.

- The cooling water to the burner was turned on.

- All electrical instrumentation was disconnected from the vessel. This was to prevent unintentionally grounding the tesla coil through a voltmeter or the pressure transmitter.
- The facility was purged using nitrogen and bypass air flows.
- The tesla coil was activated resulting in an arc being thrown to the burner head.
- The fuel valve was opened followed several seconds later by the air valve.
- The tesla coil was shut off.
- The presence of a flame was ascertained by noting thermocouple output and by feeling warm gases escaping through the open side port.

After a flame had been ignited, the vessel was sealed at the side port. The vessel was then pressurized, if so desired, by slowly closing the exhaust regulating valve. The system was allowed to come to a steady state as noted by a pressure reading and the temperature of the post flame gases.

In case of flame extinction during operation (as noted by flame thermocouple readings), the fuel supply valve was immediately closed by the operator. The vessel was then depressurized, and the above procedure was followed in re-igniting the flame.

3.3 EXPERIMENTAL PROCEDURE

From the results of computer modeling and past research, it was seen that several variables are very important in the formation of NO_2 . It was decided that experimental

work should focus on these variables and their effect on the rate and extent of NO conversion to NO₂. Those variables examined experimentally were temperature, pressure, and the presence of unburned hydrocarbons. Twenty six sets of data were collected using the high pressure flow reactor. These runs encompassed data taken at temperatures in the following ranges: below 800 K, 800 K - 1000 K, 1000 K - 1200 K, and above 1200 K. Pressure was varied between atmospheric and 9.85 atmospheres. Data sets were taken both with and without methane and nitric oxide injection. Table 1 gives a summary of the experimental runs. Those runs which appear to be at the same conditions are at different flow rates. All flames were run fuel lean at or around an equivalence ratio of 0.75.

For a typical experimental run, the burner was ignited as described in the previous section. After sealing the pressure vessel, the flow rates of the various lines into the facility were adjusted to yield the desired conditions. If it was to be a pressurized run, the exhaust valve was closed down to the point at which the desired pressure was obtained. Increasing pressure in the vessel resulted in increased probe pressure and increased flow into the reaction chamber of the CLA. Since the analyzer was calibrated at atmospheric conditions, increased pressure changed the calibration. In order to compensate for this, the flow conditions into the CLA were noted during data acquisition. Since the analyzer calibration is a straight line calibration, this information was easily used to adjust the atmospheric calibration curve to yield true concentrations. This was achieved by increasing delivery flow of the calibration gas into the analyzer until flow into the reaction chamber was equal to the flow at running pressure. The NO reading at this point was noted, and a calibration correction factor was calculated.

Table 1. Experimental Run Conditions

Run	Pressure (atm)	Temp (K)	[CH₄]_{inj} (ppm)	[NO]_{inj} (ppm)
1	1.20	885	0	196
2	1.20	891	2117	195
3	1.20	891	1097	194
4	1.19	1139	1188	197
5	1.20	1272	1293	212
6	1.20	887	1140	0
7	1.31	752	1054	186
8	3.00	867	1044	173
9	4.45	865	1015	159
10	7.20	867	1474	180
11	0.96	862	1671	189
12	1.21	734	1068	165
13	6.81	664	1222	189
14	4.02	857	1772	185
15	5.00	1071	1324	204
16	4.99	772	892	162
17	1.20	874	2294	238
18	5.01	872	1199	183
19	4.95	867	0	193
20	4.97	862	1313	0
21	4.93	669	868	172
22	9.54	872	891	144
23	8.54	882	836	132
24	5.13	981	902	144
25	1.41	847	719	164
26	1.40	847	1008	165

Data acquisition was begun at the zero point. This point was defined as the point at which the sample probe met the injection bulb. It is analogous to the injection point of the computer model, and species concentrations at this point will be denoted in the same manner as in the computer model (with a subscripted "o"). NO and NO_x measurements were obtained from the center of the flow at 5 mm to 20 mm intervals beginning at the zero point. NO and NO_x measurements from the CLA tended to be somewhat unsteady. The degree of unsteadiness seemed to be affected by the flow conditions in the reactor. Increased unsteadiness in NO and NO_x measurements was noted at points around the injector where increased turbulence would be expected. Real time NO and NO_x profiles, however, became more steady downstream as the flow apparently laminarized. Figure 3.9 shows a tracing of the CLA output as recorded on a strip chart recorder. It shows both a point close to the injector and one greater than 100 mm from the injection point. This figure illustrates the transient nature of the NO and NO_x readings around the injection point. NO and NO_x data points were obtained at each spatial point in the flow by "eyeballing" a time average of the analyzer output.

Reactor flow conditions were also monitored during the time of data acquisition. There was usually some slight change in pressure and bulk flow temperature during the period of data acquisition. Again, a time average was estimated for these properties. If a significant change was seen, it was noted on the run data sheet. Typically, data acquisition began 10 to 15 minutes after flame ignition. This allowed the facility to be sealed and come to quasi-steady state. Data acquisition usually took about 20 minutes. No more than three runs were ever conducted in succession. This was due to a limited supply of gases and the fact that the vessel tended to get extremely hot after more than an hour of operation.

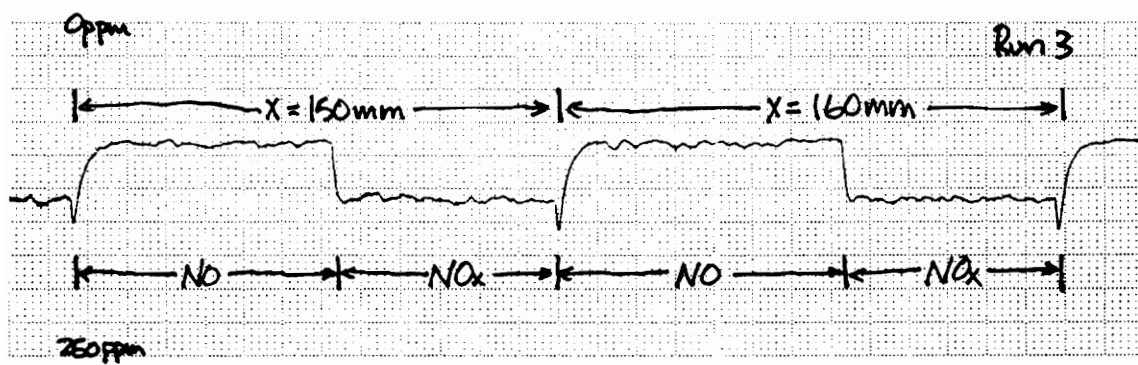
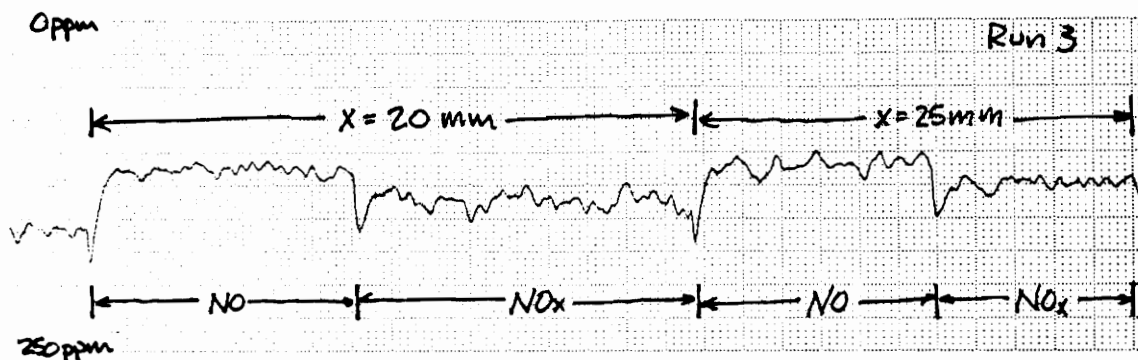


Figure 3.9. Typical real time NO/NO_x output from the CLA.

Experimental data was processed using a FORTRAN program (Appendix F). Thermocouple junctions were kept at room temperature. The thermocouple readings were then corrected for the junction temperature, and temperature was determined from thermocouple tables. The temperature in Kelvin was input to the data processing program. Thermocouple radiation effects were neglected. Other input to the data processing program included atmospheric conditions, flow into the facility, vessel pressure, post flame gas density, and measurements of NO and NO_x. The program output mass flow rates into the facility, mass flow through the burner and liner, post flame gas velocity, [CH₄]_{inj} and [NO]_{inj}, and NO, NO₂, and NO_x profiles. (The methane injection point is slightly different than the zero point of data acquisition. However, it was assumed that [CH₄]_o was equal to the concentration of CH₄ at the injection point. Therefore, [CH₄]_o = [CH₄]_{inj}.)

A number of assumptions were made in processing the experimental data. Flow past the injection point to the end of the sampling range was assumed to be plug flow. This was probably a reasonable assumption considering that the flow was developing over the sample range from the injector. In conjunction with a gas density assumption, the plug flow assumption allowed gas velocity to be calculated simply. It was assumed that gas density of the post flame flow was equal to the density of the flow at equilibrium conditions. Post flame gas density was then determined by running a STANJAN [25] equilibrium calculation at the experimental pressure and temperature. Temperature of the post flame gases was assumed to be at a constant bulk temperature past the point of injection as noted by the bulk flow thermocouple. As mentioned in a previous section, before the liner slots were sealed, a significant temperature gradient was noted in the direction of the flow. By sealing the slots, entrainment of the cooling N₂ flow was eliminated. Consequently, the large temperature gradient was also eliminated. Any

entrainment through the small opening occupied by the thermocouple probe was neglected. Through experimental observation and varying the placement of the probe, it was determined that the bulk flow temperature assumption was reasonable after the slots had been sealed. Temperature appeared to be relatively constant both along and across the flow.

A final assumption was that the system was at steady state throughout data acquisition. By observing the vessel pressure and temperature, this was seen to be untrue for some runs. However, the variations in conditions were not significant and shall be taken into account in an uncertainty analysis (App. G). Although quite a few assumptions were made, they are suitable for the goals of this study. They still allow general trends to be seen.

CHAPTER 4 - EXPERIMENTAL RESULTS

The results of the experimental portion of this study will be presented in this chapter. The effects of temperature, pressure, and unburned hydrocarbons on NO to NO₂ conversion will be examined. All oxides of nitrogen concentration are reported on a volumetric basis, wet.

4.1 NO_x PROFILES

Computer modeling of the C-H-O-N system indicated that total NO_x is always conserved in the relatively cool post flame gases. The experimental results, in contrast, do not always indicate a conservation of NO_x. This is especially true at near-atmospheric pressures. In the majority of near-atmospheric cases, there is a maximum value of NO_x at or around the injection point. This then decreases to a minimum 3-5 cm from the injection point. Downstream from this minimum, NO_x is either approximately constant or it increases slightly (Fig. 4.1). This change in NO_x concentration may be a chemical effect or an effect of mixing characteristics of the experimental system. The NO_x profile appears to only be affected by a change in pressure or flow rates. Similar profiles are seen when [NO], [CH₄], and temperature are varied for a given pressure (Fig. 4.2).

At higher pressures, the NO_x profile becomes more constant and more closely resembles the computer modeling predictions. This is illustrated in Figure 4.3 in which NO_x profiles at various pressures are presented. The near-atmospheric profile characteristics noted around the injection point disappear. There is still some variation in

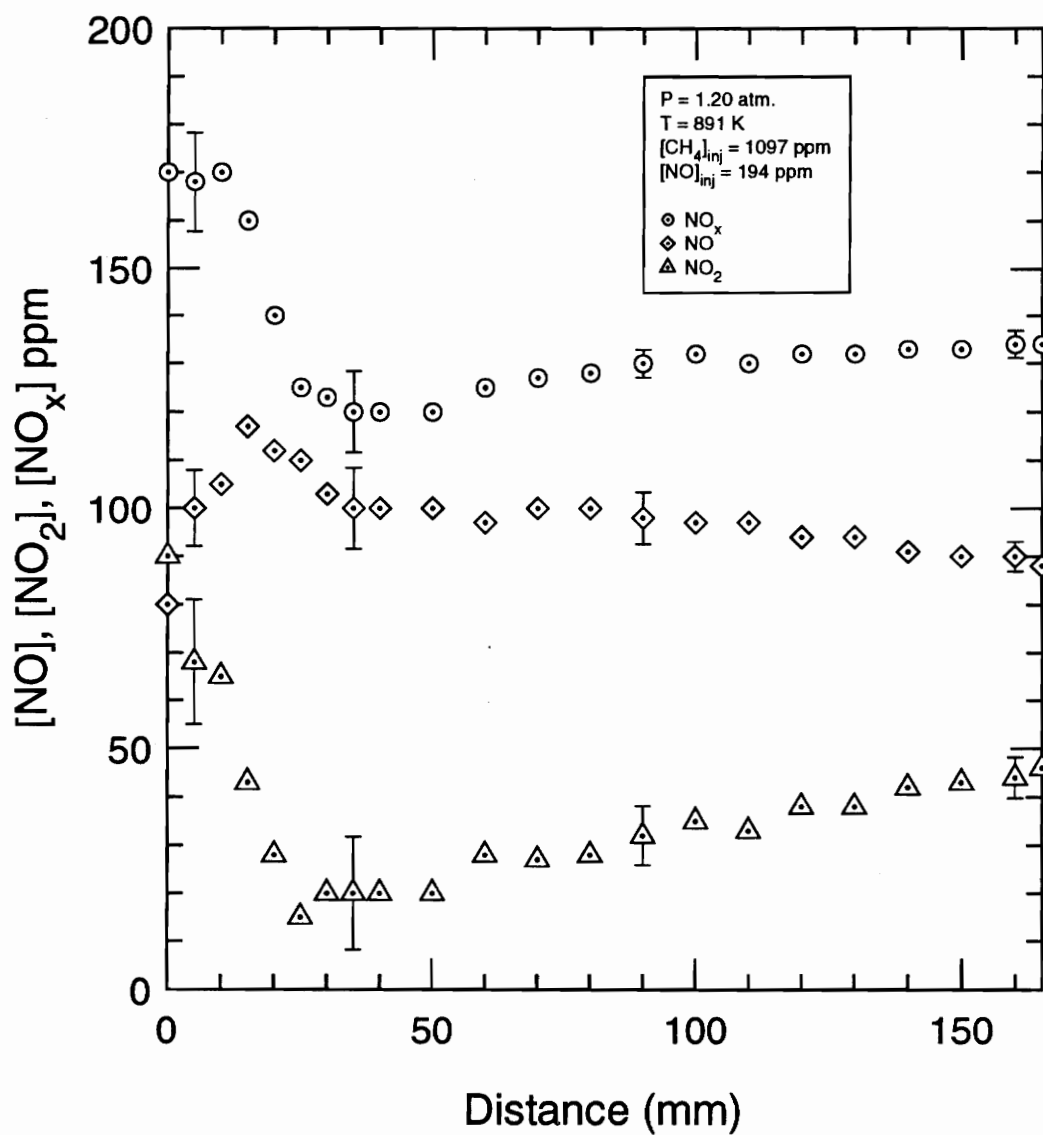


Figure 4.1. Oxides of nitrogen profiles.

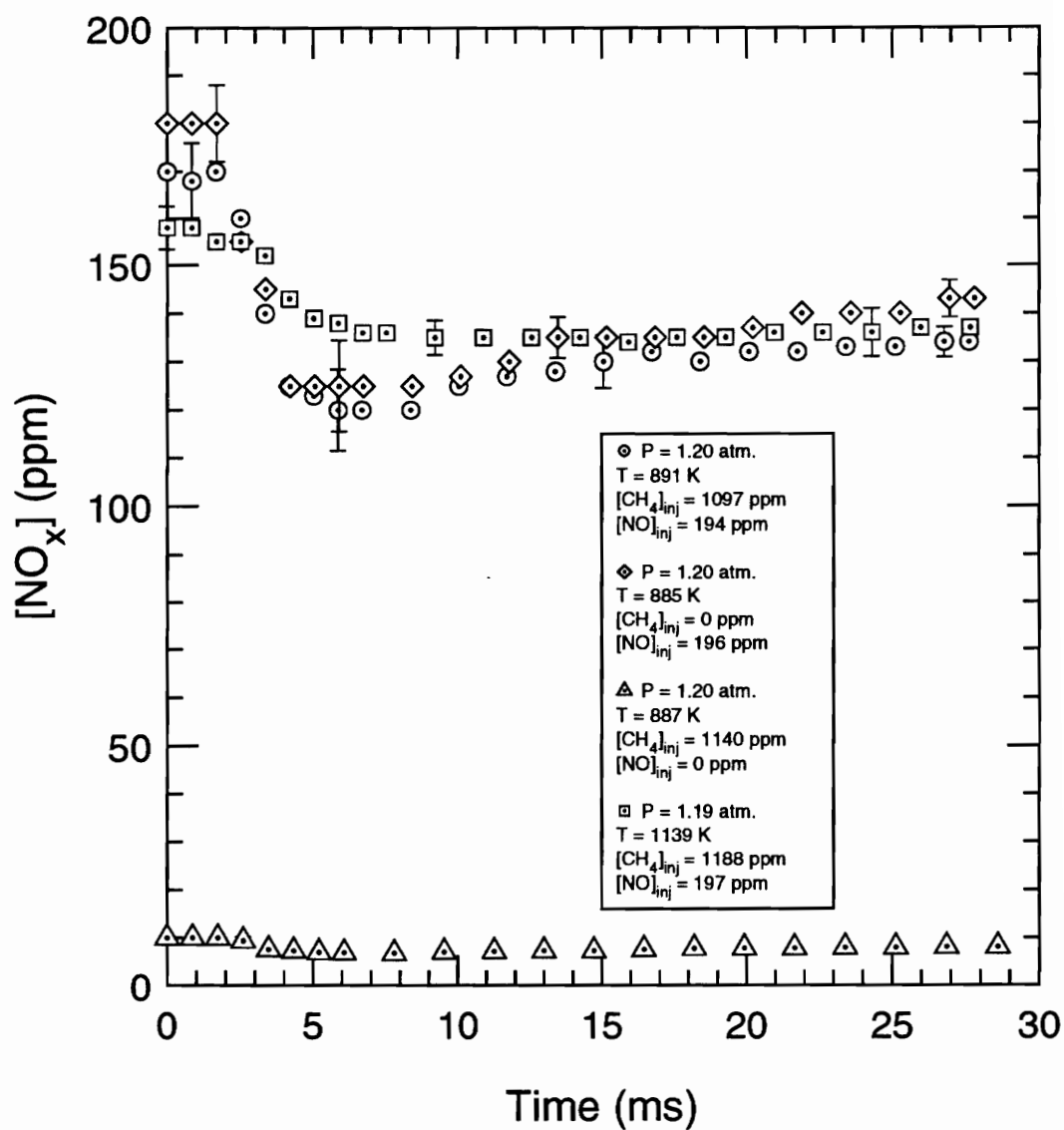


Figure 4.2. NO_x profiles for various conditions.

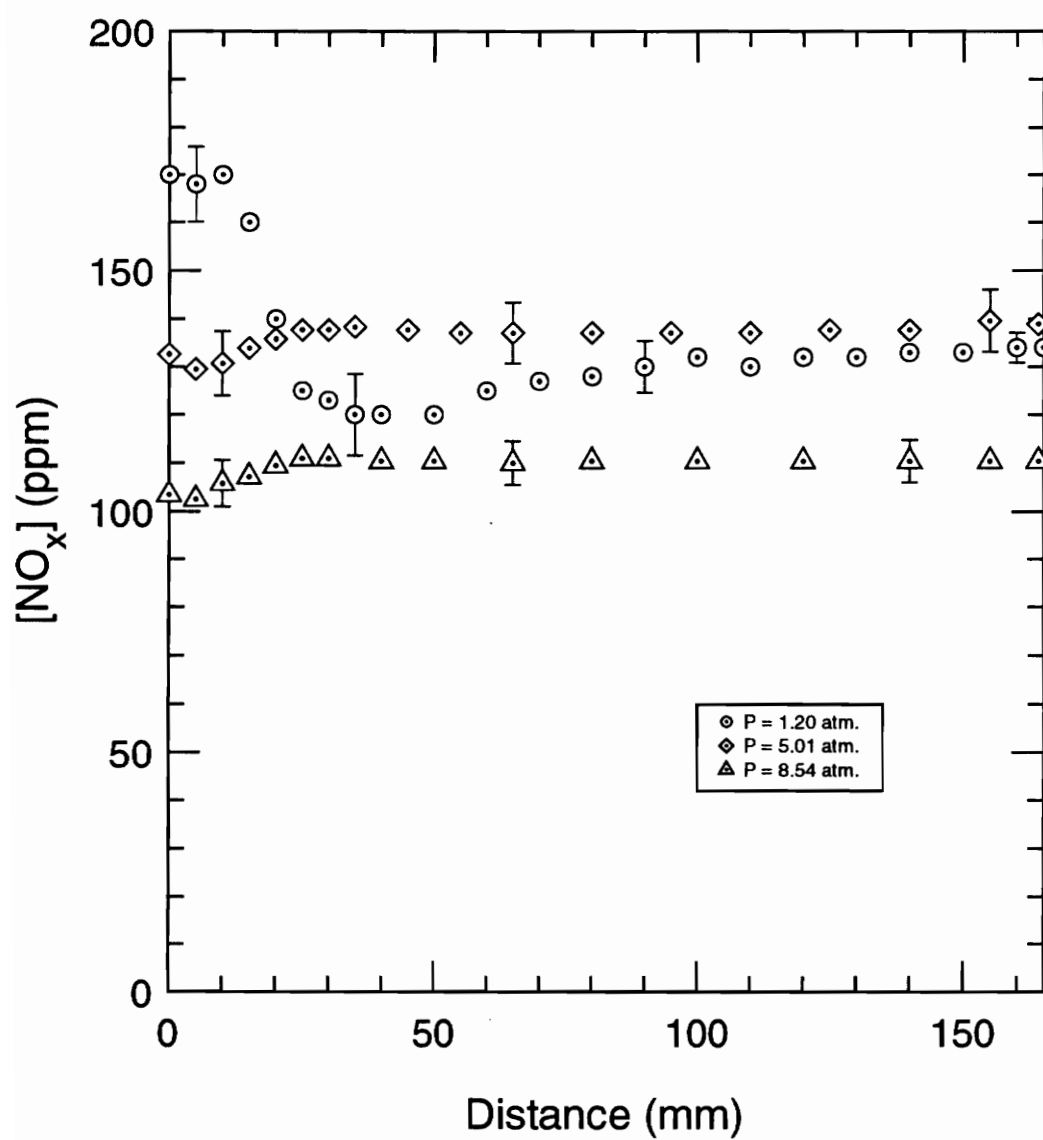


Figure 4.3. NO_x profiles for various pressures.

NO_x concentrations around the injection point, but it is not nearly as great as in the near-atmospheric case. Similar to the near-atmospheric cases, the profiles become more constant around 3 cm. It should be kept in mind, however, that residence time between data points is greater at higher pressures. For some cases, this may have the effect of "smoothing out" some NO_x changes around the injection point.

4.2 TEMPERATURE

Experimental data was collected at temperatures between 664 K and 1272 K. The results show that temperature does indeed have a profound effect on NO_2 formation. There was a definite temperature range in which significant NO_2 production occurred. For a given pressure, peak levels of NO_2 were noted around 1000 K. However, above 1000 K, NO_2 formation diminished as shown in Figure 4.4(a). Figure 4.4 shows NO_2/NO_x profiles at various temperatures for pressures of approximately one and five atmospheres. It should also be noted that as temperature decreases below 1000 K, NO_2 formation is seen to fall off. Slight differences in pressure were neglected in comparing results. Although more NO is converted to NO_2 at higher pressure, it can be seen that there is a similar temperature range which is conducive to the conversion process. This temperature "window" becomes more apparent when NO_2/NO_x is plotted as a function of temperature at a given residence time (Fig. 4.5).

4.3 PRESSURE

The majority of experimental data was taken at near-atmospheric conditions and at five atmospheres. All near-atmospheric data was taken at pressures between 0.94 and

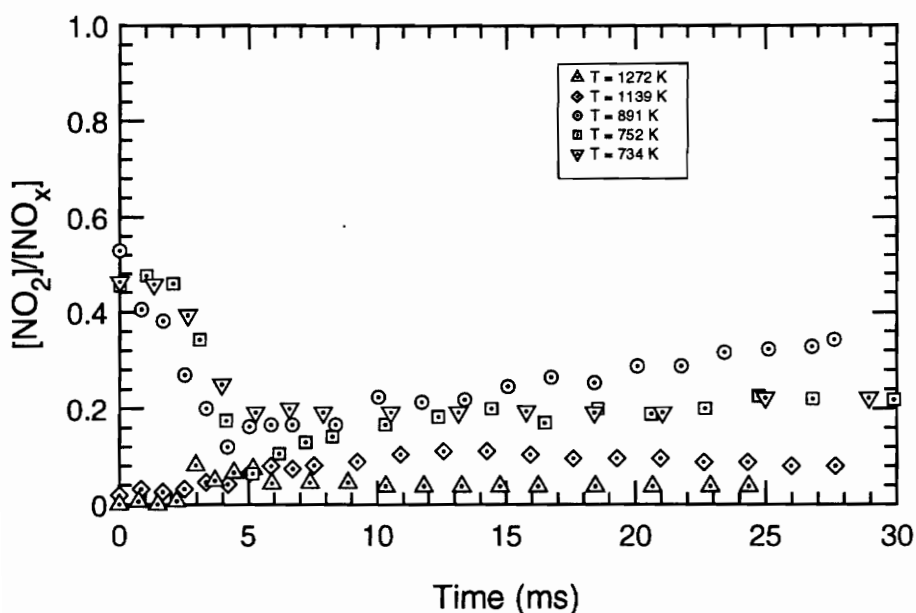


Figure 4.4(a). The effect of temperature on NO_2 formation.
 $P \approx 1.2 \text{ atm.}$, $[\text{CH}_4]_{\text{inj}} \approx 1000 \text{ ppm}$, $[\text{NO}]_{\text{inj}} = 165\text{-}212 \text{ ppm}$

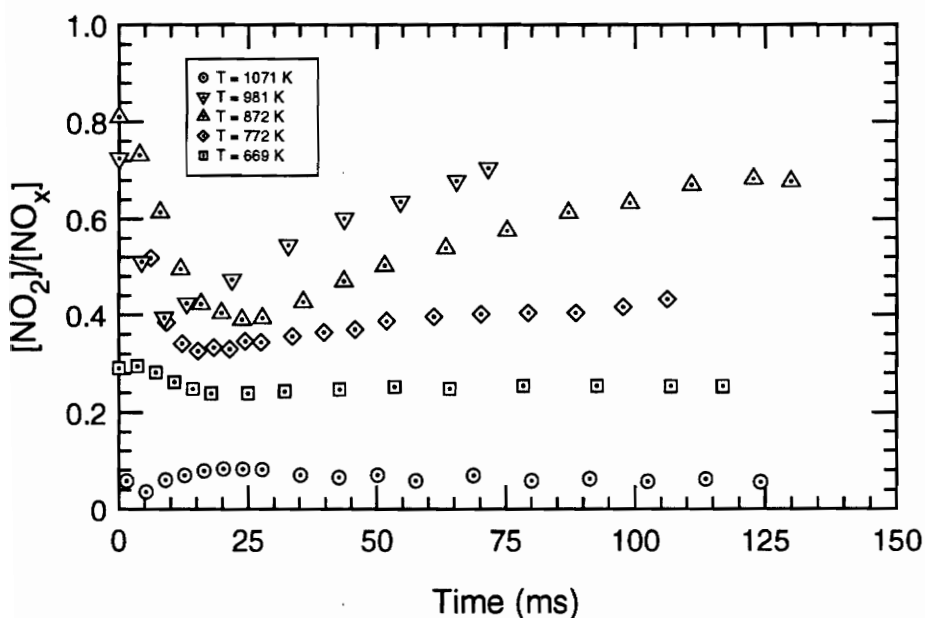


Figure 4.4(b). The effect of temperature on NO_2 formation.
 $P \approx 5 \text{ atm.}$, $[\text{CH}_4]_{\text{inj}} \approx 1000 \text{ ppm}$, $[\text{NO}]_{\text{inj}} = 144\text{-}204 \text{ ppm}$

Figure 4.4. The effect of temperature on NO_2 formation.

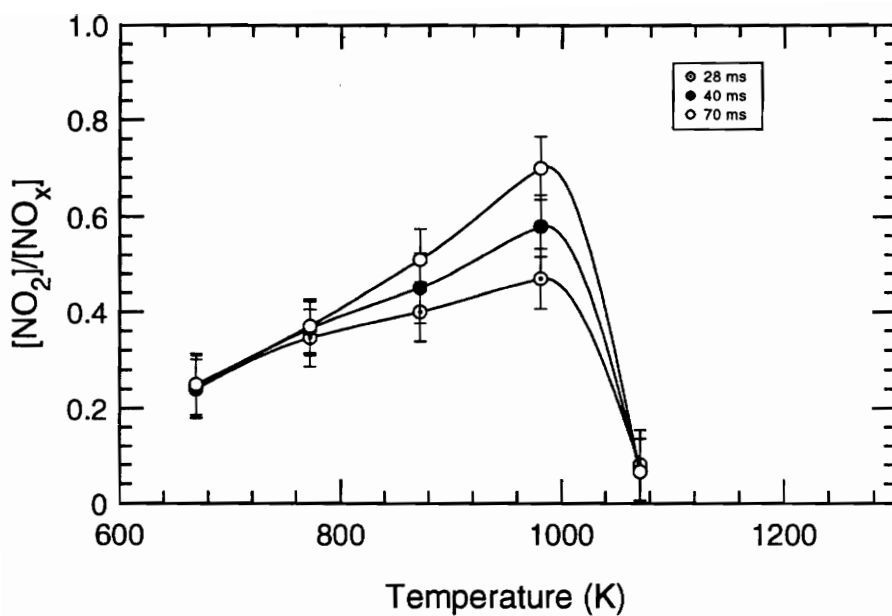


Figure 4.4(a). Temperature profiles for data at $P \approx 1.2$ atm. and $[\text{CH}_4]_{\text{inj}} \approx 1000$ ppm.

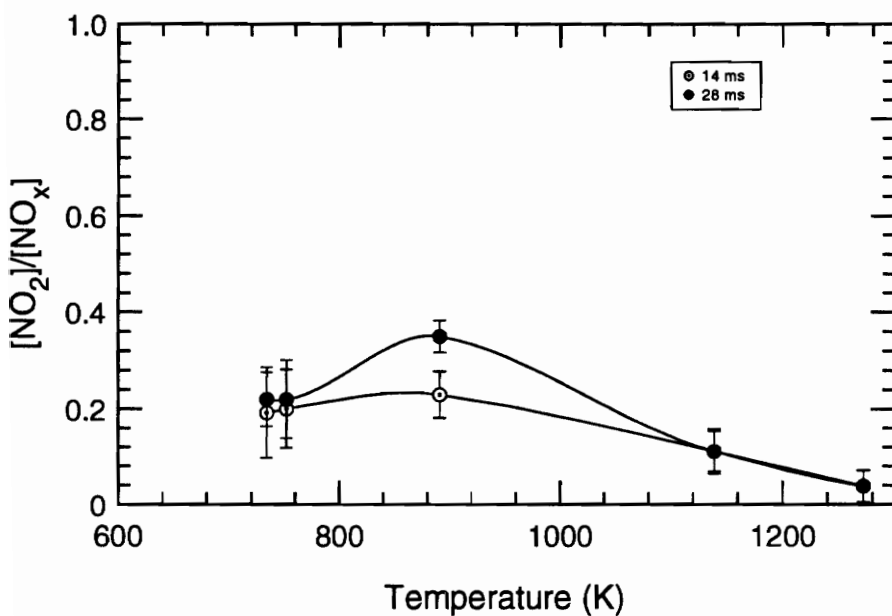


Figure 4.4(b). Temperature profiles for data at $P \approx 5.0$ atm. and $[\text{CH}_4]_{\text{inj}} \approx 1000$ ppm.

Figure 4.5. NO_2/NO_x temperature profiles for experimental results at several residence times.

1.41 atmospheres. Pressure differences in the near-atmospheric tests were neglected. The majority of near-atmospheric runs were at 1.20 atm. The barometric pressure in the laboratory was approximately 0.93 atm. for all experimental runs. Twelve runs were conducted at near-atmospheric conditions, seven runs at five atmospheres, and the remainder at various other pressures.

The highest pressure run was conducted at 9.54 atm. The data from this run, however, will not be considered because the high pressure exceeded the critical pressure for choking through the rotameters. The resulting back pressure affected flow into the facility. Therefore, flow conditions into the facility were unknown, and values such as $[\text{CH}_4]_{\text{inj}}$, $[\text{NO}]_{\text{inj}}$, flow velocity, and equivalence ratio could not be determined. The results from the run showed NO_2/NO_x levels much below those anticipated. This was most likely the result of a change in those indeterminate conditions described above, especially $[\text{CH}_4]_{\text{inj}}$.

In general, increasing pressure resulted in increased NO_2/NO_x . Without hydrocarbon injection, NO_2/NO_x profiles are seen to be relatively constant, and there is an increase in NO_2/NO_x as pressure increases (Fig 4.6). Between 1.2 and 5.0 atm., NO_2 formation approximately doubles. Figure 4.7 shows NO_2/NO_x profiles for a variety of pressures in the temperature range 800 K - 1000 K with hydrocarbon injection. The greatest NO- NO_2 conversion occurred at 8.54 atm. In this case, NO_2/NO_x approached 0.90 within the 150 ms residence time. It should be kept in mind that the different residence times for various runs also have different mixing characteristics. The slight temperature differences between runs may also have affected the results considering the mechanism's sensitivity to temperature. This may explain some of the apparent anomalies between the runs.

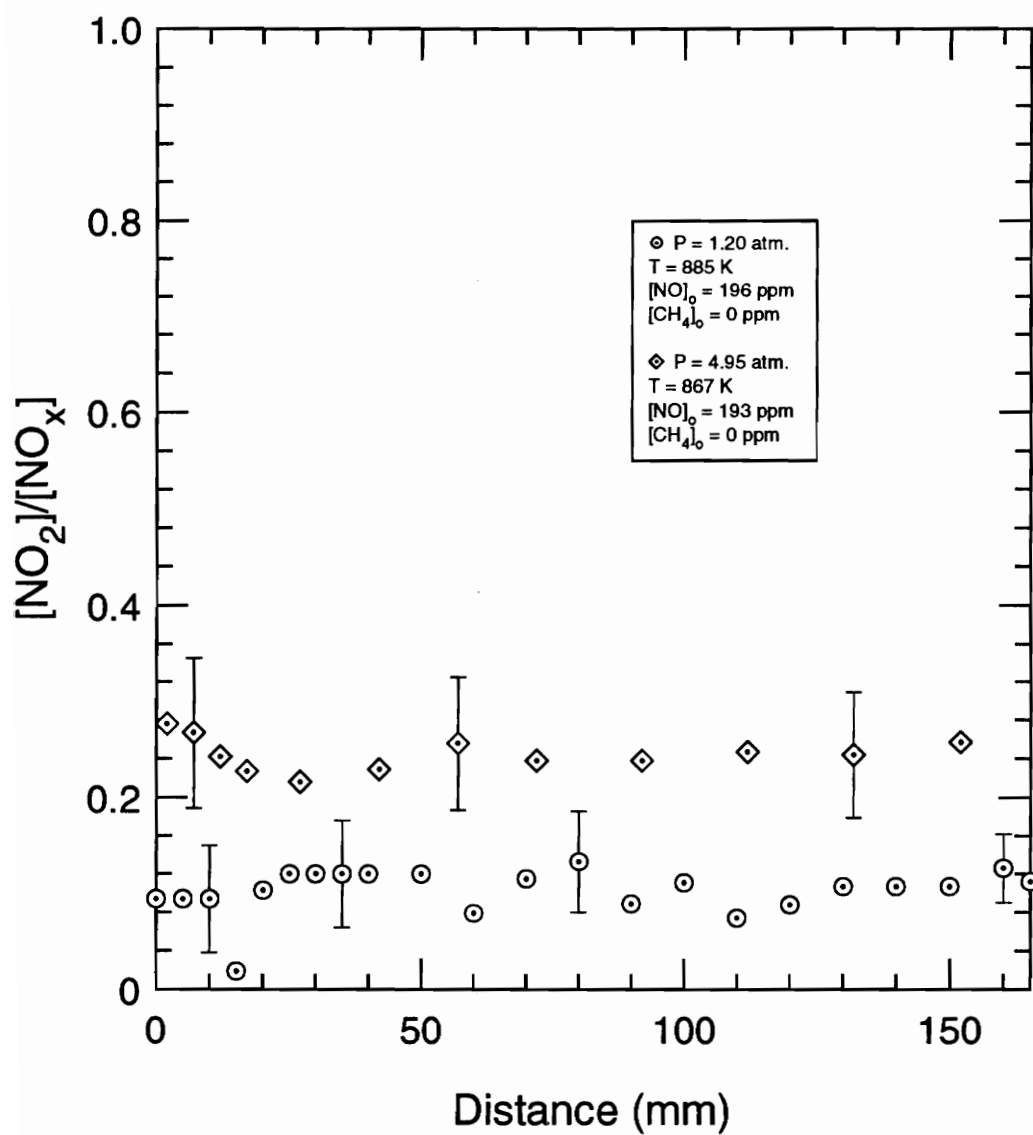


Figure 4.6. The effect of pressure on NO₂/NO_x.
No methane injection cases.

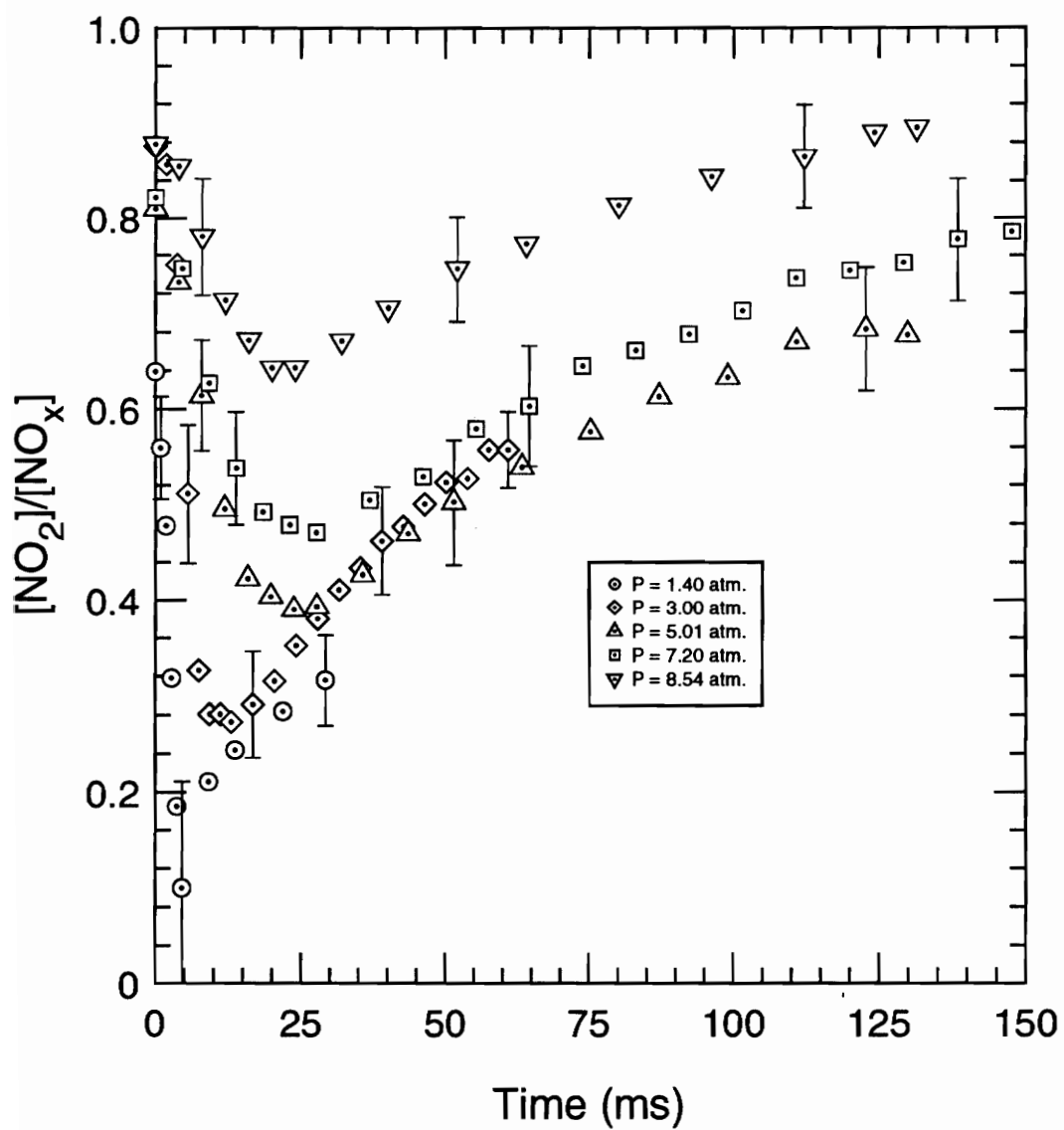


Figure 4.7. The effect of pressure on NO_2 formation.
 $T = 847\text{--}882$ K, $[\text{CH}_4]_{\text{inj}} = 836\text{--}1474$ ppm, $[\text{NO}]_{\text{inj}} = 132\text{--}183$ ppm.

Figure 4.8 shows the direct relationship between pressure and temperature in another temperature range. These two runs are at 4.9 atm. and 6.8 atm. and at temperatures of 669 K and 664 K respectively. Data regarding the effect of pressure in the temperature region above 1000 K is not presented because no two runs at different pressures had similar enough conditions to offer a good basis of comparison.

4.4 UNBURNED HYDROCARBONS

Experimental data supported claims of past research that unburned hydrocarbons have a significant promotional effect on the conversion of NO to NO₂. It was noted in the computer modeling results section, that an important ratio may in fact be [CH₄]₀/[NO]₀. Figure 4.9 shows a comparison of varying levels of [CH₄]₀ and [NO]₀ at near-atmospheric pressure and five atmospheres in the 800 K - 1000 K temperature range. It was difficult to measure [NO]₀ at the injection point because of the mixing characteristics of the system. To offer a more consistent basis of comparison, [NO]₀ will be assumed to be equal to the value of (1-NO₂/NO_x) with no CH₄ at a given pressure multiplied by [NO_x] at the end of the sample range. Similar results are seen at both near-atmospheric pressure and 5 atm. As [CH₄]₀/[NO]₀ increases, NO₂ formation also appears to increase. The increase is very dramatic with relatively small additions of hydrocarbon. However, continuing to increase the amount of injected hydrocarbon with [NO]₀ held constant has little further effect on NO₂ formation.

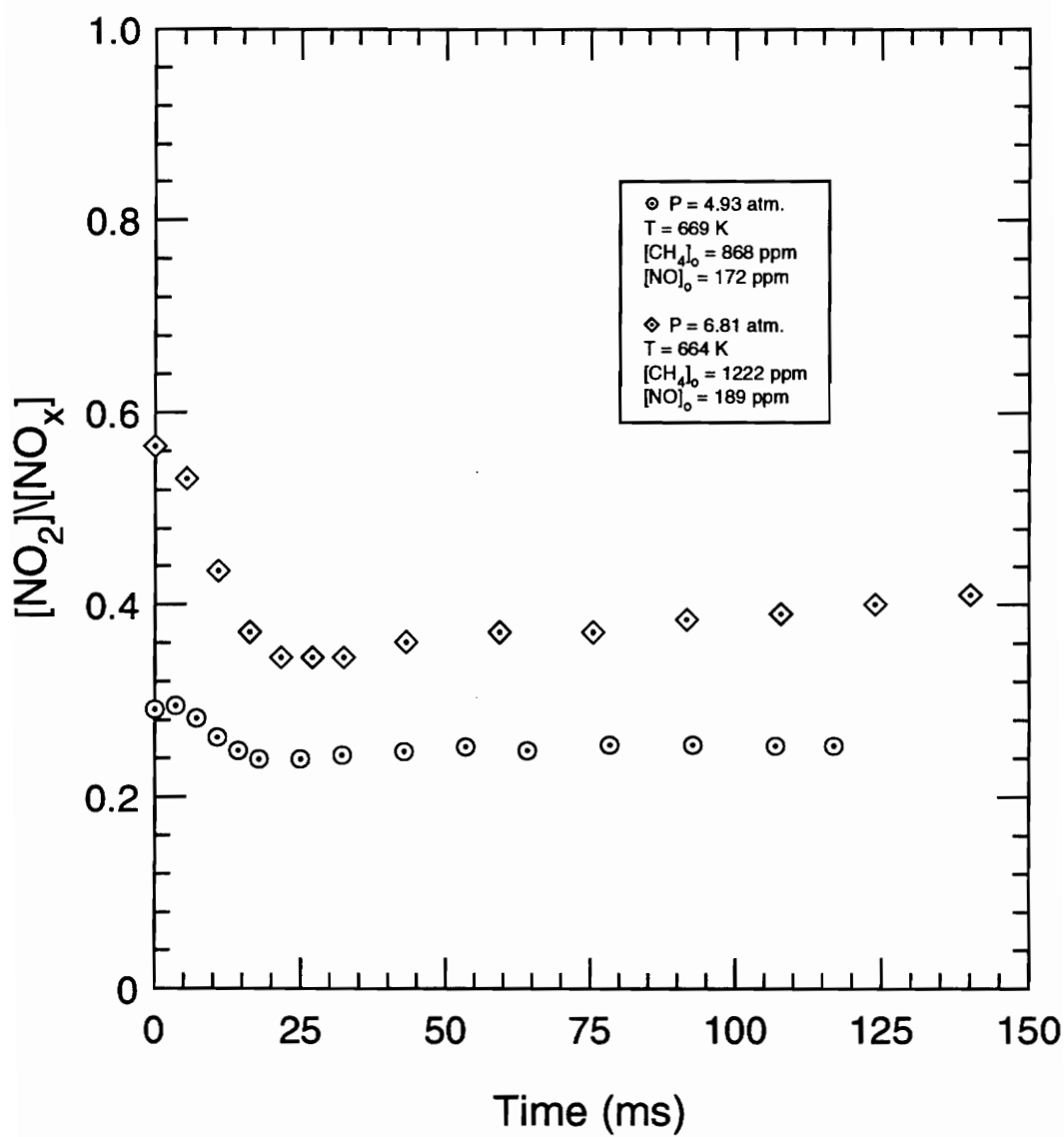


Figure 4.8. The effect of pressure on NO_2 formation.

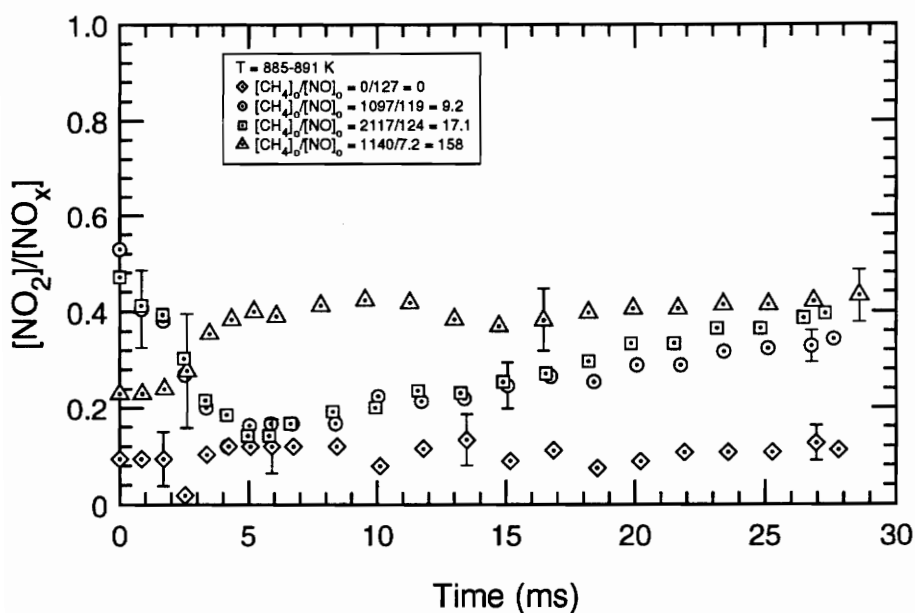


Figure 4.9(a). Hydrocarbon promotion at 1.2 atm.

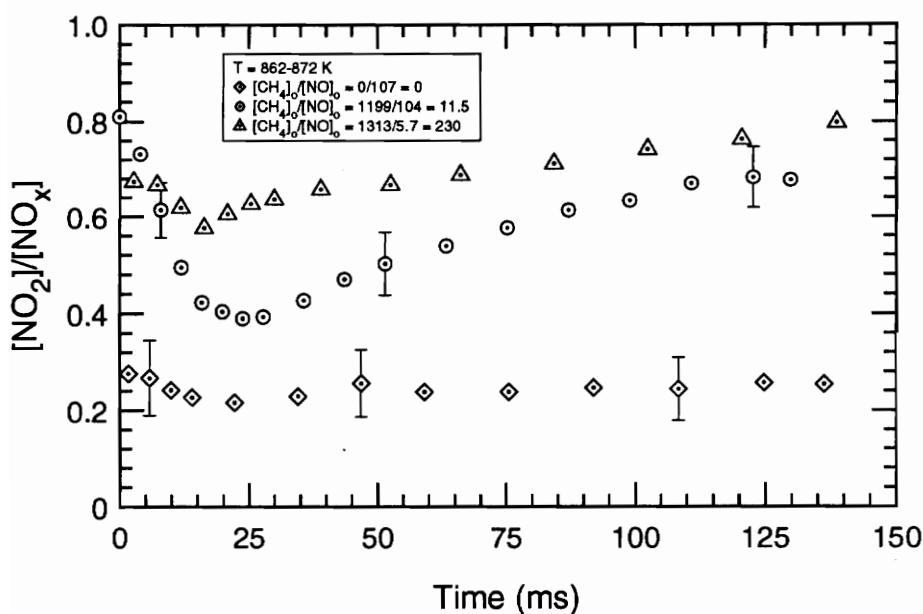


Figure 4.9(b). Hydrocarbon promotion at 5 atm.

Figure 4.9. The effect of hydrocarbon promotion on the conversion of NO to NO_2 .

4.5 FLOW RATE CONSIDERATIONS

Changing flow rates into the facility while holding other variables constant effectively changes the velocity through the liner. This has a significant effect on NO_2/NO_x profiles as can be seen in Figure 4.10. Slower velocity flows tended to have lower NO_2/NO_x levels. This is most likely a result of mixing characteristics. It should, however, be kept in mind in considering these experimental results. At a given pressure, it is probably most valid to compare runs of similar residence times. This effect of flow velocity may not be as significant at higher pressures, as mixing appears to be faster at superatmospheric pressure. The question of mixing characteristics of the facility and the effect on experimental results shall be addressed at length in the discussion chapter of this thesis.

4.6 SUMMARY

Experimental work investigated the three areas that modeling suggested were important in the NO - NO_2 conversion process. A temperature window approximately between 800 and 1000 K was seen to be most conducive to NO_2 formation. Pressure had a direct relation on NO_2/NO_x . As pressure increased, the amount of NO converted to NO_2 also increased. Methane greatly promoted NO_2 formation. For $[\text{CH}_4]_0/[\text{NO}]_0 > 10$, NO conversion to NO_2 was significantly enhanced.

Contrary to modeling results, total NO_x did not appear to be conserved in the post flame zone. It was noted, however, that mixing characteristics of the facility should be considered in evaluating these experimental results.

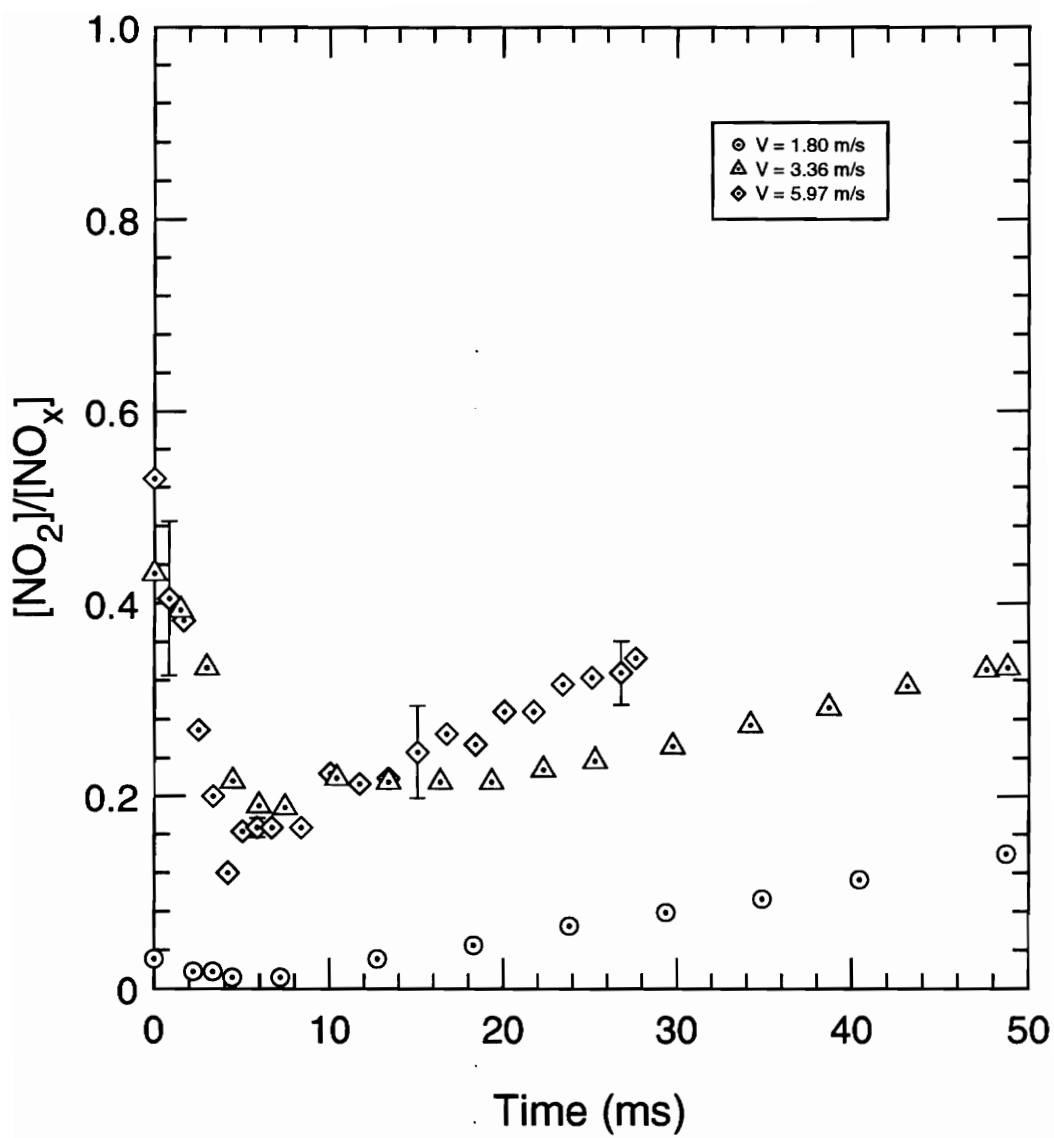
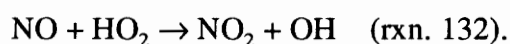


Figure 4.10. The effect of flow rate on NO_2/NO_x profiles.
 $P = .96\text{-}1.2 \text{ atm.}$, $T = 862\text{-}891 \text{ K}$, and $[\text{CH}_4]/[\text{NO}]_0 = \text{O}(10)$

CHAPTER 5 - DISCUSSION

A greater understanding of the mechanism of NO-NO₂ conversion in combustion systems has been achieved since this study was initiated. Evidence has mounted that the major pathway for NO-NO₂ conversion is in fact the HO₂ mechanism:



In their recent study, Marinov *et al.* [11] examined the pathways for the conversion of NO to NO₂ through computer modeling. These pathways included the HO₂ mechanism described by reaction 132 above, the hydrocarbon pathway which Bromly *et al.* proposed,



and several multistep mechanisms. Marinov and his colleagues [11] reported that "...chemical modeling analysis clearly determined that [the HO₂] pathway accounted for practically all of the percent conversion of NO to NO₂."

The kinetics modeling of this study has indicated that NO₂ formation is sensitive not only to reaction 132, but also reaction 114:

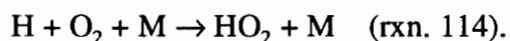


Figure 5.1 illustrates this sensitivity. By decreasing the "A" kinetic parameter for reaction 132, a reduction in the rate at which NO is converted to NO₂ is achieved. The maximum value of NO₂/NO_x is also somewhat reduced. The figure is somewhat deceptive in this regard as the maximum value is not achieved within the limits of the

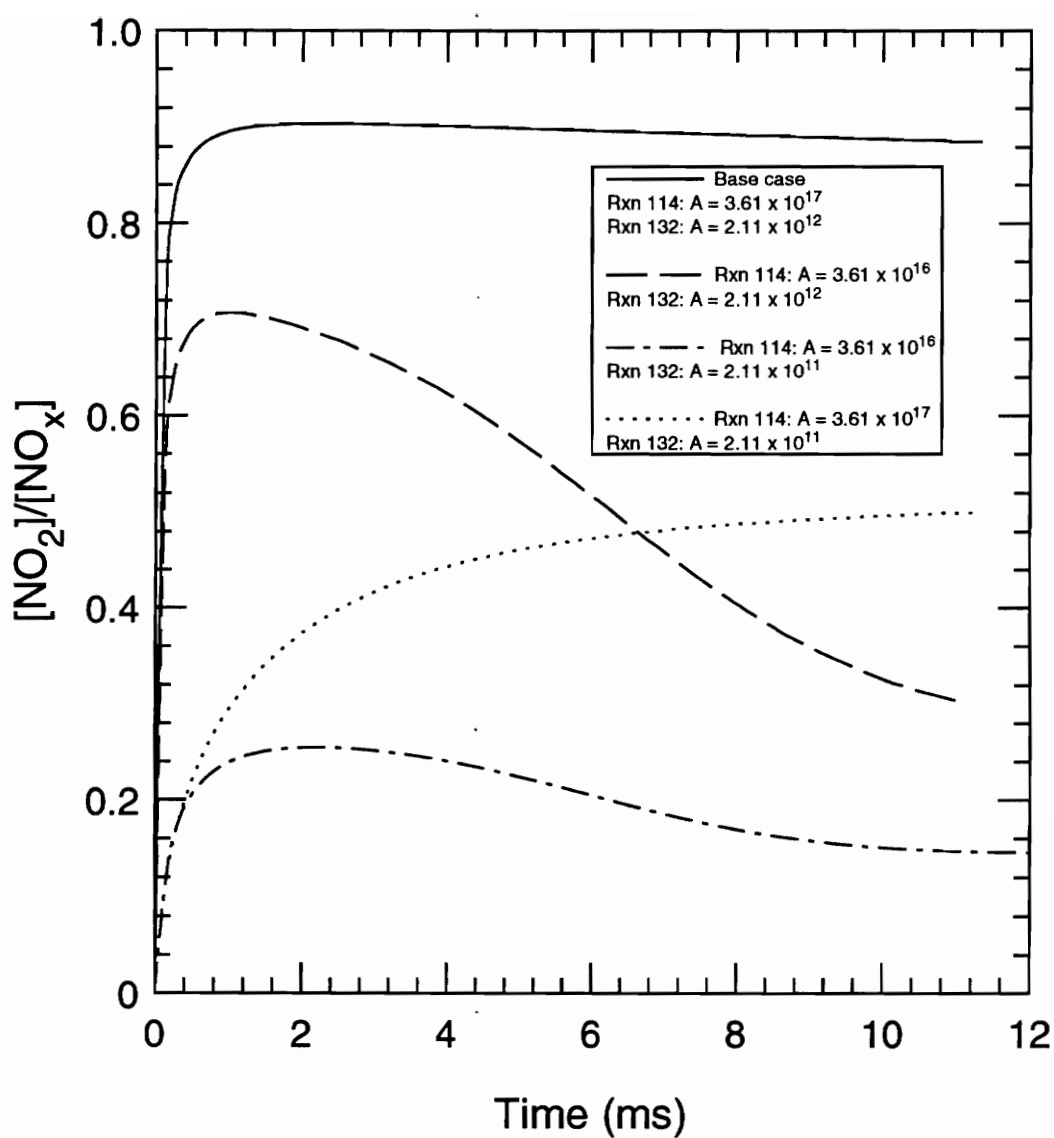
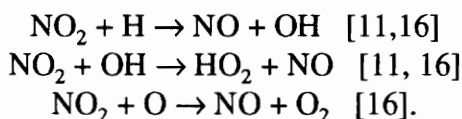


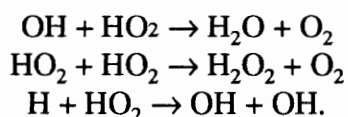
Figure 5.1. The effect of kinetic parameters on predicted conversion of NO to NO_2 . $P = 10 \text{ atm.}$, $T = 1100 \text{ K}$, and $[\text{CH}_4]_0 = 1010 \text{ ppm}$.

graph. A reduction in the "A" parameter for reaction 114 has a greater effect on peak NO_2/NO_x levels and results in less NO conversion to NO_2 . These results offer more evidence that the HO_2 mechanism is the predominant pathway for NO to NO_2 conversion.

The following reactions appear to be the main pathway for NO_2 destruction:



Marinov *et al.* [11] suggest the following reactions may indirectly reduce NO_2 formation by limiting HO_2 radical concentration through the following reactions:



These reactions are sensitive to free radical concentrations, particularly of H, O, and OH. Figure 5.2 shows time profiles of these radicals, HO_2 , and NO_2 for the computer model run at 1100 K and 10 atm. using the Miller & Bowman mechanism. At such a low temperature, it is seen that these radicals are extremely short lived. Their concentrations change significantly within 2 ms then remain at a quasi-steady state. The OH concentration drops several orders of magnitude in this time period as NO_2 forms. Similar plots can be generated for various temperatures to yield similar profiles. They are not shown here. However, the ratio of HO_2/OH at 150 ms, where HO_2 and OH have both reached relatively steady states, is given in Table 2 for various temperature runs. This table shows that significant NO conversion only occurs when $[\text{HO}_2]$ remains greater than $[\text{OH}]$. Marinov *et al.* [11] reported similar results in their computer modeling of a perfectly stirred reactor.

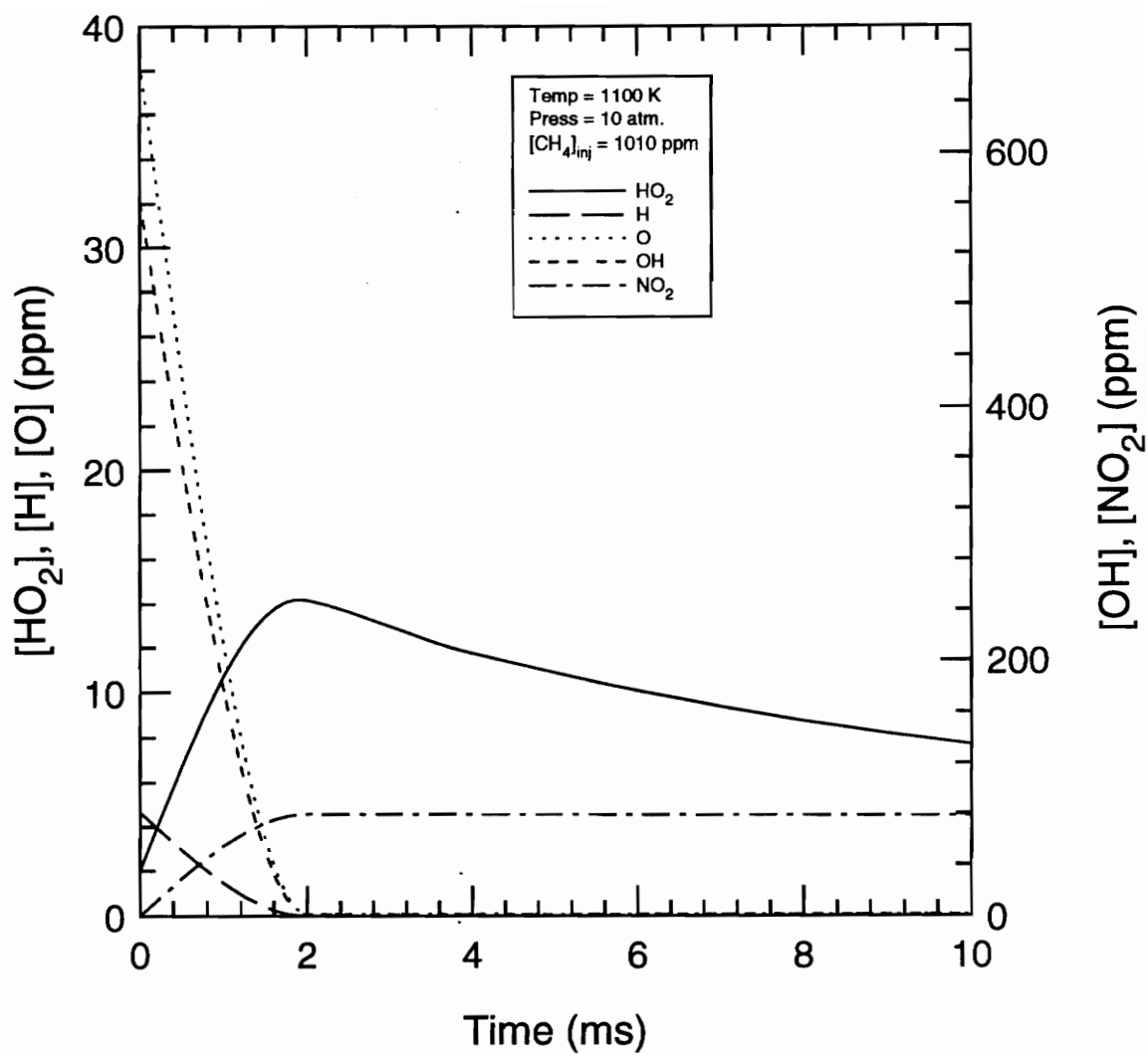
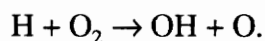


Figure 5.2. Selected species profiles.

Table 2. Comparison of HO_2/OH and NO_2/NO_x at 150 ms as predicted by the computer model.

Temperature (K)	$(\text{HO}_2/\text{OH})_{150 \text{ ms}}$	$(\text{NO}_2/\text{NO}_x)_{150 \text{ ms}}$
700	872	1.000
850	105	0.995
1000	15.5	0.955
1100	2.48	0.772
1300	0.0250	0.026
1600	0.0108	0.008

At higher temperatures, the formation of HO₂ via the 3-body reaction (114) is limited by competition with the reaction,



In the temperature range above approximately 1100 K, this reaction is favored over the HO₂ producing 3-body reaction (rxn. 114). This results in less HO₂ formed and more OH and O formed which in turn attack HO₂ and NO₂. Destruction of NO₂ and HO₂ then becomes significant and NO is favored.

How does this greater understanding of the mechanism of NO-NO₂ conversion apply to the real system -- the gas turbine combustor? In order to better understand the mechanism in a pragmatic manner, it is important to quantify under which conditions there occurs a significant conversion. From the results of the computer modeling and experimental work, there appears to be three major parameters of importance in the conversion process. They are temperature, pressure, and the presence of unburned hydrocarbons (UHC's). Their relative significance and how they apply to the industrial gas turbine shall be discussed in this chapter.

Before evaluating the value of experimental results and comparing them to computer modeling results, several areas affecting the experimental results must be evaluated. These are mixing considerations and probe effects.

5.1 MIXING CONSIDERATIONS

An important question in a practical sense in examination of the formation process of NO₂ from NO is whether the process is mixing or kinetic controlled. The computer

modeling did not take mixing into account. In the model, mixing was instantaneous and complete. Unfortunately, real world systems are never this convenient. Mixing inside the test facility is, therefore, an area worthy of consideration in interpreting the experimental results.

There has been some controversy regarding the relative advantages and disadvantages of turbulent flow reactors vs. laminar flow reactors. The main disadvantage associated with laminar flow reactors is slow mixing. Turbulent flow reactors are more ideal for rapid mixing. The local fluctuations in temperature and concentrations of species, however, have an ultimate effect on the kinetics of the turbulent flow system. Gouldin [26] examined the turbulent flow reactor and attempted to quantify chemical kinetics and mixing associated with turbulent flow combustors. Although in the high pressure flow reactor of this study there was some turbulence at the mixing point around the injector, Gouldin's results do not apply to this system because the flow quickly laminarizes past the injection point. The experimental facility of this study was in essence a laminar flow reactor that was designed to optimize mixing as described in section 3.1.2. Unfortunately, the liner was not constructed to specifications and, therefore, had a slightly larger inside diameter than intended. This had two effects. It slowed the velocity of the flow through that portion of the liner and resulted in poorer mixing due to a larger throat between injector bulb and liner.

5.1.1 Mixing and NO_x Profiles

If one examines NO_x as a function of residence time at a given pressure, similar profiles become apparent (Fig. 5.3) For NO_x at near-atmospheric conditions,

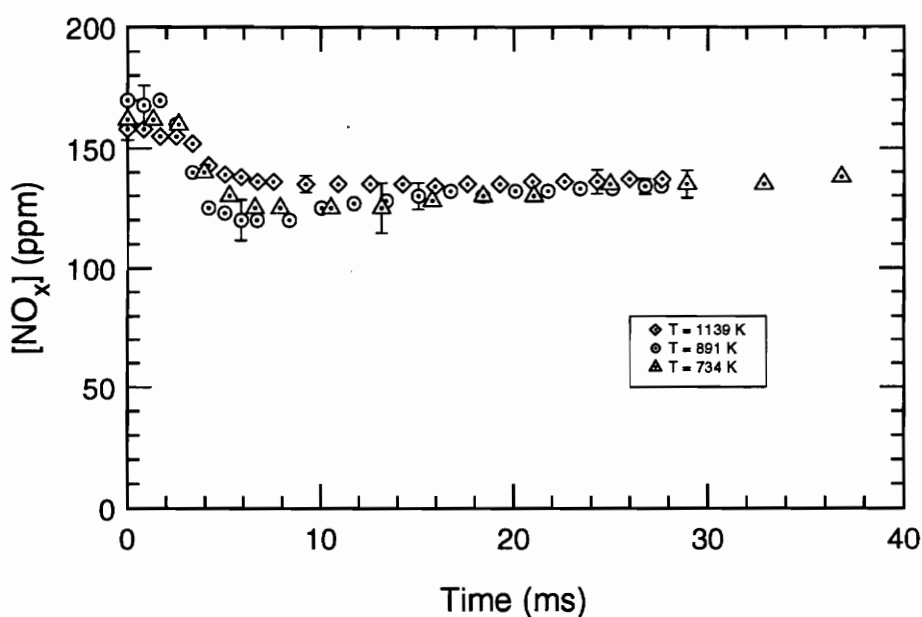


Figure 5.3(a). NO_x profiles at 1.2 atm.

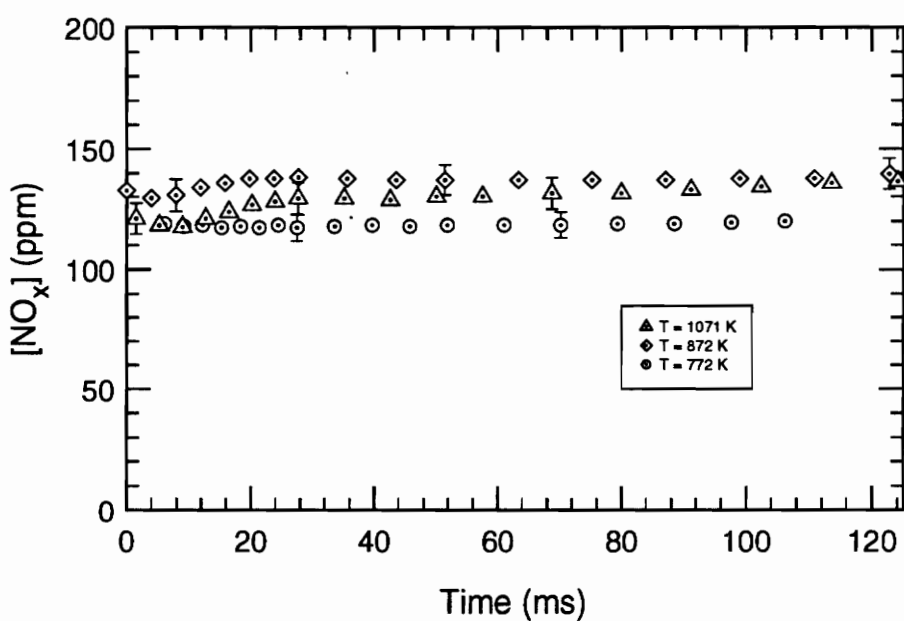


Figure 5.3(b). NO_x profiles at 5 atm.

Figure 5.3. NO_x profile similarities at a given pressure.

concentration is at a maximum at $t = 0$ (i.e., that point where the probe meets the injector bulb). It then decreases relatively quickly to a minimum at which point it begins to slowly increase again or remains relatively constant. This was not expected and could be the result of mixing around the injection point.

There is some evidence suggesting that the system was fairly well mixed by approximately 3-5 cm past the injection point. This is the area where a minimum in NO_x was noted for the near-atmospheric tests. There are two different mixing factors which must be considered. First is the post flame gas flow mixing with the bypass air. This mixing was driven by shear layer flow effects, diffusion, and buoyancy effects. To aid in this mixing, the liner converged from an inside diameter of 11.75 cm to 2.94 cm (Fig. 5.4). The burner was approximately centered in the liner. If the mixing of bypass air with the post flame gases was incomplete, higher NO_x concentrations would have been expected in the center of the flow. Approximately 3 cm after the liner converges, the flow encountered the bulb of the injector and passed through the annulus created between the injector bulb and liner wall. There was a 26% reduction in area as the flow passed through the annulus. It was in this area that methane mixed with the post flame flow. Methane was injected normal to the flow at the annulus in six jets spaced 60° apart. The injector was not exactly centered in the liner, rather it was offset slightly creating an asymmetric annulus. As a result of this, the probe did not meet the injector exactly in the center of the injector. Instead, it was closer to one side. Due to the geometry of the system, it is possible that higher NO_x concentrations were present in the center of the flow if there was incomplete mixing prior to the flow encountering the injector bulb. Therefore, mixing and flow phenomena may be responsible for locally high levels of NO_x .

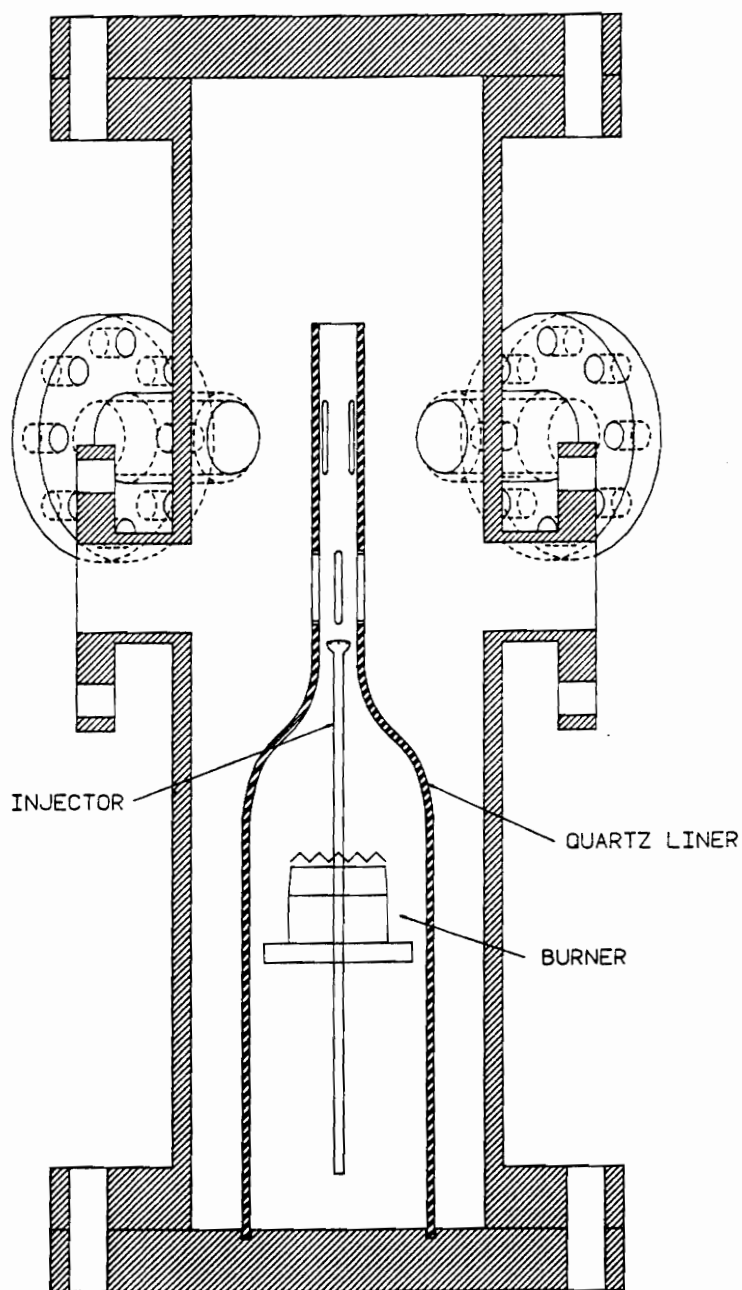


Figure 5.4. Schematic showing the relative positions of the injector, liner, and burner.

As the flow mixed past the injector, it would have been expected that NO_x concentration would have leveled off downstream as the flow became well mixed. This is seen past 3 cm where NO_x levels off somewhat, increasing only slightly for the near-atmospheric case. This slight increase may indicate that some mixing is still taking place even toward the end of the sample range. It would not be expected that total NO_x would be formed in the post flame gases. At those temperatures explored ($< 1300 \text{ K}$), NO_x chemistry has frozen out.

At bulk temperatures greater than 800 K , diffusion flamelets were noted at the injection point. These flamelets appeared to converge to the center of the flow approximately 3 to 5 cm above the injector top. It is possible that this was a source of thermal NO_x formation which could explain locally high levels around the injection point. It is also conceivable that Fenimore - "prompt" - NO may have been formed around the injection point. As the injected methane passed by the flame, some pyrolysis may have occurred. Methane fragments - CH , CH_2 , CH_3 - may then have participated in prompt NO reactions at the injection point where air is in excess. If there had been significant NO_x formation at the injection point, one would not expect to see a similar profile in the case in which no CH_4 was injected. In comparing the two cases, it can be seen that both the injection and no-injection cases have nearly identical NO_x profiles (Fig. 5.5). Therefore, any chemical effect at the injection point seems unlikely. By excluding chemical effect as a source of elevated NO_x concentration around the injection point, it follows that it must be a mixing phenomenon.

Unlike near-atmospheric flows, superatmospheric flows exhibited longer residence times and more constant NO_x profiles. In order to better understand the differences in NO_x profiles at various conditions, Reynolds numbers for each run were calculated for

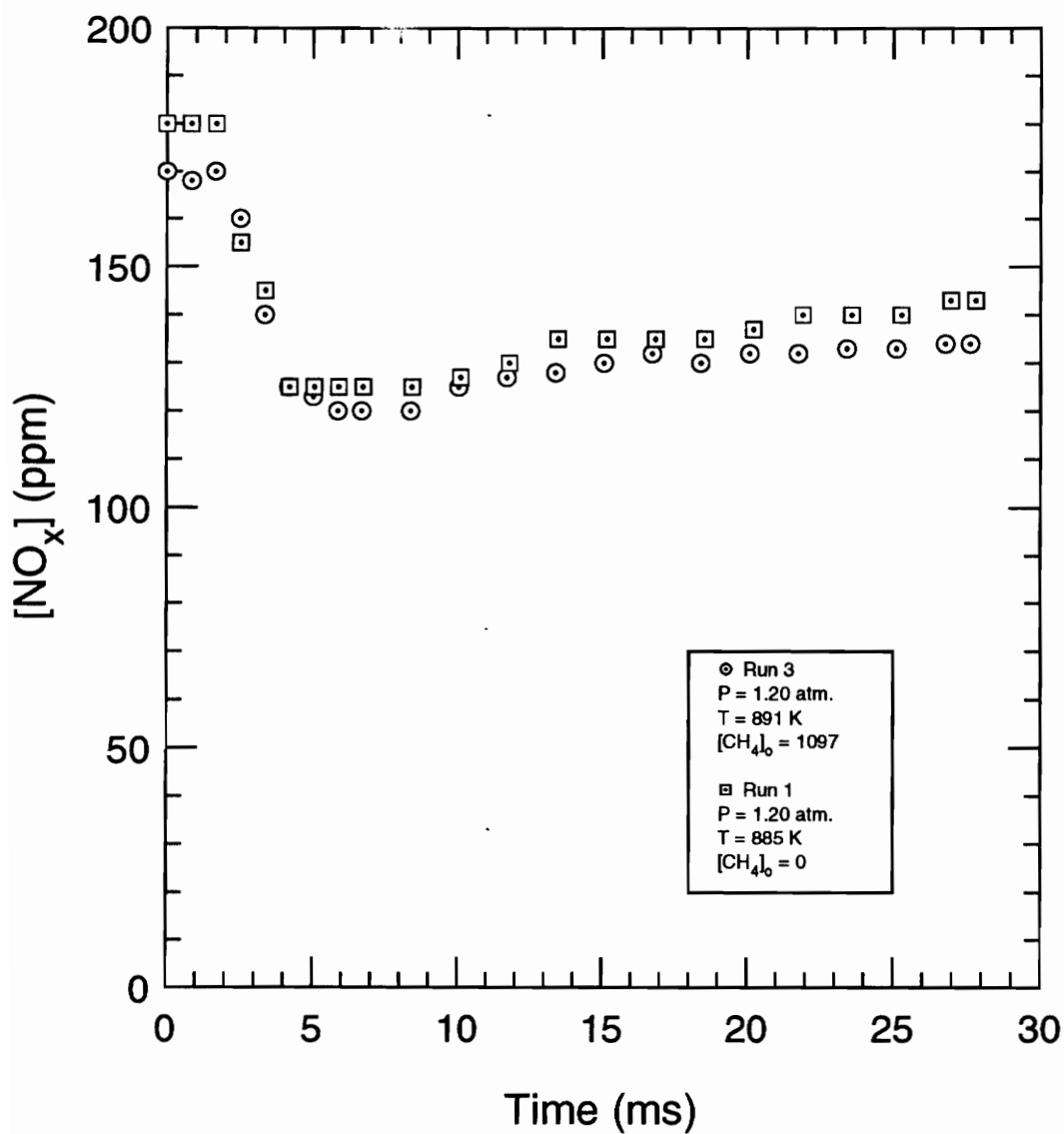


Figure 5.5 Comparison of NO_x profiles at 1.2 atm.
for CH_4 injection and no CH_4 injection cases

flow in the upper portion of the liner. The following assumptions were made in the calculation:

- Viscosity was determined using the power law, $\mu/\mu_o = (T/T_o)^n$, where μ_o is the viscosity at a given temperature T_o and n is an exponent dependent on the working fluid [27].
- For the purpose of calculating a viscosity, the working fluid was assumed to be air ($n = 0.7$).
- Viscosity is much more dependent on temperature than pressure [27]; therefore, pressure was not taken into account in the viscosity calculation.

Most experimental tests had Reynolds numbers in or close to the transition regime, $2000 < Re_D < 4000$. Table 3 shows Reynolds numbers for each run. Two runs were well within the laminar regime with $Re_D < 1000$. Examination of NO_x real time data as recorded on the strip chart recorder for these runs reveal NO and NO_x point sampling profiles with very little fluctuation. Higher Reynolds number flows tended to have much greater fluctuations. Flows with $1000 < Re_D < 2000$ tended to exhibit fluctuation around the injection point but smoothed out somewhat downstream (Fig. 5.6). This indicates that the flow was more turbulent as it passed by the injector, but then laminarized downstream. Turbulence around the injection point should have aided in mixing; however, as the flow mixed, some locally high NO_x levels may have been created as noted previously.

In examining NO_x as a function of residence time, it does appear that these profiles have some dependence on Reynolds number. For a given pressure, flows with similar Reynolds numbers have similar NO_x profiles, providing more evidence to the assertion

Table 3. Reynolds Numbers for Experimental Runs

Run	Re	Temperature (K)	Pressure (atm.)	Residence Time (ms)
1	2098	885	1.20	27.8
2	2090	891	1.20	27.3
3	2088	891	1.20	27.6
4	1354	1139	1.19	27.7
5	1279	1272	1.20	24.4
6	2033	887	1.20	28.6
7	2459	752	1.31	34.0
8	2460	867	3.00	61.0
9	2750	865	4.45	81.3
10	2358	867	7.20	151.4
11	992	862	0.96	48.8
12	1868	734	1.21	43.1
13	3043	664	6.81	176.7
14	1310	857	4.02	154.2
15	1403	1071	5.00	124.1
16	3045	772	4.99	106.2
17	644	874	1.20	90.9
18	1894	872	5.01	129.9
19	1829	867	4.95	136.3
20	1681	862	4.97	151.4
21	3284	669	4.93	116.9
22	2486	872	9.54	200.4
23	3122	882	8.54	131.4
24	2896	981	5.13	71.6
25	2454	847	1.41	29.3
26	2557	847	1.40	29.2

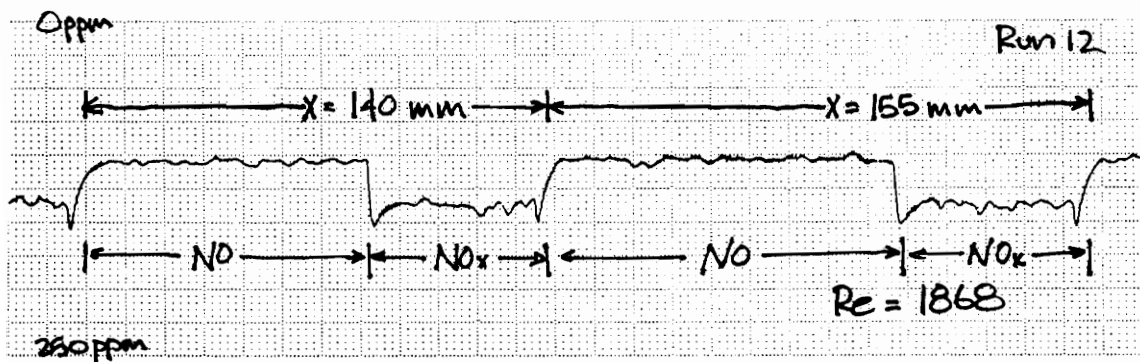
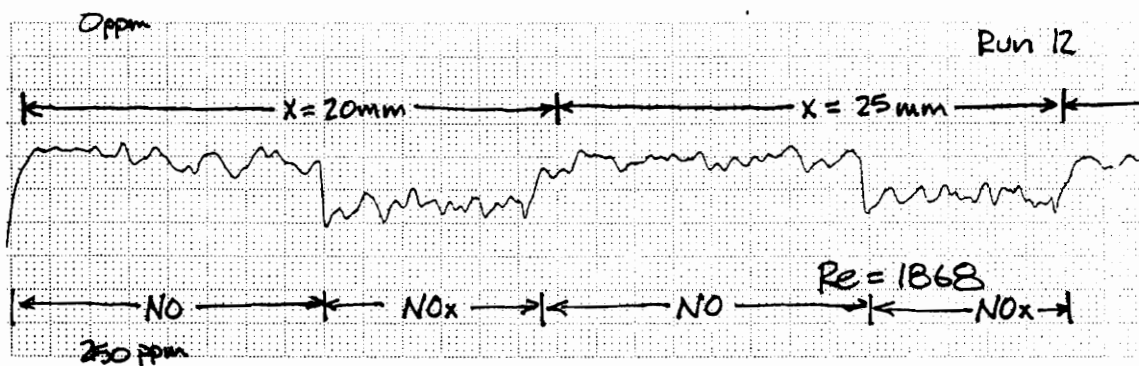
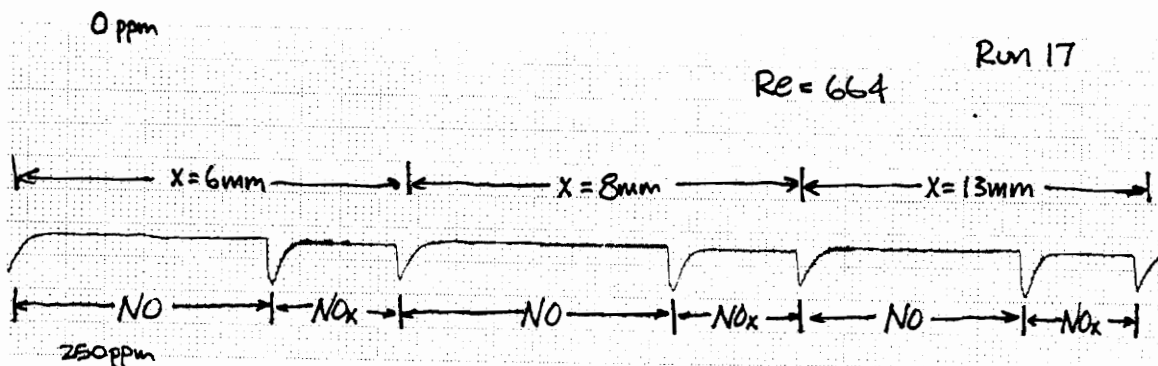


Figure 5.6. Real time NO/NO_x output from CLA for Re = 664 and for Re = 1868.

that variations in NO_x are in fact mixing phenomena. At higher Reynolds numbers seen in lower temperature runs, the NO_x vs. residence time profile smoothes out quite a bit, perhaps indicating that the system had mixed more completely (Fig. 5.7). Although significant changes do not appear around the injection point for these transition flows, they may not be as apparent due to greater residence times between data points. In comparing runs of different residence times, however, it seems more likely that mixing is significantly faster for these conditions, and, therefore, the flow has a more uniform NO_x profile spatially around the injector.

5.1.2. Mixing and NO_2/NO_x Profiles

In comparing NO_2 formation for cases in which CH_4 is injected and cases in which it is not, it becomes apparent that there was NO_2 being formed at the injection point (Fig. 5.8). NO_2/NO_x then decreased as the flow mixed. In the region past the NO_2/NO_x minimum, there is an increase in NO_2/NO_x . This behavior of the system can be explained by mixing effects. The region between $t = 0$ and the NO_2/NO_x minimum shall be referred to as region I. The region past the NO_2/NO_x minimum shall be called region II.

At the injection point, there were regions of locally high methane concentration. NO was quickly converted to NO_2 here. As the gases flowed downstream and mixed in region I, both CH_4 and NO_2 concentrations decreased as the flow became diluted with regard to these species at the center. At the minimum in NO_2/NO_x , mixing catches up with kinetics, and NO is converted to NO_2 at a slower rate. Therefore, it appears that in region I, NO_2 formation is mixing controlled, and in region II it is kinetic controlled.

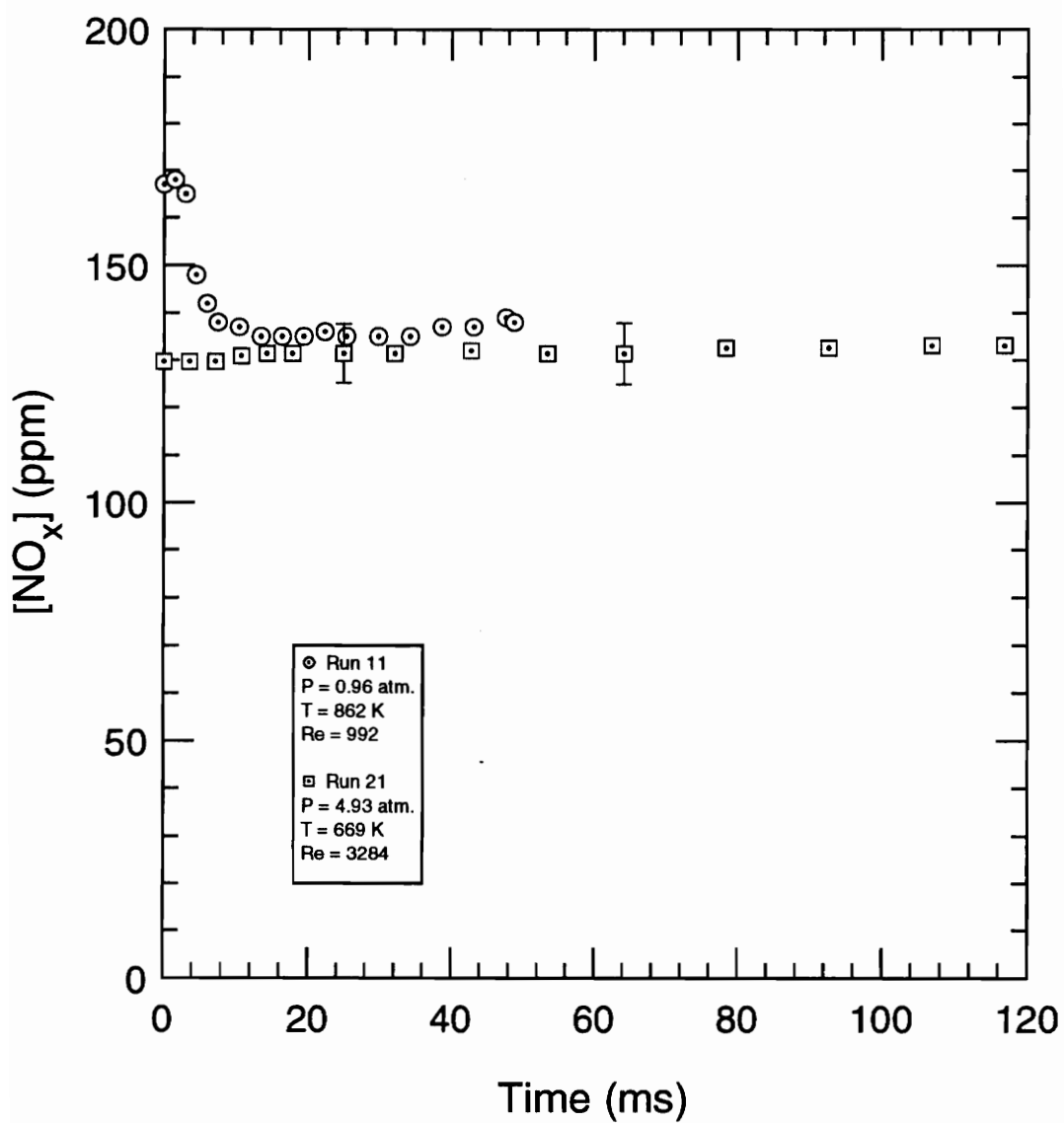


Figure 5.7 Comparison of NO_x profiles with dissimilar Reynolds numbers.

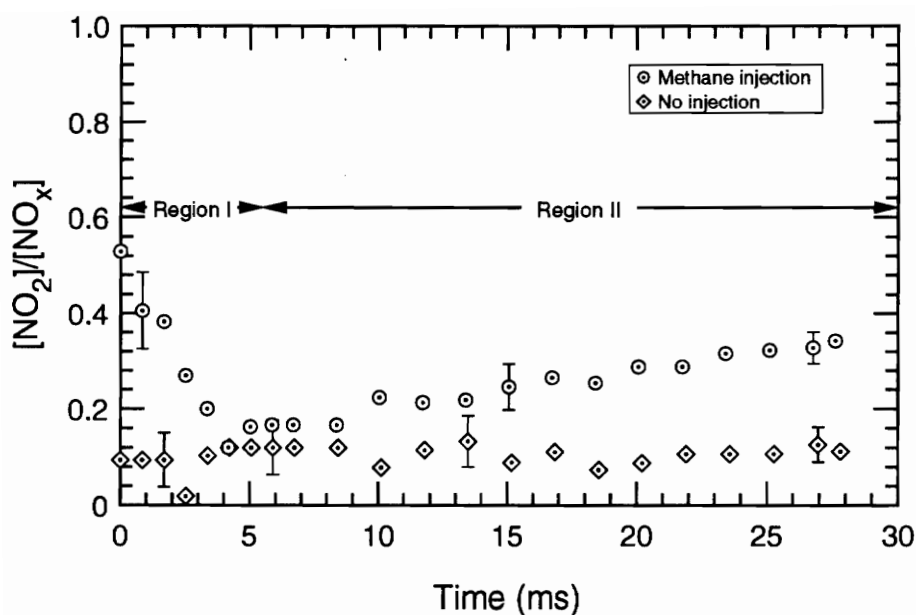


Figure 5.8(a). NO_2/NO_x profiles at 1.2 atm. and 890 K with $[\text{NO}]_0 \approx 195$ ppm.

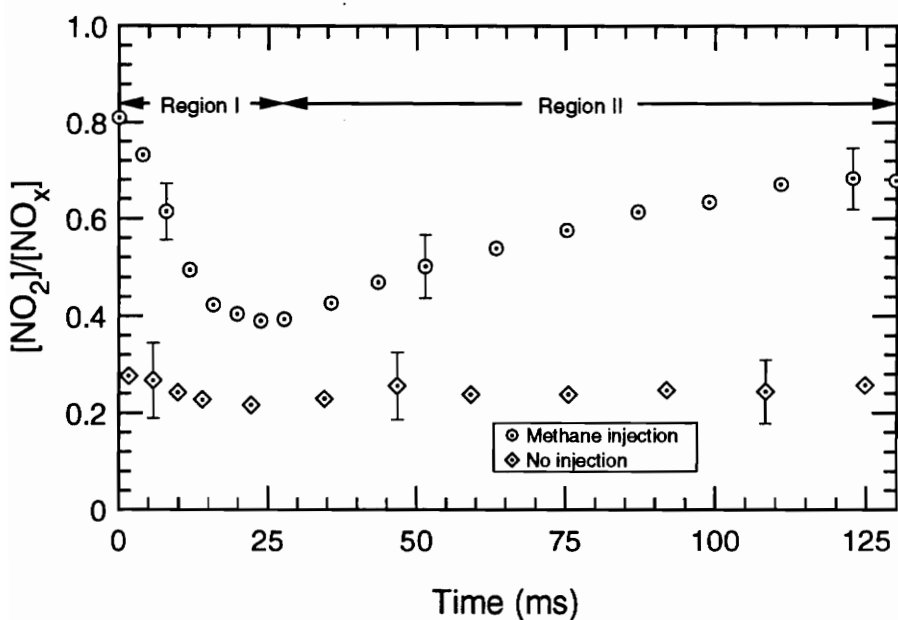


Figure 5.8(b). NO_2/NO_x profiles at 5 atm. and 870 K with $[\text{NO}]_0 \approx 185$ ppm.

Figure 5.8. Comparison of NO_2/NO_x profiles with and without methane injection.

Based on the observations noted to this point, several conclusions regarding mixing can be made.

1. Mixing affects NO_x residence time profiles.
2. Higher pressure flows exhibit more complete mixing due to longer residence times and higher Reynolds numbers which indicate increased turbulence, especially around the injection point.
3. If mixing is taken into account, it is reasonable to assume that NO_x is conserved, even though the profiles do not appear to support this at first glance.
4. NO-NO_2 conversion is mixing controlled in the region around the injection point. By 3-5 cm past the point of injection the process appears to be kinetic controlled.

5.2 PROBE EFFECTS

Probe effects continue to be an area of controversy in NO_2 research. It has been suggested that NO_2 may be formed in the probe, thus yielding inaccurate measurement of NO_2 in the combustion system. Indeed, in early NO_2 research the possibility of probe formed NO_2 was not addressed. Based on previous studies, it is believed that probe formed NO_2 can be minimized, if not eliminated, through low pressure sampling in an uncooled probe. In order to sample at low pressure, the CLA used to measure NO and NO_x concentrations was modified as described in section 3.1.3.

Computer modeling of the probe using CHEMKIN II with a linear temperature reduction over a 4 second residence time at 0.13 atm. showed nearly complete destruction of NO_2 within 100 ms. Based on the experimental results and previous research, it would appear that modeling of the probe using the Miller & Bowman mechanism and the plug flow reactor model is not accurate. It may be that kinetic parameters are not appropriate for such low pressures. Other variables not taken into account in the model, such as wall effects, may be important in the probe case. Therefore, the simple plug flow reactor model used for the experimental system does not appear to accurately predict NO- NO_2 conversion in the probe where conditions are not as well known.

The experimental data offers evidence that probe formed NO_2 is insignificant. Since the plumbing involved in sampling is fairly extensive some cooling of the sample occurs as the sample flows to the reaction chamber of the CLA. If probe formed NO_2 were significant, one would expect to see it over a broad range of experimental temperatures because the flow would most likely pass through the ideal conversion temperature at some point in its path to the reaction chamber. At 5 atm., significant NO_2 formation occurred at 981 K. However, at 1071 K very little NO_2 formation was seen under similar injection and pressure conditions (Fig. 5.9). If probe effects were significant, it would be expected that NO_2 would be formed in the probe as the flow cooled to the 800 K - 1000 K range. This is apparently not the case. More evidence that probe formed NO_2 is insignificant comes from lower experimental temperature ranges in which NO_2 formation is seen to decrease. Unless probe formed NO_2 is extremely transient, and NO_2 is destroyed as well as created, significant probe effects do not occur. This experimental data therefore indicates that probe formed NO_2 is not an issue under probing conditions used in this study. This can be stated with some confidence;

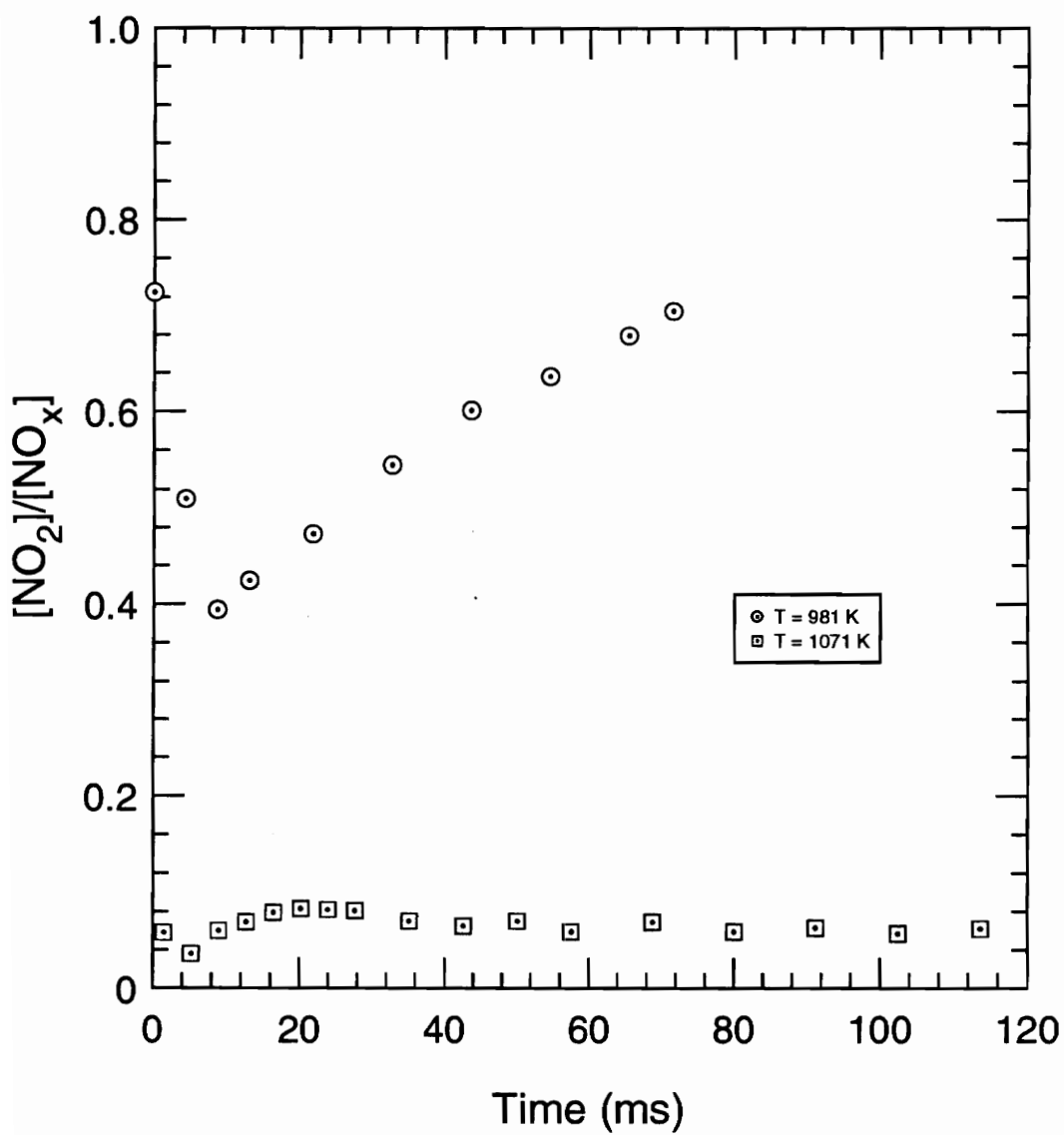


Figure 5.9 NO₂/NO_x profiles at 5 atm. and similar temperature and injection conditions.

however, the ideal manner in which to address the issue would be to eliminate the sampling probe through use of optical measurement techniques such as Laser Induced Florescence (LIF) and Fourier Transform Infrared Spectroscopy (FTIR).

5.3 IMPORTANT VARIABLES REGARDING NO-NO₂ CONVERSION

It has been shown that mixing is an important factor in assessing the experimental data of this study. Keeping this consideration in mind, the effects of several important variables - temperature, pressure, and unburned hydrocarbons - on the conversion of NO to NO₂ can be examined more closely.

5.3.1 Temperature

Modeling, experimental data, and past research indicate that the formation of NO₂ from NO is an extremely temperature sensitive process. Bromly *et al.* [9] reported in their recent study that "at a given residence time, the system goes from being inert (no NO conversion) to completely reacted (100% NO→NO₂) over just a few degrees of temperature." Experimental data from this study supports these observations.

Initial computer modeling with the Miller & Bowman mechanism revealed significant NO₂ conversion only at relatively low temperatures (below approximately 1200 K). NO-NO₂ conversion would therefore appear to be a post flame phenomenon. Temperatures in the flame zone would be much too high to support the conversion. This supports previous studies in which NO₂ was seen to be formed only in the periphery of the flame in areas of large temperature gradients [7, 8]. This is also the area of a

diffusion flame in which one would expect to see locally elevated levels of UHC's - another promotion factor in NO_2 formation.

The modified Miller & Bowman mechanism predicted an upper temperature limit similar to the original mechanism; however, unlike the Miller & Bowman mechanism, a lower temperature limit also became evident (Fig. 5.10). This indicated that there may be a temperature window in which NO is readily converted to NO_2 .

Experimental data supported the predictions of the modified mechanism. In the experimental work a clearly defined region was apparent in which significant NO_2 formation took place. This "temperature window" is more easily visualized when plotted as $[\text{NO}_2]/[\text{NO}_x]$ at a point in time as a function of temperature. The computer results for both mechanisms along with an experimentally obtained curve are plotted in Figure 5.10. Points for these curves are taken at 150 ms in the case of the computer model. By this point, NO_2/NO_x has reached a steady state or is approaching a steady state. The reaction does not appear to have proceeded to this extent for the experimental case; therefore, different residence times were chosen. A similar temperature window is noted at the experimental residence times. It should be noted that the Miller & Bowman mechanism does not predict a lower limit to the temperature window that the experimental data and the modified mechanism indicate.

To offer a better basis of comparison, the maximum value of the experimental data curve at 5 atm. was matched with the modified Miller & Bowman model. Points were then taken at this point in time from the model. The resulting curves are shown in Figure 5.11. In comparing the modified mechanism curve with that obtained experimentally, the curves are similar. The modified mechanism, however, predicts a

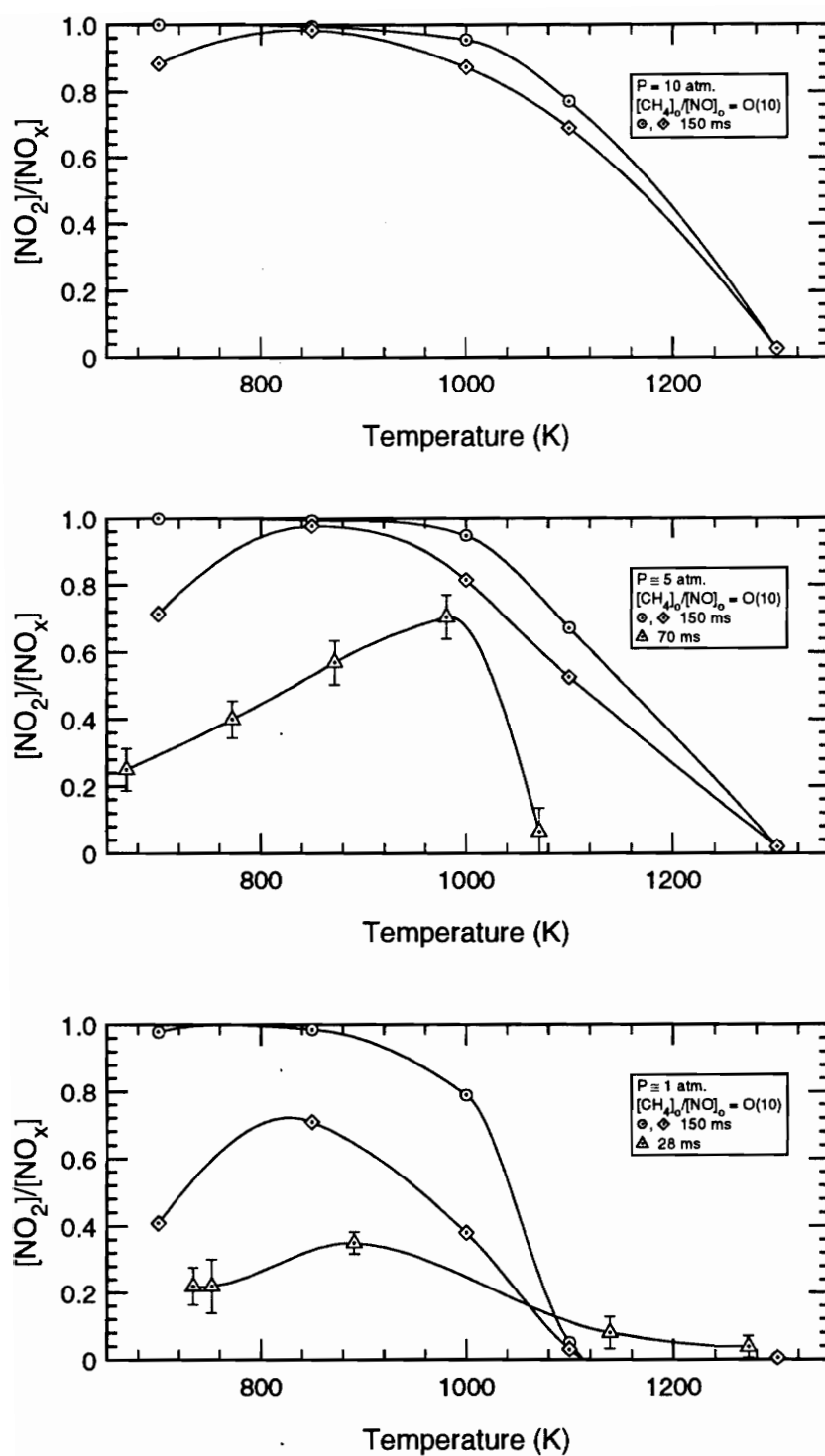


Figure 5.10. Temperature effect on NO_2 formation
 \odot Miller & Bowman Mechanism, \diamond Modified Miller & Bowman Mechanism. \triangle Experimental data.

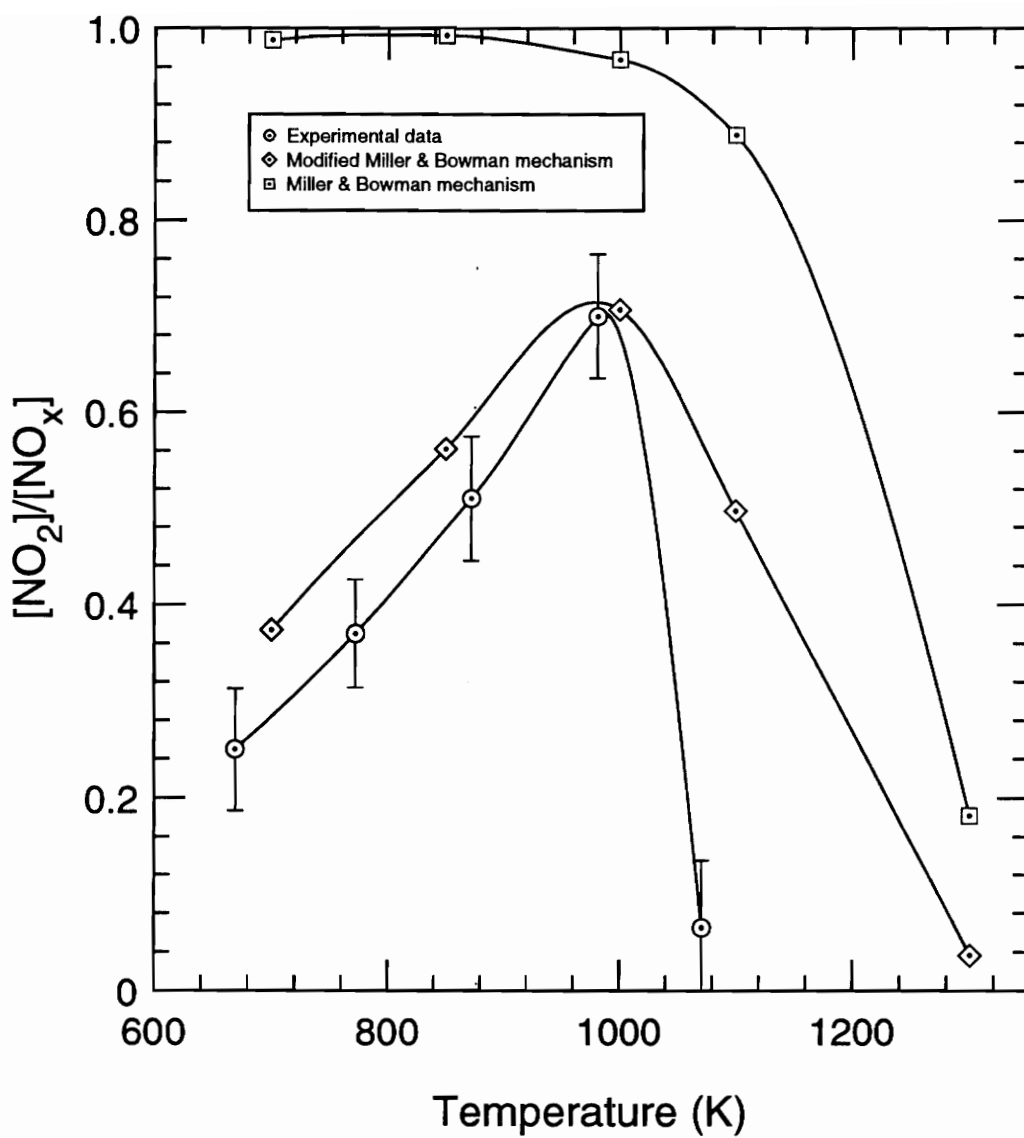
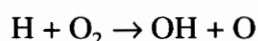


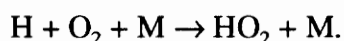
Figure 5.11. Comparison of NO_2/NO_x temperature profile for modeling and experimental results. Experimental points taken at 28 ms. Modeling points taken at 10 ms. $P = 5 \text{ atm.}$, $[\text{CH}_4]_0 \cong 1000 \text{ ppm.}$

slightly higher upper temperature limit that does not drop off as quickly as experimental data indicates.

In examining these temperature curves, it should be noted that the lower boundary observed in experimental testing and predicted by the modified Miller & Bowman mechanism is of a different nature than the upper boundary. Above approximately 1000 K, the formation of NO₂ quickly decreases as temperature increases. Some NO₂ which is formed in this temperature region is destroyed relatively quickly. This is because the reaction



is favored at higher temperatures over the 3-body reaction



More NO₂ destroying radicals - OH, O - are then produced at higher temperatures, and less HO₂ is formed. The net result is decreased NO₂ production. In the area of the lower "boundary", NO continues to be converted to NO₂, but at a much slower rate. The very rapid conversion seen in the ideal temperature range does not occur at lower temperatures. The "window" then is a temperature range in which NO conversion to NO₂ not only is favored, but occurs rapidly.

5.3.2 Pressure

The effects of pressure on NO₂ formation have not been investigated experimentally heretofore. It does appear to be another variable that is important in the conversion of NO to NO₂. If the reaction $\text{H} + \text{O}_2 + \text{M} \rightarrow \text{HO}_2 + \text{M}$ is indeed an

important reaction, increasing pressure would increase the probability of a three body reaction occurring as the mean free path of the molecules decreases. If HO_2 production is increased, NO_2 production should also increase due to the reaction of HO_2 with NO (rxn. 132).

Both experimental results and modeling provide evidence that pressure is an important consideration in the conversion of NO to NO_2 . At first glance, the experimental results in regard to pressure appear somewhat ambiguous. Different residence times and mixing conditions make it difficult to compare various runs. In general, both experimental data and modeling show an increase in NO_2 production as pressure increases. Figure 5.12 shows $(\text{NO}_2/\text{NO}_x)_{\text{max}}$ as a function of pressure for the Miller & Bowman mechanism. The modified mechanism shows a similar curve, but maximum NO_2/NO_x values are not as great and occur at greater residence times. Maximum values of NO_2/NO_x were not achieved in the experimental sampling range. However, if NO_2/NO_x is plotted at a given residence time for various pressures, an increase in NO_2 production is seen at higher pressures (Fig 5.13). The spread of the data is most likely the result of varying mixing conditions.

Data indicates that the temperature region favoring rapid and significant NO conversion changes as pressure changes. The upper temperature limit of NO conversion increases as pressure increases (Fig. 5.10). The lower limit appears to decrease with a pressure increase. In short, as pressure increases modeling suggests that the NO_2 temperature window grows larger. The greatest change occurs between 1 and 5 atmospheres.

It is difficult to interpret experimental data due to the varied flow conditions at which experimental data was taken. The data does support the modeling prediction that

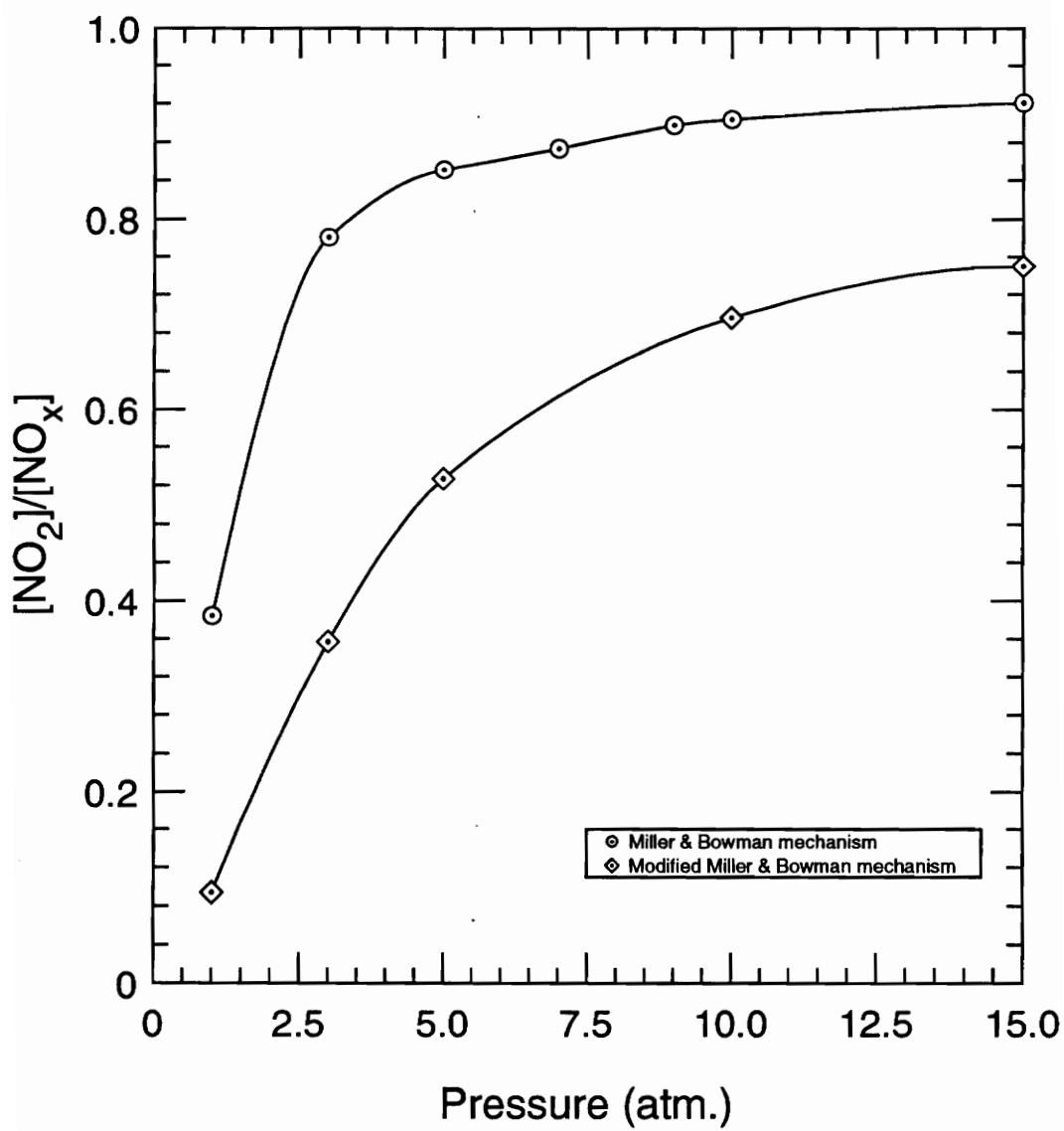


Figure 5.12. The effect of pressure on NO₂ formation.
 $T = 1100 \text{ K}$, $[\text{CH}_4]_0 \cong 1000 \text{ ppm}$

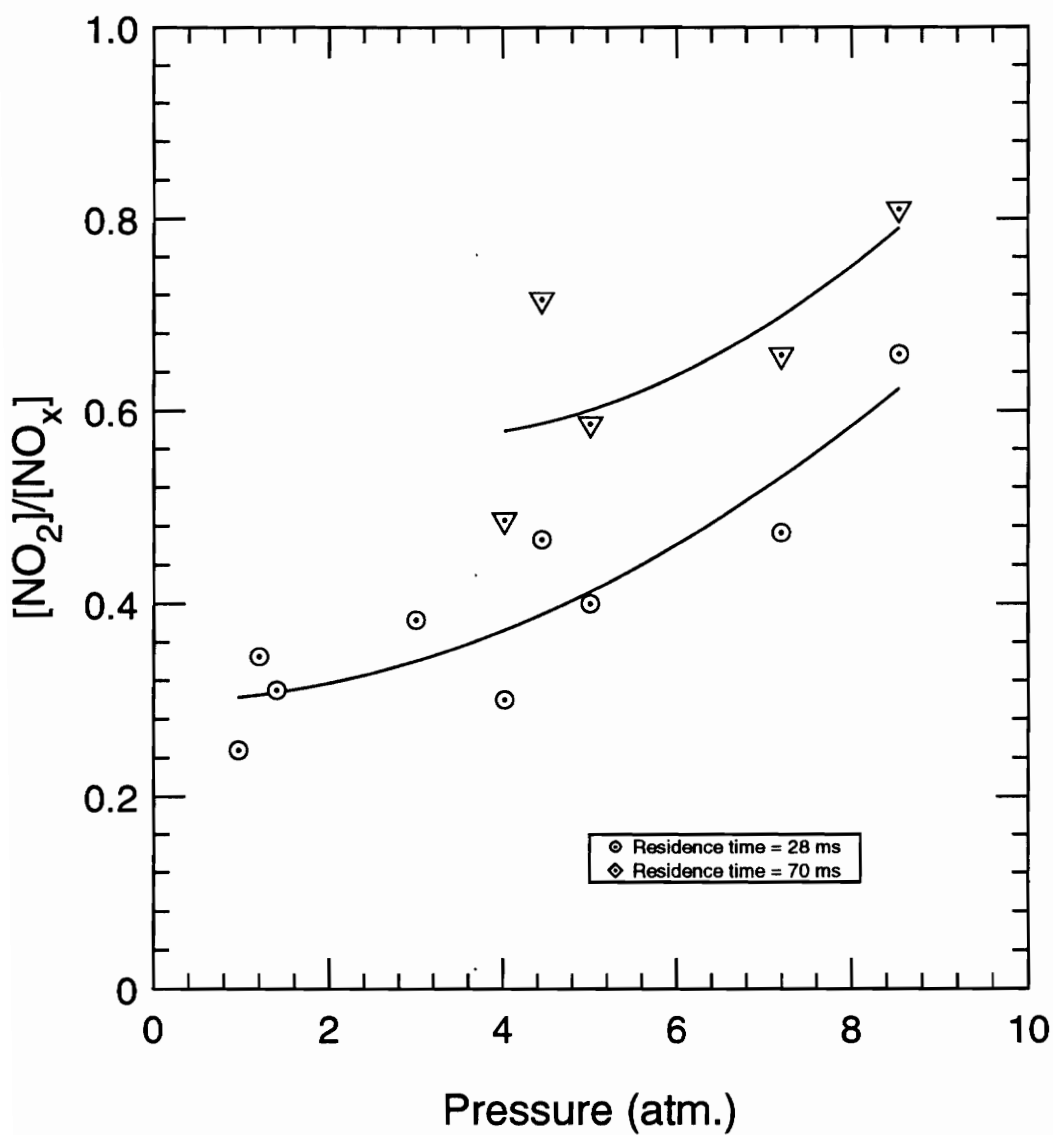


Figure 5.13. The effect of pressure on NO₂ formation.
 T = 847-891 K, [CH₄]₀ ≅ 1000 ppm

rapid and complete NO-NO₂ conversion if favored at superatmospheric pressures when a hydrocarbon promoter is present. Not much can be said about peak NO₂/NO_x levels because for most experimental cases maximum NO₂/NO_x was never reached within the sampled residence times. Optimum NO₂/NO_x formation appears to occur between 900 and 1000 K regardless of pressure. The upper temperature limit is much steeper at 5 atmospheres, but this may be a result of the residence time at which the profile's data points were taken and not a characteristic dependent on pressure.

5.3.3 Unburned Hydrocarbons

It has been well documented in past research that the presence of unburned hydrocarbons greatly increases NO-NO₂ conversion. Recent studies have confirmed reports from previous studies that trace amounts of hydrocarbons greatly promote NO conversion to NO₂. These studies have investigated the effectiveness of various hydrocarbons in the promotion of the conversion of NO to NO₂ [9-11].

Hori *et al.* [10] studied the effectiveness of six hydrocarbons in promoting the conversion of NO to NO₂. They found that methane was the least effective and n-butane the most effective. They also reported that "...fuel addition required to obtain a certain conversion of NO to NO₂ depends on initial NO level." Bromly *et al.* [9], in their study of the effects of n-butane on NO-NO₂ conversion, defined a ratio of [NO] to [n-butane]. This takes into account both initial [NO] levels as well as hydrocarbon concentration. They found that the value of this ratio affected the temperature required "...to bring about the reaction."

In this study, CH₄ was selected to be injected into the post flame gas flow. The current results agree with past research in that the presence of UHC's is indeed an important factor in NO-NO₂ conversion. When no CH₄ was injected, the conversion was dramatically reduced. However, when a small amount of CH₄ was injected, NO₂ production significantly increased. As a baseline injection for computer modeling, approximately 1000 ppm was injected. Doubling this had little effect on NO₂ formation. Similarly, halving it also had little effect. However, when the injection concentration was decreased an order of magnitude, a significant reduction in NO₂ formation was noted. The question naturally arises as to how much injected hydrocarbon is required for optimum NO₂ formation.

The results (experimental and modeling) also indicated that [NO]_o is a variable in NO₂ production. In general, as [NO]_o decreases with injected CH₄ held constant, NO₂/NO_x increases. Taking this into account, as well as the relationship with [CH₄]_o described above, a ratio [CH₄]_o/[NO]_o, similar to Bromly's ratio, can be defined. This ratio is sensitive to changes in both injected CH₄ and NO, and, therefore, may be a useful quantity in predicting those conditions conducive to NO-NO₂ conversion. Computer modeling showed that the value of this ratio is indeed useful; however, the individual values of [CH₄]_o and [NO]_o must also be taken into account in predicting the extent of NO₂ formation. This is because the two variables appear to have a slightly disproportionate effect on NO₂ production. Bromly *et al.* [9] report that [NO]/[n-butane] = 1 is an important quantity. Similarly, results of this study found [CH₄]_o/[NO]_o ≅ 1 to be important. At [CH₄]_o/[NO]_o ratios greater than one, there is an increase in NO₂/NO_x. For [CH₄]_o/[NO]_o > 10, the maximum effect of the hydrocarbon has apparently already been reached and there is little further increase in NO₂/NO_x. As [CH₄]_o/[NO]_o approaches zero, there is significantly less NO-NO₂ conversion (Fig. 5.14).

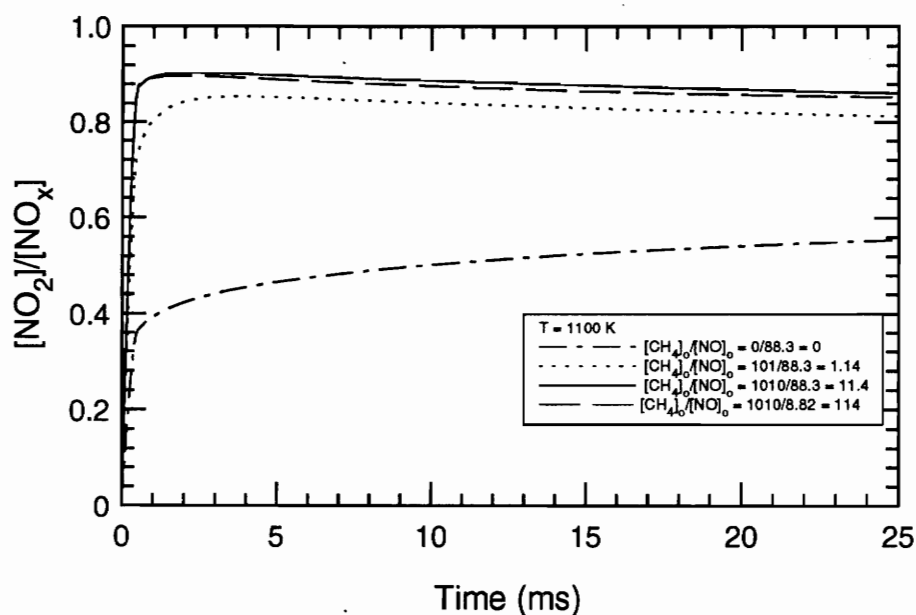


Figure 5.14(a). Hydrocarbon promotion at 10 atm.
(Computer model)

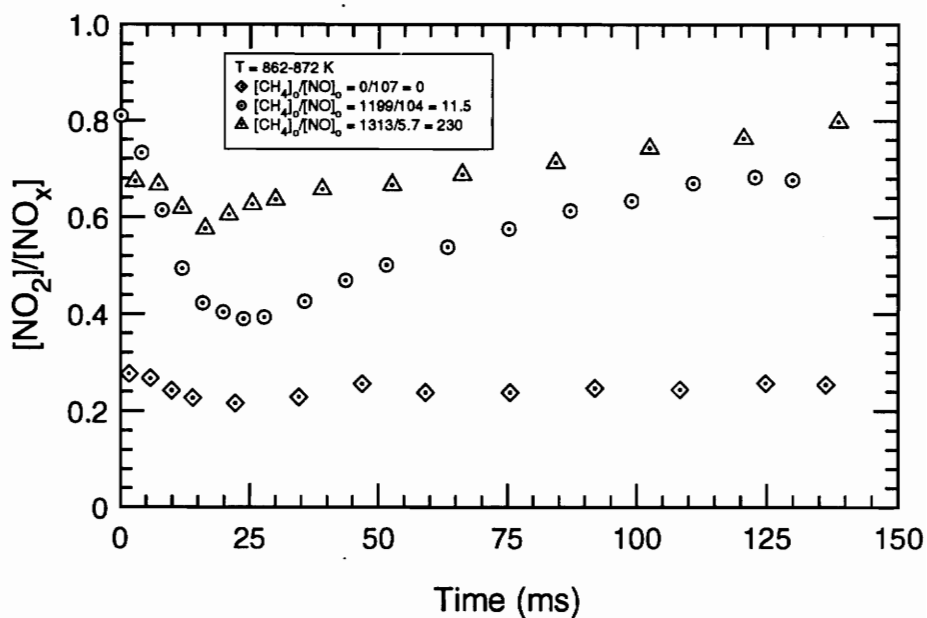


Figure 5.14(b). Hydrocarbon promotion at 5 atm.
(Experimental data)

Figure 5.14. The effect of hydrocarbon promotion on the conversion of NO to NO_2 .

This was noted in both experimental and modeling results. Similar experimental results at both 1 and 5 atm. indicate that pressure probably does not significantly affect the $[\text{CH}_4]_0/[\text{NO}]_0$ ratio necessary to enhance NO-NO₂ conversion.

5.3.4 Comparison of Promoting Factors

In assessing the relative importance of the three promoting factors on NO-NO₂ conversion, it would appear that the order of decreasing importance is the presence of unburned hydrocarbons, temperature, and pressure.

This study as well as past studies indicate that hydrocarbons play an essential role in NO-NO₂ conversion. It has been shown that in their absence, NO is not converted to NO₂ even if the system is within the ideal temperature range. Modeling has suggested that CO may play a similarly important role in the conversion process; however, this has not been explored experimentally, and modeling results indicate that it is a poorer promoting factor than methane. Although water does have a slight chemical effect on NO₂ formation, its main contribution is thermal in nature. This study only examined the effects of one hydrocarbon - methane - on NO-NO₂ conversion. Recent studies have compared the promotional effects of different hydrocarbons on NO-NO₂ conversion and have shown methane to be the poorest of the hydrocarbon promoters [9-11]. Even if methane is the least effective NO₂ promoting hydrocarbon agent, its effect on the conversion of NO to NO₂ is still significant.

The conversion mechanism has been shown to be extremely temperature sensitive. Experimental data as well as some of the modeling indicate that there is a temperature region or window, outside of which NO conversion does not occur or occurs at a much

slower rate. Research by Hori *et al.* [10] also supports this idea of a temperature window.

A hydrocarbon promoter and temperature are two essential factors in NO-NO₂ conversion. Outside of parameters involved with these variables, NO₂ formation does not occur or is drastically decreased. Pressure is not as essential as hydrocarbons and temperature, but as pressure increases, the rate at which NO is converted to NO₂ is seen to increase. The results indicate that pressure may in fact affect the peak values of NO₂/NO_x as well as the temperature range of optimal conversion. Pressure, however, is not as important as the first two factors because NO-NO₂ formation can not be eliminated by changing the pressure above 1 atmosphere. Although NO₂ formation may not be as fast or great at 1 atmosphere as it is at 10 atmospheres, this study as well as past studies have shown that NO conversion still does occur to significant levels.

5.4 APPLICATION TO THE INDUSTRIAL GAS TURBINE

It has been shown that temperature, pressure, and the presence of unburned hydrocarbons are important factors in the conversion of NO to NO₂. Their relative importance in the conversion process has also been discussed. This section will address how these factors may apply to the industrial gas turbine.

With methane as a hydrocarbon promoter, the region most conducive to NO₂ formation seems to be between approximately 800 K and 1000 K. As temperature increases past 1000 K, experimental data shows that NO₂ formation decreases dramatically. One would not expect to see the low temperatures necessary for the conversion to take place in the combustor of an industrial gas turbine, except for perhaps

locally where cooling air mixes with hot combustion gases in the can. This suggests that NO conversion is not occurring in the combustor or that it is only occurring locally. If it is occurring in the combustor, it is most likely at the cooling air injection points. It seems unlikely, though, that NO₂ would survive mixing with the hotter gases in the combustor where free radical concentration would be significant. If NO₂ formation is not occurring in the combustor, conversion more likely takes place as the gases expand and cool through the turbine.

Based on modeling and experimental results examining the effects of pressure, it would be expected that NO₂ formation in an actual gas turbine would occur at a point where pressure is still relatively high. This is where the conversion would take place most rapidly and possibly to the greatest extent. The most ideal pressures would then be in the combustor or early stages of the turbine. As the gases expand through the turbine, the conversion process would slow considerably. Residence time then becomes an important variable in examining NO-NO₂ conversion in the industrial gas turbine.

Hydrocarbons must be considered in terms of their ratio with [NO] to be of use in explaining possible sources of high NO₂ formation. For a turbine run in dry low NO_x mode, NO may be decreased; however, if UHC's remain constant or increase, the decrease in NO may push the system into an NO-NO₂ conversion regime ($[CH_4]/[NO] > 1$). In this regime, the majority of NO may be converted to NO₂. If NO₂ levels increase enough, it may result in visible stack emissions. Therefore, although total NO_x is decreased, the resulting increase in NO₂/NO_x may result in visible stack emissions.

It should also be noted that there may be other promoting species, such as CO. Therefore, as NO_x emissions are decreased, they must be accompanied by a decrease in

UHC's and possibly CO. This may help to explain why NO₂ has not been a problem until recently. NO_x reductions have finally reached the point where they have surpassed UHC and CO reductions. It may be that further reductions in these areas will be necessary before further NO_x reductions can be achieved while avoiding significant NO₂ production.

CHAPTER 6 - SUMMARY, CONCLUSIONS, AND RECOMMENDATIONS

6.1 SUMMARY AND CONCLUSIONS

The conversion of NO to NO₂ continues to be a problem in industry. In order to address the issue, a study of this conversion process was undertaken. Particular interest was given to the effect of pressure on the mechanism and how the results apply to the industrial gas turbine.

Computer modeling of the system was undertaken. Based on the modeling results and past research, a high pressure flow reactor was designed and built. This facility was used to collect experimental data on NO-NO₂ conversion.

The experimental and modeling results point to three variables which are of particular importance to the conversion process. These are temperature, the presence of unburned hydrocarbons, and pressure.

It was found that rapid, significant conversion only took place over a temperature range of several hundred degrees. Experimentally this temperature window was determined to be between approximately 800 and 1000 K. The upper limit of this temperature window appears to be quite abrupt. At 70 ms and under similar conditions, NO₂/NO_x increases from approximately .07 to .70 as temperature changes from 981 to 1071 K. Within less than 100 K, the system becomes essentially inert (i.e., no conversion of NO to NO₂). The lower limit is the result of a relatively gradual decrease in the rate at which NO is converted to NO₂. These temperature constraints on the

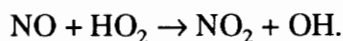
mechanism limit NO_2 production to occurring in the relatively cool post flame region of a combustion system.

A conversion promoter appears to be another essential element in significant NO conversion. Hydrocarbons have been shown to be excellent species in promoting NO- NO_2 conversion. Modeling also suggests that carbon monoxide may be another promoter, but its effect on the conversion has not yet been investigated experimentally. The relative concentration of methane with respect to NO concentration has been shown to be an important consideration. For $[\text{CH}_4]/[\text{NO}] > 1$, significant conversion was seen to occur. It was seen experimentally that at 5 atm. and approximately 870 K, NO_2/NO_x was approximately .25 for the no injection case, .70 for $[\text{CH}_4]_0/[\text{NO}]_0 = 11.5$, and .80 for $[\text{CH}_4]_0/[\text{NO}]_0 = 230$. Above the upper limit of the temperature window (~ 1000 K), the presence of hydrocarbons had little effect on NO- NO_2 conversion.

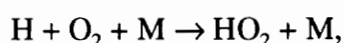
Although pressure does not seem to have as dramatic an impact on NO- NO_2 conversion as temperature and hydrocarbon promotion, it is a contributing factor in the process. At higher pressure, increased levels of NO_2/NO_x were noted, both with and without hydrocarbon promotion. In exploring the effect of pressure alone (no hydrocarbon injection), as pressure of the reactor was increased from 1.20 to 4.95 atm., NO_2/NO_x was seen to increase from .12 to .25. Pressure, therefore, is an important variable in consideration of pressurized combustion systems.

The model does indeed appear to be a good tool in predicting incidences of significant NO to NO_2 conversion. Experimental data suggested that the rate of NO_2 formation is not as rapid as the model indicated. The important consideration, however, is that the model, particularly when incorporating the modified Miller & Bowman mechanism, predicted those trends seen in the experimental tests.

The results of this study yield more evidence that the major pathway for NO₂ formation is, in fact, the HO₂ mechanism,



The existence of an upper temperature limit to NO₂ formation and the increase in NO-NO₂ conversion noted at superatmospheric conditions suggest that the 3-body reaction,



which forms HO₂ is indeed important in the mechanism.

6.2 RECOMMENDATIONS

Although it has become generally accepted that NO is converted to NO₂ mainly through the HO₂ mechanism, experimental studies, including this one, have not measured HO₂ or other important free radicals which affect the conversion process. It would therefore be desirable to conduct some experiments using optical measurement techniques such as laser induced fluorescence (LIF) or Fourier transform infrared spectroscopy (FTIR). An advantage to optical measurement techniques is that they would eliminate the controversy of probe formed NO₂. The current experimental apparatus was designed with optical access in mind. This could be achieved quite easily by machining the side flanges to fit windows.

In addition to those species mentioned above, it would be advantageous to measure hydrocarbon concentrations in order to more closely investigate the relationship between hydrocarbons, temperature, and pressure and their effect on NO₂ formation. Since modeling has indicated that other species may have promotional effects similar to those

of hydrocarbons, it would be beneficial to investigate the effect of carbon monoxide addition and to determine if there are any other species which have a promotional effect on the conversion of NO to NO₂.

Further experimental work must be carried out in conjunction with computer modeling. Although the modified Miller & Bowman mechanism appears to more accurately represent experimental results than the original Miller & Bowman mechanism, the kinetic parameters must continue to be refined in order to most accurately represent experimental observation.

Use of the high pressure flow reactor facility revealed some shortcomings of the design which, short of a total redesign, could be improved upon for future work. One of the main problems encountered in the experimental portion of this study was relatively slow mixing conditions. Because NO to NO₂ conversion does appear to be a rapid process, quick, efficient mixing was desired. A smaller inside diameter for the upper portion of the liner would aid this. Another factor which could help is turbulence induction around the injection point. Physical turbulence inductors could be implemented in this area. It could also be beneficial to inject the secondary reactant at an angle so as to induce swirl. Optical ports would prove useful in using flow visibility techniques as a tool in assessing the mixing characteristics of the facility.

The burner proved to be satisfactory at atmospheric conditions; however, as pressure in the facility increased, the flame zone became thinner and was drawn closer to the burner head. The burner head was water cooled. As the flame drew closer to the burner head, it tended to be quenched. Since heat was being drawn off through the burner, the temperature of post flame gases decreased as pressure increased. In order to combat this, flow through the burner had to be increased as pressure increased to

maintain a given temperature. Higher temperature runs (> 1100 K) were impossible at high pressure due to the effect described above. A flat flame burner is desirable for this application, but one of a different design could prove more useful.

A great deal of time was spent modifying the CLA to sample at low pressure. Optical measurement techniques would make this a moot point; however, if future work were to include probe sampling, some work on the modified CLA would be in order. Although the system served its purpose, it was not very robust. Calibration was extremely sensitive to the NO sampling pathway regulating valve. Lower probe pressures may also be desirable. Unfortunately, as pressure in the system was decreased, the flow became increasingly unsteady, making it impossible to calibrate the instrument. Short of a complete system redesign, this problem may be alleviated somewhat with the introduction of surge tanks upstream to both vacuum pumps.

REFERENCES

1. Allen, J.D., "Probe Sampling of Oxides of Nitrogen from Flames," *Combustion and Flame*, 24, 133 (1975).
2. Johnson, G.M., Smith, M.Y., and Mulcahy, M.F.R., "The Presence of NO₂ in Premixed Flames," Seventeenth (International) Symposium on Combustion, The Combustion Institute, 647 (1978).
3. Kramlich, J.C. and Malte, P.C., "Modeling and Measurement of Sample Probe Effects on Pollutant Gases Drawn from Flame Zones," *Combustion Science and Technology*, 18, 91 (1978).
4. Hori, M., "Effects of Probing Conditions on NO₂/NO_x Ratios," *Combustion Science and Technology*, 23, 131 (1980).
5. Amin, H., "Effect of Heterogeneous Removal of Oxygen Atoms on Measurement of Nitrogen Dioxide in Combustion Gas Sampling Probes," *Combustion Science and Technology*, 15, 31 (1977).
6. Chen, J.Y., McLean, W.J., and Gouldin, F.C., "The Oxidation of NO to NO₂ During Combustion Quenching Processes," WSS Paper 79-17, (1979).
7. Hargraves, K.J.A., Harvey, R., Roper, F.G., and Smith, D.B., "Formation of NO₂ By Laminar Flames," Eighteenth (International) Symposium on Combustion, The Combustion Institute, 133 (1981).
8. Sano, T., "NO₂ Formation in the Mixing Region of Hot Burned Gas with Cool Air," *Combustion Science and Technology*, 38, 129 (1984).
9. Bromly, J.H., Barnes, F.J., Mandyczewsky, R., Edwards, T.J., and Haynes, B.S., "An Experimental Investigation of the Mutually Sensitised Oxidation of Nitric Oxide and n-Butane," Twenty-Fourth (International) Symposium on Combustion, The Combustion Institute (1992).

10. Hori, M., Matsunaga, N., and Malte, P.C., "The Effect of Hydrocarbons on the Conversion of Nitric Oxide to Nitrogen Dioxide," WSS/CI 92-36, (1992).
11. Marinov, N.M., Steele, R.C., Hori, M., and Malte, P.C., "The Effect of Hydrocarbons on the Promotion of Nitric Oxide to Nitrogen Dioxide in a Well-Stirred Reactor," WSS/CI (1993).
12. Jaasma, D. and Borman, G., "Peculiarities Associated with the Measurement of Oxides of Nitrogen Produced by Diffusion Flames," *Combustion Science and Technology*, 23, 83 (1980).
13. Hori, M., "Nitrogen Dioxide Formation by the Mixing of Hot Combustion Gas with Cold Air," Twenty-Second (International) Symposium on Combustion, The Combustion Institute, 1175 (1988).
14. Sano, T., "NO₂ Formation in the Mixing Region of Hot Burned Gas with Cool Air - Effect of Surrounding Air," *Combustion Science and Technology*, 43, 259 (1985).
15. Hori, M., "Experimental Study of Nitrogen Dioxide Formation in Combustion Systems," Twenty-First (International) Symposium on Combustion, The Combustion Institute, 1181 (1986).
16. Miller, J.A. and Bowman, C.T., "Mechanism and Modeling of Nitrogen Chemistry in Combustion," *Prog. Energy Combust. Sci.*, 15, 287 (1989).
17. Johnson, G.M. and Smith, M.Y., Short Communication: "Emissions of Nitrogen Dioxide from a Large Gas-Turbine Power Station," *Combustion Science and Technology*, 19, 67 (1978).
18. Kee, R.J., Rupley, F.M., and Miller, J.A., "CHEMKIN II: A FORTRAN Chemical Kinetics Package for the Analysis of Gas Phase Chemical Kinetics," Sandia Report SAND89-8009, UC-401, Sandia National Laboratories (1989).
19. Roby, R.J., *A Study of Fuel-Nitrogen Reactions in Rich, Premixed Flames*, Ph.D. Dissertation, Stanford University (1987).
20. Eskin, L.D. and Seitzman, J.M., *Proplot*, version 1.01, Cogent Software (1987).

21. Miller, J.A. and Bowman, C.T., "Erratum: Mechanism and Modeling of Nitrogen Chemistry in Combustion," *Combustion Science and Technology*, 16, 347 (1990).
22. Carter, C.D., King, G.B., and Laurendeau, N.M., "A Combustion Facility for High-Pressure Flame Studies by Spectroscopic Methods," *Rev. Sci. Instrum.*, 60, 8 (1989).
23. Kimball-Linne, M.A., *Flow Reactor Studies of NH_3/NO Reaction Kinetics, From 1050° K to 1450° K*, Ph.D. Dissertation, Stanford University (1984).
24. Instruction Manual: Model 10AR Chemiluminescent NO/NO_x Analyzer, Thermo Environmental Corp.
25. Reynolds, W.C., STANJAN, version 3.89, Stanford University (1987).
26. Gouldin, F.C., "Controlling Emissions from Gas Turbines - The Importance of Chemical Kinetics and Turbulent Mixing," *Combustion Science and Technology*, 7, 33 (1973).
27. White, F.M., *Fluid Mechanics*, second edition, 28 (1986).

APPENDIX A

Reaction Mechanism

The reactions of the mechanism used in this study were taken from the Miller and Bowman mechanism published in reference [16]. Although the mechanism does not include all species nor reactions that Miller and Bowman took into account, it is referred to as the "Miller & Bowman" mechanism in this thesis.

Miller & Bowman Mechanism [16]

$$(k = A T^{\beta} \exp(-E/RT))$$

	A	β	E
1. $2CH_3+M=C_2H_6+M$	9.03E+16	-1.2	654.0
H2 Enhanced by 2.0			
CO Enhanced by 2.0			
CO2 Enhanced by 3.0			
H2O Enhanced by 5.0			
2. $CH_3+H+M=CH_4+M$	6.00E+16	-1.0	.0
H2 Enhanced by 2.0			
CO Enhanced by 2.0			
CO2 Enhanced by 3.0			
H2O Enhanced by 5.0			
3. $CH_4+O_2=CH_3+HO_2$	7.90E+13	.0	56000.0
4. $CH_4+H=CH_3+H_2$	2.20E+04	3.0	8750.0
5. $CH_4+OH=CH_3+H_2O$	1.60E+06	2.1	2460.0
6. $CH_4+HO_2=CH_3+H_2O_2$	1.80E+11	.0	18700.0
7. $CH_3+HO_2=CH_3O+OH$	2.00E+13	.0	.0
8. $CH_3+O=CH_2O+H$	8.00E+13	.0	.0
9. $CH_3+O_2=CH_3O+O$	2.05E+19	1.6	29229.0
10. $CH_2OH+H=CH_3+OH$	1.00E+14	.0	.0
11. $CH_3O+H=CH_3+OH$	1.00E+14	.0	.0
12. $CH_3+OH=CH_2+H_2O$	7.50E+06	2.0	5000.0
13. $CH_3O+M=CH_2O+H+M$	1.00E+14	.0	25000.0
14. $CH_2OH+M=CH_2O+H+M$	1.00E+14	.0	25000.0
15. $CH_3O+H=CH_2O+H_2$	2.00E+13	.0	.0
16. $CH_2OH+H=CH_2O+H_2$	2.00E+13	.0	.0
17. $CH_3O+OH=CH_2O+H_2O$	1.00E+13	.0	.0
18. $CH_2OH+OH=CH_2O+H_2O$	1.00E+13	.0	.0
19. $CH_3O+O=CH_2O+OH$	1.00E+13	.0	.0
20. $CH_2OH+O=CH_2O+OH$	1.00E+13	.0	.0
21. $CH_3O+O_2=CH_2O+HO_2$	6.30E+10	.0	2600.0
22. $CH_2OH+O_2=CH_2O+HO_2$	1.48E+13	.0	1500.0
23. $CH_2+H=CH+H_2$	1.00E+18	1.6	.0
24. $CH_2+OH=CH+H_2O$	1.13E+07	2.0	3000.0
25. $CH_2+OH=CH_2O+H$	2.50E+13	.0	.0
26. $CH+O_2=HCO+O$	3.30E+13	.0	.0
27. $CH+O=CO+H$	5.70E+13	.0	.0
28. $CH+OH=HCO+H$	3.00E+13	.0	.0
29. $CH+CO_2=HCO+CO$	3.40E+12	.0	690.0
30. $CH+H=C+H_2$	1.50E+14	.0	.0
31. $CH+H_2O=CH_2O+H$	1.17E+15	.8	.0
32. $CH+CH_2O=CH_2CO+H$	9.46E+13	.0	515.0
33. $CH+CH_2=C_2H_2+H$	4.00E+13	.0	.0
34. $CH+CH_3=C_2H_3+H$	3.00E+13	.0	.0

	A	β	E
35. $CH+CH_4=C_2H_4+H$	6.00E+13	.0	.0
36. $C+O_2=CO+O$	2.00E+13	.0	.0
37. $C+OH=CO+H$	5.00E+13	.0	.0
38. $C+CH_3=C_2H_2+H$	5.00E+13	.0	.0
39. $C+CH_2=C_2H+H$	5.00E+13	.0	.0
40. $CH_2+CO_2=CH_2O+CO$	1.10E+11	.0	1000.0
41. $CH_2+O=CO+2H$	5.00E+13	.0	.0
42. $CH_2+O=CO+H_2$	3.00E+13	.0	.0
43. $CH_2+O_2=CO_2+2H$	1.60E+12	.0	1000.0
44. $CH_2+O_2=CH_2O+O$	5.00E+13	.0	9000.0
45. $CH_2+O_2=CO_2+H_2$	6.90E+11	.0	500.0
46. $CH_2+O_2=CO+H_2O$	1.90E+10	.0	1000.0
47. $CH_2+O_2=HCO+OH$	4.30E+10	.0	500.0
48. $CH_2O+OH=HCO+H_2O$	3.43E+09	1.2	447.0
49. $CH_2O+H=HCO+H_2$	2.19E+08	1.8	3000.0
50. $CH_2O+M=HCO+H+M$	3.31E+16	.0	81000.0
51. $CH_2O+O=HCO+OH$	1.80E+13	.0	3080.0
52. $HCO+OH=H_2O+CO$	1.00E+14	.0	.0
53. $HCO+M=H+CO+M$	2.50E+14	.0	16802.0
<i>CO Enhanced by 1.9</i>			
<i>H2 Enhanced by 1.9</i>			
<i>CH4 Enhanced by 2.8</i>			
<i>CO2 Enhanced by 3.0</i>			
<i>H2O Enhanced by 5.0</i>			
54. $HCO+H=CO+H_2$	1.19E+13	.3	.0
55. $HCO+O=CO+OH$	3.00E+13	.0	.0
56. $HCO+O=CO_2+H$	3.00E+13	.0	.0
57. $HCO+O_2=HO_2+CO$	3.30E+13	.4	.0
58. $CO+O+M=CO_2+M$	6.17E+14	.0	3000.0
59. $CO+OH=CO_2+H$	1.51E+07	1.3	758.0
60. $CO+O_2=CO_2+O$	1.60E+13	.0	41000.0
61. $HO_2+CO=CO_2+OH$	5.80E+13	.0	22934.0
62. $C_2H_6+CH_3=C_2H_5+CH_4$	5.50E-01	4.0	8300.0
63. $C_2H_6+H=C_2H_5+H_2$	5.40E+02	3.5	5210.0
64. $C_2H_6+O=C_2H_5+OH$	3.00E+07	2.0	5115.0
65. $C_2H_6+OH=C_2H_5+H_2O$	8.70E+09	1.1	1810.0
66. $C_2H_4+H=C_2H_3+H_2$	1.10E+14	.0	8500.0
67. $C_2H_4+O=CH_3+HCO$	1.60E+09	1.2	746.0
68. $C_2H_4+OH=C_2H_3+H_2O$	2.02E+13	.0	5955.0
69. $CH_2+CH_3=C_2H_4+H$	3.00E+13	.0	.0
70. $H+C_2H_4+M=C_2H_5+M$	2.21E+13	.0	2066.0
<i>H2 Enhanced by 2.0</i>			
<i>CO Enhanced by 2.0</i>			
<i>CO2 Enhanced by 3.0</i>			
<i>H2O Enhanced by 5.0</i>			
71. $C_2H_5+H=2CH_3$	1.00E+14	.0	.0
72. $C_2H_5+O_2=C_2H_4+HO_2$	8.43E+11	.0	3875.0
73. $C_2H_2+O=CH_2+CO$	1.02E+07	2.0	1900.0
74. $C_2H_2+O=HCCO+H$	1.02E+07	2.0	1900.0

	A	β	E
75. $H_2 + C_2H = C_2H_2 + H$	4.09E+05	2.4	864.0
76. $H + C_2H_2 + M = C_2H_3 + M$.54E+12	.0	2410.0
<i>H2 Enhanced by 2.0</i>			
<i>CO Enhanced by 2.0</i>			
<i>CO2 Enhanced by 3.0</i>			
<i>H2O Enhanced by 5.0</i>			
77. $C_2H_3 + H = C_2H_2 + H_2$	4.00E+13	.0	.0
78. $C_2H_3 + O = CH_2CO + H$	3.00E+13	.0	.0
79. $C_2H_3 + O_2 = CH_2O + HCO$	4.00E+12	.0	250.0
80. $C_2H_3 + OH = C_2H_2 + H_2O$	5.00E+12	.0	.0
81. $C_2H_3 + CH_2 = C_2H_2 + CH_3$	3.00E+13	.0	.0
82. $C_2H_3 + C_2H = 2C_2H_2$	3.00E+13	.0	.0
83. $C_2H_3 + CH = CH_2 + C_2H_2$	5.00E+13	.0	.0
84. $OH + C_2H_2 = C_2H + H_2O$	3.37E+07	2.0	14000.0
85. $C_2H_2 + O = C_2H + OH$	3.16E+15	.6	15000.0
86. $CH_2CO + H = CH_3 + CO$	1.13E+13	.0	3428.0
87. $CH_2CO + O = CO_2 + CH_2$	1.75E+12	.0	1350.0
88. $CH_2CO + H = HCCO + H_2$	5.00E+13	.0	8000.0
89. $CH_2CO + O = HCCO + OH$	1.00E+13	.0	8000.0
90. $CH_2CO + OH = HCCO + H_2O$	7.50E+12	.0	2000.0
91. $CH_2CO + M = CH_2 + CO + M$	3.00E+14	.0	70980.0
92. $C_2H + O_2 = 2CO + H$	5.00E+13	.0	1500.0
93. $H + HCCO = CH_2 + CO$	1.00E+14	.0	.0
94. $O + HCCO = H + 2CO$	1.00E+14	.0	.0
95. $HCCO + O_2 = 2CO + OH$	1.60E+12	.0	854.0
96. $CH + HCCO = C_2H_2 + CO$	5.00E+13	.0	.0
97. $2HCCO = C_2H_2 + 2CO$	1.00E+13	.0	.0
98. $CH_2 + CH_4 = 2CH_3$	4.00E+13	.0	.0
99. $CH_2 + C_2H_6 = CH_3 + C_2H_5$	1.20E+14	.0	.0
100. $CH_2 + O_2 = CO + OH + H$	3.00E+13	.0	.0
101. $CH_2 + H_2 = CH_3 + H$	7.00E+13	.0	.0
102. $C_2H + O = CH + CO$	5.00E+13	.0	.0
103. $C_2H + OH = HCCO + H$	2.00E+13	.0	.0
104. $2CH_2 = C_2H_2 + H_2$	4.00E+13	.0	.0
105. $CH_2 + HCCO = C_2H_3 + CO$	3.00E+13	.0	.0
106. $C_2H_2 + O_2 = HCCO + OH$	2.00E+08	1.5	30100.0
107. $C_2H_2 + M = C_2H + H + M$	4.20E+16	.0	107000.0
108. $C_2H_4 + M = C_2H_2 + H_2 + M$	1.50E+15	.0	55800.0
109. $C_2H_4 + M = C_2H_3 + H + M$	1.40E+16	.0	82360.0
110. $H_2 + O_2 = 2OH$	1.70E+13	.0	47780.0
111. $OH + H_2 = H_2O + H$	1.17E+09	1.3	3626.0
112. $O + OH = O_2 + H$	4.00E+14	-.5	.0
113. $O + H_2 = OH + H$	5.06E+04	2.7	6290.0
114. $H + O_2 + M = HO_2 + M$	3.61E+17	-.7	.0
<i>H2O Enhanced by 18.6</i>			
<i>CO2 Enhanced by 4.2</i>			
<i>H2 Enhanced by 2.9</i>			
<i>CO Enhanced by 2.1</i>			
<i>N2 Enhanced by 1.3</i>			

	A	β	E
115. $H+O_2+O_2=HO_2+O_2$	6.70E+19	-1.4	.0
116. $OH+HO_2=H_2O+O_2$	7.50E+12	.0	.0
117. $H+HO_2=2OH$	1.40E+14	.0	1073.0
118. $O+HO_2=O_2+OH$	1.40E+13	.0	1073.0
119. $2OH=O+H_2O$	6.00E+08	1.3	.0
120. $2H+M=H_2+M$	1.00E+18	-1.0	.0
121. $2H+H_2=2H_2$	9.20E+16	-.6	.0
122. $2H+H_2O=H_2+H_2O$	6.00E+19	-1.3	.0
123. $2H+CO_2=H_2+CO_2$	5.49E+20	-2.0	.0
124. $H+OH+M=H_2O+M$	1.60E+22	-2.0	.0
<i>H2O Enhanced by 5.0</i>			
125. $H+O+M=OH+M$	6.20E+16	-.6	.0
<i>H2O Enhanced by 5.0</i>			
126. $2O+M=O_2+M$	1.89E+13	.0	1788.0
127. $H+HO_2=H_2+O_2$	1.25E+13	.0	.0
128. $2HO_2=H_2O_2+O_2$	2.00E+12	.0	.0
129. $H_2O_2+M=2OH+M$	1.30E+17	.0	45500.0
130. $H_2O_2+H=HO_2+H_2$	1.60E+12	.0	3800.0
131. $H_2O_2+OH=H_2O+HO_2$	1.00E+13	.0	1800.0
132. $HO_2+NO=NO_2+OH$	2.11E+12	.0	-479.0
133. $NO_2+H=NO+OH$	3.50E+14	.0	1500.0
134. $NO_2+O=NO+O_2$	1.00E+13	.0	600.0
135. $NH+O_2=HNO+O$	1.00E+13	.0	12000.0
136. $NH+O_2=NO+OH$	7.60E+10	.0	1530.0
137. $NH+NO=N_2O+H$	4.33E+14	5	.0
138. $N_2O+H=N_2+OH$	7.60E+13	.0	15200.0
139. $NH+OH=HNO+H$	2.00E+13	.0	.0
140. $NH+OH=N+H_2O$	5.00E+11	.5	2000.0
141. $NH+N=N_2+H$	3.00E+13	.0	.0
142. $NH+H=N+H_2$	1.00E+13	.0	.0
143. $NH_2+O=HNO+H$	6.63E+14	-.5	.0
144. $NH_2+O=NH+OH$	6.75E+12	.0	.0
145. $NH_2+OH=NH+H_2O$	4.00E+06	.0	1600.0
146. $NH_2+H=NH+H_2$	6.92E+13	.0	3650.0
147. $NH_2+NO=NNH+OH$	6.40E+15	-1.3	.0
148. $NH_2+NO=N_2+H_2O$	6.20E+15	-1.3	.0
149. $NH_3+OH=NH_2+H_2O$	2.04E+06	2.0	566.0
150. $NH_3+H=NH_2+H_2$	6.36E+05	2.4	10171.0
151. $NH_3+O=NH_2+OH$	2.10E+13	.0	9000.0
152. $NNH+M=N_2+H+M$	2.00E+14	.0	20000.0
153. $NNH+NO=N_2+HNO$	5.00E+13	.0	.0
154. $NNH+H=N_2+H_2$	1.00E+14	.0	.0
155. $HNO+M=H+NO+M$	1.50E+16	.0	48680.0
<i>H2O Enhanced by 10.0</i>			
<i>O2 Enhanced by 2.0</i>			
<i>H2 Enhanced by 2.0</i>			
<i>N2 Enhanced by 2.0</i>			
156. $HNO+OH=NO+H_2O$	3.60E+13	.0	.0
157. $HNO+H=H_2+NO$	5.00E+12	.0	.0

	A	β	E
158. $N+NO=N_2+O$	3.27E+12	.3	.0
159. $N+O_2=NO+O$	6.40E+09	1.0	6280.0
160. $N+OH=NO+H$	3.80E+13	.0	.0
161. $CH_4+O=CH_3+OH$	1.02E+09	1.5	8604.0
162. $CH+C_2H_2=C_3H_2+H$	1.00E+14	.0	.0
163. $CH+N_2=HCN+N$	3.00E+11	.0	13600.0
164. $CN+N=C+N_2$	1.04E+15	.5	.0
165. $CH_2+N_2=HCN+NH$	1.00E+13	.0	74000.0
166. $C+NO=CN+O$	6.60E+13	.0	.0
167. $CH+NO=HCN+O$	1.10E+14	.0	.0
168. $CH_3+NO=HCN+H_2O$	1.00E+11	.0	15000.0
169. $CH_2+NO=HCN+OH$	2.00E+13	.0	.0
170. $CH_2+N=HCN+H$	5.00E+13	.0	.0
171. $CH+N=CN+H$	1.30E+13	.0	.0
172. $CO_2+N=NO+CO$	1.90E+11	.0	3400.0
173. $HCCO+N=HCN+CO$	5.00E+13	.0	.0
174. $C_2H_3+N=HCN+CH_2$	2.00E+13	.0	.0
175. $C_3H_3+N=HCN+C_2H_2$	1.00E+13	.0	.0
176. $HCN+OH=CN+H_2O$	1.45E+13	.0	10929.0
177. $OH+HCN=HNCO+H$	1.98E-03	4.0	1000.0
178. $OH+HCN=NH_2+CO$	7.83E-04	4.0	4000.0
179. $HCN+O=NCO+H$	1.38E+04	2.6	4980.0
180. $HCN+O=NH+CO$	3.45E+03	2.6	4980.0
181. $HCN+O=CN+OH$	2.70E+09	1.6	26600.0
182. $CN+H_2=HCN+H$	2.95E+05	2.5	2237.0
183. $CN+O=CO+N$	1.80E+13	.0	.0
184. $CN+O_2=NCO+O$	5.60E+12	.0	.0
185. $CN+OH=NCO+H$	6.00E+13	.0	.0
186. $CN+HCN=C_2N_2+H$	2.00E+13	.0	.0
187. $CN+NO_2=NCO+NO$	3.00E+13	.0	.0
188. $CN+N_2O=NCO+N_2$	1.00E+13	.0	.0
189. $C_2N_2+O=NCO+CN$	4.57E+12	.0	8880.0
190. $NO_2+M=NO+O+M$	1.10E+16	.0	66000.0
191. $NCO+H=NH+CO$	5.00E+13	.0	.0
192. $NCO+O=NO+CO$	2.00E+13	.0	.0
193. $NCO+N=N_2+CO$	2.00E+13	.0	.0
194. $NCO+OH=NO+CO+H$	1.00E+13	.0	.0
195. $NCO+M=N+CO+M$	3.10E+16	.5	48000.0
196. $NCO+NO=N_2O+CO$	1.00E+13	.0	390.0
197. $NCO+H_2=HNCO+H$	8.58E+12	.0	9000.0
198. $HNCO+H=NH_2+CO$	2.00E+13	.0	3000.0
199. $N_2O+OH=N_2+HO_2$	2.00E+12	.0	10000.0
200. $N_2O+M=N_2+O+M$	1.60E+14	.0	51600.0
201. $N_2O+O=N_2+O_2$	1.00E+14	.0	28200.0
202. $N_2O+O=NO+NO$	1.00E+14	.0	28200.0
203. $NNH+OH=N_2+H_2O$	5.00E+13	.0	.0
204. $NNH+NH_2=N_2+NH_3$	5.00E+13	.0	.0
205. $NNH+NH=N_2+NH_2$	5.00E+13	.0	.0
206. $NNH+O=N_2O+H$	1.00E+14	.0	.0

	A	β	E
207. $HNO+NH_2=NH_3+NO$	2.00E+13	.0	1000.0
208. $OH+C_2H_2=CH_2CO+H$	2.18E-04	4.5	1000.0
209. $OH+C_2H_2=CH_3+CO$	4.83E-04	4.0	2000.0
210. $C_2H+C_2H_2=C_4H_2+H$	3.00E+13	.0	.0
211. $CH_2+C_2H_2=C_3H_3+H$	1.20E+13	.0	6600.0
212. $C_4H_2+OH=C_3H_2+HCO$	6.66E+12	.0	410.0
213. $C_3H_2+O_2=HCO+HCCO$	1.00E+13	.0	.0
214. $C_3H_3+O_2=CH_2CO+HCO$	3.00E+10	.0	2868.0
215. $C_3H_3+O=CH_2O+C_2H$	2.00E+13	.0	.0
216. $C_3H_3+OH=C_3H_2+H_2O$	2.00E+13	.0	.0
217. $C_2H_2+C_2H_2=C_4H_3+H$	2.00E+12	.0	45900.0
218. $C_4H_3+M=C_4H_2+H+M$	1.00E+16	.0	59700.0
219. $C_4H_2+O=C_3H_2+CO$	1.20E+12	.0	.0

NOTE: A units mole·cm·sec·K, E units cal/mole

APPENDIX B
Thermodynamic Data Base
From NACOMB87.DAT

THERMODYNAMIC DATA BASE

C(S)	J 3/61	C 10 00 00 OS	300.000 5000.000	1
0.13604942E 01	0.19182237E-02	-0.84040389E-06	0.16448707E-09 -0.11672670E-13	2
-0.65713870E 03	-0.80070207E 01	-0.44778053E 00	0.53691002E-02 -0.39775571E-06	3
-0.40459298E-08	0.21134939E-11	-0.94280688E 02	0.16840791E 01 2.	4
C	J 3/61	C 100 000 000 OG	300.000 5000.000	1
0.25810663E 01	-0.14696202E-03	0.74388084E-07	-0.79481079E-11 0.58900977E-16	2
0.85216294E 05	0.43128879E 01	0.25328705E 01	-0.15887641E-03 0.30682082E-06	3
-0.26770064E-09	0.87488827E-13	0.85240422E 05	0.46062374E 01	4
C+	L12/66	C 1E -100 000 OG	300.000 5000.000	1
0.25118274E 01	-0.17359784E-04	0.95042676E-08	-0.22188518E-11 0.18621892E-15	2
0.21667721E 06	0.42861298E 01	0.25953840E 01	-0.40686645E-03 0.68923669E-06	3
-0.52664878E-09	0.15083377E-12	0.21666281E 06	0.38957298E 01	4
C-	J 9/65	C 1E 100 000 OG	300.000 5000.000	1
0.24470591E 01	0.11286428E-03	-0.78591462E-07	0.19778614E-10 -0.11105555E-14	2
0.69972969E 05	0.42356992E 01	0.24925640E 01	0.53153068E-04 -0.13307994E-06	3
0.13951379E-09	-0.52150992E-13	0.69955757E 05	0.39811657E 01	4
CH	J12/67	C 1H 10 00 OG	300.000 5000.000	1
0.22673116E 01	0.22043000E-02	-0.62250191E-06	0.69689940E-10 -0.21274952E-14	2
0.70838037E 05	0.87889352E 01	0.35632752E 01	-0.20031372E-03 -0.40129814E-06	3
0.18226922E-08	-0.86768311E-12	0.70405506E 05	0.17628023E 01	4
CH+	J12/71	C 1H 1E -1 OG	300.000 5000.000	1
0.27466401E+01	0.15496991E-02	-0.52858324E-06	0.86132075E- -0.50909775E-14	2
0.19483672E+06	0.46994695E+01	0.35601593E+01	-0.22478101E-03 -0.26341623E-06	3
0.16716214E-08	-0.89478626E-12	0.19460363E+06	0.41570213E+00	4
CH2	J12/72	C 1H 2 0 OG	300.000 5000.000	1
0.27525479E+01	0.39782047E-02	-0.14921731E-05	0.25956899E-09 -0.17110673E-13	2
0.45547759E+05	0.66534799E+01	0.35883347E+01	0.21724137E-02 -0.13323408E-05	3
0.19469445E-08	-0.89431394E-12	0.45315188E+05	0.22627869E+01	4
CH2CO		C 2H 2O 1 G	300. 5000.	1
2.64750000E+00	1.44453000E-02	-0.93435500E-05	2.37345000E-09 0.00000000E+00	2
-5.70000000E+03	9.86474460E+00	2.64750000E+00	1.44453000E-02 -0.93435500E-05	3
2.37345000E-09	0.00000000E+00	-5.70000000E+03	9.86474460E+00	4
CH2O	J 3/61	C 1H 2O 10 OG	300.000 5000.000	1
0.28364249E 01	0.68605298E-02	-0.26882647E-05	0.47971258E-09 -0.32118406E-13	2
-0.15236031E 05	0.78531169E 01	0.37963783E 01	-0.25701785E-02 0.18548815E-04	3
-0.17869177E-07	0.55504451E-11	-0.15088947E 05	0.47548163E 01	4

CH2OH		C 1H 3O 1 G	300.000	5000.000	1
0.63368688E+01	0.45510226E-02	-0.21093260E-05	0.41259997E-09	-0.27800781E-13	2
-0.96832313E+04	-0.11239777E+02	0.30464578E+01	0.80451022E-02	0.24033189E-05	3
-0.71893524E-08	0.28578380E-11	-0.83207148E+04	0.75517490E+01		4
CH3	J 6/69	C 1H 3O 00 OG	300.000	5000.000	1
0.28400327E 01	0.60869086E-02	-0.21740338E-05	0.36042576E-09	-0.22725300E-13	2
0.16449813E 05	0.55056751E 01	0.34666350E 01	0.38301845E-02	0.10116802E-05	3
-0.18859236E-08	0.66803182E-12	0.16313104E 05	0.24172192E 01		4
CH3O		C 1H 3O 1 G	300.000	5000.000	1
0.63368688E+01	0.45510226E-02	-0.21093260E-05	0.41259997E-09	-0.27800781E-13	2
-0.87598421E+03	-0.11239777E+02	0.30464578E+01	0.80451022E-02	0.24033189E-05	3
-0.71893524E-08	0.28578380E-11	0.48653233E+03	0.75517490E+01		4
CH4	J 3/61	C 1H 400 000 OG	300.000	5000.000	1
0.15027072E 01	0.10416798E-01	-0.39181522E-05	0.67777899E-09	-0.44283706E-13	2
-0.99787078E 04	0.10707143E 02	0.38261932E 01	-0.39794581E-02	0.24558340E-04	3
-0.22732926E-07	0.69626957E-11	-0.10144950E 05	0.86690073E 00		4
CN	J 6/69	C 1N 10 00 OG	300.000	5000.000	1
0.36036285E 01	0.33644390E-03	0.10028933E-06	-0.16318166E-10	-0.36286722E-15	2
0.51159833E 05	0.35454505E 01	0.37386307E 01	-0.19239224E-02	0.47035189E-05	3
-0.31113000E-08	0.61675318E-12	0.51270927E 05	0.34490218E 01		4
CN+	J12/70	C 1N 1E -10 OG	300.000	5000.000	1
0.36522919E+01	0.81427579E-03	-0.20853348E-06	0.29071604E-10	-0.17865094E-14	2
0.21560182E+06	0.43916910E+01	0.36175018E+01	-0.20179550E-02	0.79359855E-05	3
-0.77300616E-08	0.24798477E-11	0.21578134E+06	0.53579527E+01		4
CN-	J12/70	C 1N 1E 10 OG	300.000	5000.000	1
0.29471725E+01	0.14988427E-02	-0.57579547E-06	0.10177789E-09	-0.67478503E-14	2
0.63644338E+04	0.63743952E+01	0.37034310E+01	-0.14896426E-02	0.31864701E-05	3
-0.14831305E-08	0.48121663E-13	0.62335826E+04	0.27722843E+01		4
CO	J 9/65	C 1O 100 000 OG	300.000	5000.000	1
0.29840696E 01	0.14891390E-02	-0.57899684E	-06 0.10364577E-09	-0.69353550E-14	2
-0.14245228E 05	0.63479156E 01	0.37100928E	01-0.16190964E-02	0.36923594E-05	3
-0.20319674E-08	0.23953344E-12	-0.14356310E	05 0.29555351E 01		4
CO2	J 9/65	C 1O 200 000 OG	300.000	5000.000	1
0.44608041E	01 0.30981719E-02	-0.12392571E-05	0.22741325E-09	-0.15525954E-13	2
-0.48961442E	05-0.98635982E 00	0.24007797E 01	0.87350957E-02	-0.66070878E-05	3
0.20021861E	-08 0.63274039E-15	-0.48377527E 05	0.96951457E 01		4
CO2-	J12/66	C 1O 2E 100 OG	300.000	5000.000	1
0.45454640E 01	0.26054316E-02	-0.10928732E-05	0.20454421E-09	-0.14184542E-13	2
-0.54761968E 05	0.18317369E 01	0.34743737E 01	0.16913805E-02	0.73533803E-05	3
-0.99554255E-08	0.36846719E-11	-0.54249049E 05	0.83834329E 01		4

C2H		C 2H 1	G	300.000	5000.000	1
0.45648394E+01	0.20059461E-02	-0.49348481E-06	0.74284901E-10	-0.54309610E-14		2
0.62282356E+05	-0.19872781E+01	0.24076798E+01	0.10174531E-01	-0.13836531E-04		3
0.10476414E-07	-0.30759392E-11	0.62816474E+05	0.87170410E+01			4
C2H2	J 3/61	C 2H 200 000 0G	300.000	5000.000		1
0.45751083E 01	0.51238358E-02	-0.17452354E-05	0.28673065E-09	-0.17951426E-13		2
0.25607428E 05	-0.35737940E 01	0.14102768E 01	0.19057275E-01	-0.24501390E-04		3
0.16390872E-07	-0.41345447E-11	0.26188208E 05	0.11393827E 02			4
C2H3		C 2H 3	G	300.000	5000.000	1
0.61400977E+01	0.37377094E-02	-0.27031722E-06	-0.15377419E-09	0.21952953E-13		2
0.31211517E+05	-0.96864340E+01	0.29617599E+01	0.89272478E-02	-0.75394764E-06		3
-0.28486517E-08	0.11892601E-11	0.32396554E+05	0.79274876E+01			4
C2H4	J 9/65	C 2H 400 000 0G	300.000	5000.000		1
0.34552152E 01	0.11491803E-01	-0.43651750E-05	0.76155095E-09	-0.50123200E-13		2
0.44773119E 04	0.26987959E 01	0.14256821E 01	0.11383140E-01	0.79890006E-05		3
-0.16253679E-07	0.67491256E-11	0.53370755E 04	0.14621819E 02			4
C2H5		C 2H 5 0 0G	300.000	5000.000	1000.00	1
0.33121281E+01	0.13950736E-01	-0.50743188E-05	0.82857310E-09	-0.50269772E-13		2
0.12277491E+05	0.41015129E+01	0.29107187E+01	0.92690215E-02	0.90435051E-05		3
-0.11535964E-07	0.32795678E-11	0.12738983E+05	0.77862067E+01			4
C2H6	L 5/72	C 2H 6 0 0G	300.000	1500.000		1
0.21555281E+01	0.14779861E-01	0.23352804E-05	-0.64146428E-08	0.19036925E-11		2
-0.11524517E+05	0.10776316E+02	0.21415788E+01	0.10529720E-01	0.18730274E-04		3
-0.26691187E-07	0.10049332E-10	-0.11410486E+05	0.11647757E+02			4
C2N2	J 3/61	C 2N 200 000 0G	300.000	5000.000		1
0.65968935E 01	0.38694131E-02	-0.15516161E-05	0.28141546E-09	-0.19069442E-13		2
0.34883726E 05	-0.10001801E 02	0.39141782E 01	0.14011008E-01	-0.17404350E-04		3
0.12012779E-07	-0.33565772E-11	0.35514550E 05	0.32384353E 01			4
C3H2		C 3H 2	G	300.000	5000.000	1
0.79426799E+01	0.32122819E-02	-0.17244707E-06	-0.13701012E-09	0.18399355E-13		2
0.50684927E+05	-0.18999670E+02	0.24911352E+01	0.14011657E-01	0.23898325E-05		3
-0.17056545E-07	0.90278239E-11	0.52310689E+05	0.99652415E+01			4
C3H3		C 3H 3	G	300.000	5000.000	1
0.57469726E+01	0.96155313E-02	-0.38051491E-05	0.68993907E-09	-0.46561597E-13		2
0.36529931E+05	-0.58634502E+01	0.30908408E+01	0.13549582E-01	0.27253533E-05		3
-0.14363185E-07	0.71981410E-11	0.37356544E+05	0.84916890E+01			4
C4H2		C 4H 2	G	300.000	4000.000	1
0.90831114E+01	0.58389517E-02	-0.18490676E-05	0.25895282E-09	-0.12860016E-13		2
0.51243411E+05	-0.24044444E+02	0.31946607E+01	0.20400085E-01	-0.34472061E-05		3
-0.17628748E-07	0.10800297E-10	0.52693302E+05	0.61287466E+01			4

C4H3		C 4H 3	G	300.000	4000.000	1
0.78607135E+01	0.97995789E-02	-0.35577026E-05	0.58884173E-09	-0.36403343E-13		2
0.51728752E+05	-0.15501684E+02	0.66140550E+00	0.38628795E-01	-0.51227651E-04		3
0.38204268E-07	-0.11611788E-10	0.53314655E+05	0.19590502E+02			4
H	J 9/65	H 100 000 000 0G		300.000	5000.000	1
0.25000000E 01	0.	0.	0.		0.	2
0.25471627E 05	-0.46011763E 00	0.25000000E 01	0.		0.	3
0.	0.	0.25471627E 05	-0.46011762E 00			4
H+	J 6/66	H 1E -100 000 0G		300.000	5000.000	1
0.25000000E 01	0.	0.	0.		0.	2
0.18403344E 06	-0.11538620E 01	0.25000000E 01	0.		0.	3
0.	0.	0.18403344E 06	-0.11538621E 01			4
H-	J 9/65	H 1E 100 000 0G		300.000	5000.000	1
0.25000000E 01	0.	0.	0.		0.	2
0.15961045E 05	-0.11524488E 01	0.25000000E 01	0.		0.	3
0.	0.	0.15961045E 05	-0.11524486E 01			4
HCCO	J29/80	C 2O 1H 1 G		300.0	5000.0	1
0.55144941E+01	0.41394403E-02	-0.15878702E-05	0.27977639E-09	-0.18584209E-13		2
+1.91731230E+04	-0.31425253E+01	0.25098874E+01	0.12171605E-01	-0.78618375E-05		3
0.35351571E-09	0.11540858E-11	2.00000000E+04	0.12399634E+02			4
HCN	L12/69	H 1C 1N 10 0G		300.000	5000.000	1
0.37068121E 01	0.33382803E-02	-0.11913320E-05	0.19992917E-09	-0.12826452E-13		2
0.14962636E 05	0.20794904E 01	0.24513556E 01	0.87208371E-02	-0.10094203E-04		3
0.67255698E-08	-0.17626959E-11	0.15213002E 05	0.80830085E 01			4
HCO	J12/70	H 1C 1O 10 0G		300.000	5000.000	1
0.34738348E+01	0.34370227E-02	-0.13632664E-05	0.24928645E-09	-0.17044331E-13		2
0.39594005E+04	0.60453340E+01	0.38840192E+01	-0.82974448E-03	0.77900809E-05		3
-0.70616962E-08	0.19971730E-11	0.40563860E+04	0.48354133E+01			4
HCO+	J12/70	H 1C 1O 1E -1G		300.000	5000.000	1
0.37411880E+01	0.33441517E-02	-0.12397121E-05	0.21189388E-09	-0.13704150E-13		2
0.98884078E+05	0.20654768E+01	0.24739736E+01	0.86715590E-02	-0.10031500E-04		3
0.67170527E-08	-0.17872674E-11	0.99146608E+05	0.81625751E+01			4
HNCO	J12/70	H 1N 1C 1O 1G		300.000	5000.000	1
0.51300390E+01	0.43551371E-02	-0.16269022E-05	0.28035605E-09	-0.18276037E-13		2
-0.14101787E+05	-0.22010995E+01	0.23722164E+01	0.13664040E-01	-0.13323158E-04		3
0.64475457E-08	-0.10402894E-11	-0.13437059E+05	0.11588263E+02			4
HNO	J 3/63	H 1N 1O 10 0G		300.000	5000.000	1
0.35548619E 01	0.32713182E-02	-0.12734071E-05	0.22602046E-09	-0.15064827E-13		2
0.10693734E 05	0.51684901E 01	0.37412008E 01	-0.20067061E-03	0.75409300E-05		3
-0.79105713E-08	0.25928389E-11	0.10817845E 05	0.50063473E 01			4

H2	J 3/61	H 20 00 00 0G	300.000 5000.000	1
0.31001901E 01	0.51119464E-03	0.52644210E-07	-0.34909973E-10 0.36945345E-14	2
-0.87738042E 03	-0.19629421E 01	0.30574451E 01	0.26765200E-02 -0.58099162E-05	3
0.55210391E-08	-0.18122739E-11	-0.98890474E 03	-0.22997056E 01	4
H2O(S)	L11/65	H 2O 100 000 0S	200.000 273.150	1
0.	0.	0.	0. 0.	2
0.	0.	-0.39269330E-01	0.16920420E-01 0.	3
0.	0.	-0.35949581E 05	0.56933784E 00	4
H2O(L)	L11/65	H 2O 100 000 0L	273.150 1000.0	1
0.	0.	0.	0. 0.	2
0.	0.	0.12712782E 02	-0.17662790E-01 -0.22556661E-04	3
0.20820908E-06	-0.24078614E-09	-0.37483200E 05	-0.59115345E 02	4
H2O	J 3/61	H 2O 100 000 0G	300.000 5000.000	1
0.27167633E 01	0.29451374E-02	-0.80224374E-06	0.10226682E-09 -0.48472145E-14	2
-0.29905826E 05	0.66305671E 01	0.40701275E 01	-0.11084499E-02 0.41521180E-05	3
-0.29637404E-08	0.80702103E-12	-0.30279722E 05	-0.32270046E 00	4
H2O2	L 2/69	H 2O 20 00 0G	300.000 5000.000	1
0.45731667E 01	0.43361363E-02	-0.14746888E-05	0.23489037E-09 -0.14316536E-13	2
-0.18006961E 05	0.50113696E 00	0.33887536E 01	0.65692260E-02 -0.14850126E-06	3
-0.46258055E-08	0.24715147E-11	-0.17663147E 05	0.67853631E 01	4
N	J 3/61	N 100 000 000 0G	300.000 5000.000	1
0.24502682E+01	0.10661458E-03	-0.74653373E-07	0.18796524E-10 -0.10259839E-14	2
0.56116040E 05	0.44487581E 01	0.25030714E 01	-0.21800181E-04 0.54205287E-07	3
-0.56475602E-10	0.20999044E-13	0.56098904E 05	0.41675664E 01	4
NCO		C 1N 1O 1 0G	298.000 6000.000 1000.00	1
0.53652081E+01	0.20130952E-02	-0.74677047E-06	0.12255391E-09 -0.73190821E-14	2
0.17225793E+05	-0.38094556E+01	0.32227991E+01	0.56548542E-02 0.27579890E-06	3
-0.50998485E-08	0.26931623E-11	0.17971971E+05	0.79024191E+01	4
NH		N 1H 1 G	300.000 5000.000	1
0.27602491E+01	0.13753462E-02	-0.44519143E-06	0.76927915E-1 -0.50175923E-14	2
0.42078281E+05	0.58571992E+01	0.33397579E+01	0.12530086E-02 -0.34916459E-05	3
0.42188120E-08	-0.15576179E-11	0.41850473E+05	0.25071807E+01	4
NH2		N 1H 2 G	300.000 5000.000	1
0.25141589E+01	0.37243452E-02	-0.13176448E-05	0.21889114E-09 -0.13940907E-13	2
0.23350231E+05	0.82483222E+01	0.41425766E+01	-0.17680285E-02 0.59665661E-05	3
-0.44238885E-08	0.12085839E-11	0.22956119E+05	0.91841706E-01	4
NH3	J 9/65	N 1H 300 000 0G	300.000 5000.000	1
0.24165177E 01	0.61871211E-02	-0.21785136E-05	0.37599090E-09 -0.24448856E-13	2
-0.64747177E 04	0.77043482E 01	0.35912768E 01	0.49388668E-03 0.83449322E-05	3
-0.83833385E-08	0.27299092E-11	-0.66717143E 04	0.22520966E 01	4

NNH		N 2H 1	G	300.	5000.	1
0.35548619E 01	0.32713182E-02	-0.12734071E-05	0.22602046E-09	-0.15064827E-13		2
0.283758886E 05	0.51684901E 01	0.37412008E 01	-0.20067061E-03	0.75409300E-05		3
-0.79105713E-08	0.25928389E-11	0.28500000E 05	0.50063473E 01			4
NO	J 6/63	N 1O 100 000 0G	300.000	5000.000		1
0.31890000E 01	0.13382281E-02	-0.52899318E-06	0.95919332E-10	-0.64847932E-14		2
0.98283290E 04	0.67458126E 01	0.40459521E 01	-0.34181783E-02	0.79819190E-05		3
-0.61139316E-08	0.15919076E-11	0.97453934E 04	0.29974988E 01			4
NO+	J 6/66	N 1O 1E -100 0G	300.000	5000.000		1
0.28885488E 01	0.15217119E-02	-0.57531241E-06	0.10051081E-09	-0.66044294E-14		2
0.11819245E 06	0.70027197E 01	0.36685056E 01	-0.11544580E-02	0.21755608E-05		3
-0.48227472E-09	-0.27847906E-12	0.11803369E 06	0.31779324E 01			4
NO2	J 9/64	N 1O 200 000 0G	300.000	5000.000		1
0.46240771E 01	0.25260332E-02	-0.10609498E-05	0.19879239E-09	-0.13799384E-13		2
0.22899900E 04	0.13324138E 01	0.34589236E 01	0.20647064E-02	0.66866067E-05		3
-0.95556725E-08	0.36195881E-11	0.28152265E 04	0.83116983E 01			4
NO2-	J 6/72	N 1O 2E 1 0G	300.000	5000.000		1
0.50160903E+01	0.21884463E-02	-0.94586144E-06	0.17939789E-09	-0.12052428E-13		2
-0.26200160E+05	-0.12861447E+01	0.29818036E+01	0.49398681E-02	0.28557293E-05		3
-0.78905297E-08	0.35391483E-11	-0.25501540E+05	0.99161680E+01			4
N2	J 9/65	N 2O 00 00 0G	300.000	5000.000		1
0.28963194E 01	0.15154866E-02	-0.57235277E-06	0.99807393E-10	-0.65223555E-14		2
-0.90586184E 03	0.61615148E 01	0.36748261E 01	-0.12081500E-02	0.23240102E-05		3
-0.63217559E-09	-0.22577253E-12	-0.10611588E 04	0.23580424E 01			4
N2O	J12/64	N 2O 100 000 0G	300.000	5000.000		1
0.47306679E 01	0.28258267E-02	-0.11558115E-05	0.21263683E-09	-0.14564087E-13		2
0.81617682E 04	-0.17151073E 01	0.26189196E 01	0.86439616E-02	-0.68110624E-05		3
0.22275877E-08	-0.80650330E-13	0.87590123E 04	0.92266952E 01			4
N2O+	J12/70	N 2O 1E -10 0G	300.000	5000.000		1
0.53926946E+01	0.22337196E-02	-0.93548832E-06	0.17466166E-09	-0.12059043E-13		2
0.15847633E+06	-0.36920186E+01	0.34273064E+01	0.63787690E-02	-0.22585149E-05		3
-0.20421800E-08	0.13481477E-11	0.15909237E+06	0.67997616E+01			4
O	J 6/62	O 100 000 000 0G	300.000	5000.000		1
0.25420596E 01	-0.27550619E-04	-0.31028033E-08	0.45510674E-11	-0.43680515E-15		2
0.29230803E 05	0.49203080E 01	0.29464287E 01	-0.16381665E-02	0.24210316E-05		3
-0.16028432E-08	0.38906964E-12	0.29147644E 05	0.29639949E 01			4
O+	L12/66	O 1E -100 000 0G	300.000	5000.000		1
0.25060486E 01	-0.14464249E-04	0.12446049E-07	-0.46858472E-11	0.65548873E-15		2
0.18794700E 06	0.43479741E 01	0.24984794E 01	0.11410972E-04	-0.29761395E-07		3
0.32246539E-10	-0.12375517E-13	0.18794908E 06	0.43864355E 01			4

O-	J 6/65	O 1E 100 000 0G	300.000 5000.000	1
0.25437173E 01	-0.53258700E-04	0.25119617E-07	-0.51851466E-11 0.39011542E-15	2
0.11480516E 05	0.45202538E 01	0.28115796E 01	-0.11905697E-02 0.18710553E-05	3
-0.13479178E-08	0.36663554E-12	0.11428431E 05	0.32402855E 01	4
OH	J12/70	O 1H 10 00 0G	300.000 5000.000	1
0.29131230E+01	0.95418248E-03	-0.19084325E-06	0.12730795E-10 0.24803941E-15	2
0.39647060E+04	0.54288735E+01	0.38365518E+01	-0.10702014E-02 0.94849757E-06	3
0.20843575E-09	-0.23384265E-12	0.36715807E+04	0.49805456E+00	4
OH+	J12/70	O 1H 1E -10 0G	300.000 5000.000	1
0.27381495E+01	0.14613173E-02	-0.46950536E-06	0.73663560E-10 -0.41410922E-14	2
0.15761683E+06	0.61343811E+01	0.35365969E+01	-0.47029254E-04 -0.62344259E-06	3
0.17601461E-08	-0.82678699E-12	0.15736677E+06	0.18477172E+01	4
OH-	J12/70	O 1H 1E 10 0G	300.000 5000.000	1
0.28881148E+01	0.96560229E-03	-0.19659254E-06	0.14053802E-10 0.12080617E-15	2
-0.18086455E+05	0.41896259E+01	0.34621427E+01	0.40525802E-03 -0.13516992E-05	3
0.17899459E-08	-0.63434810E-12	-0.18312355E+05	0.92893220E+00	4
O2	J 9/65	O 20 00 00 0G	300.000 5000.000	1
0.36219535E 01	0.73618264E-03	-0.19652228E-06	0.36201558E-10 -0.28945627E-14	2
-0.12019825E 04	0.36150960E 01	0.36255985E 01	-0.18782184E-02 0.70554544E-05	3
-0.67635137E-08	0.21555993E-11	-0.10475226E 04	0.43052778E 01	4
O2-	J12/66	O 2E 100 000 0G	300.000 5000.000	1
0.38147234E 01	0.77444546E-03	-0.30677649E-06	0.56618118E-10 -0.38229492E-14	2
-0.69910087E 04	0.29587995E 01	0.31440525E 01	0.12127972E-02 0.23812161E-05	3
-0.40914092E-08	0.16885304E-11	-0.67369752E 04	0.67688687E 01	4

APPENDIX C
CHEMKIN .grf File Manipulation Program
FILE2.FOR

C JIM HUNDERUP

REVISED 7-23-91

C THIS PROGRAM MANIPULATES THE .GRF FILE FROM CHEMKIN TO
C CREATE NEW FILES OF DATA FOR GRAPHING PURPOSES.

```
REAL X0,X1,DX,VEL,VEL1,VAVG,TU,DT,TIME,S1,S2,DUM,NOX,NO2NOX,DU,  
+   DU1,DATA,X,Y,T0  
INTEGER TUF,K,K1,LINES,INOR,INOC,INO2R,INO2C,IDU,IDU1,XVR,XVC,YVR,  
+   YVC  
CHARACTER SOURCE*12,NEWFILE*12,FC*1,SPECIE*6,XVAR*7,YVAR*7,YN*1  
DIMENSION TIME(100),SPECIE(5,11),S1(100),S2(100),NOX(100),  
+   NO2NOX(100),DATA(5,11,100),X(100),Y(100)
```

```
WRITE(*,*) 'THIS PROGRAM MANIPULATES THE .GRF FILE FROM CHEMKIN AN  
+D CREATES'  
WRITE(*,*) 'NEW FILES SUITABLE FOR GRAPHING PURPOSES.'  
WRITE(*,*) ''  
WRITE(*,*) 'CAPS LOCK MUST BE ON WHILE RUNNING THIS PROGRAM.'  
69 WRITE(*,*) ''
```

C OPEN SOURCE FILE

```
WRITE(*,199) 'ENTER THE NAME OF THE .GRF SOURCE FILE (W/EXT.): '  
199 FORMAT(1X,A,\)  
READ (*,99) SOURCE  
99 FORMAT(A12)
```

```
OPEN (1, ERR = 69, FILE = SOURCE, STATUS = 'OLD')  
REWIND 1  
WRITE(*,*) ''
```

C DETERMINE NUMBER OF LINES IN EACH BLOCK OF DATA

```
K = 0  
DO 10 I = 1,100  
  READ (1,101) FC  
101  FORMAT (A1)  
  IF (FC .EQ. 'X') K=K+1  
  IF (K .EQ. 1) K1 = K1+1  
  IF (K .EQ. 2) THEN  
    LINES = K1-4  
    GOTO 20  
  ENDIF  
10 CONTINUE  
20 CONTINUE
```

C DETERMINE LENGTH (mm), DX (mm)

```
REWIND 1  
READ (1,102) X0, X1  
102 FORMAT (////,F5.2,/,F5.2)  
DX = X1 - X0
```


LENGTH = DX*(REAL(LINES)-1.0)

C DETERMINE AVERAGE VELOCITY

```
REWIND 1
READ (1,103) VEL
103 FORMAT (////,13X,F7.2)
DO 30 I = 2, LINES
    READ(1,104) VEL1
104  FORMAT (13X,F7.2)
    VEL = VEL + VEL1
30 CONTINUE
VAVG = VEL/REAL(LINES)

WRITE(*,*) ''
WRITE(*,*) ''
```

C DETERMINE TIME ARRAY

```
WRITE (*,*) 'WHAT TIME UNITS DO YOU WANT?'
WRITE (*,199) 'ENTER 1 FOR MICROSEC., 2 FOR MS, 3 FOR SEC: '
READ (*,*) TUF
WRITE (*,*) ''
IF (TUF .EQ. 1) TU = 1.0E-6
IF (TUF .EQ. 2) TU = 1.0E-3
IF (TUF .EQ. 3) TU = 1.0
WRITE(*,199) 'ENTER TIME AT X=0: '
READ (*,*) T0
TIME(1) = T0
DT = DX/(VAVG*1000.0*TU)
DO 40 I = 2, LINES
    TIME(I) = TIME(I-1) + DT
40 CONTINUE
```

C READ COLUMN HEADERS INTO ARRAY

```
REWIND 1
LL = 11
DO 50 I = 1, 5
    IF (I .EQ. 5) LL = 2
    DO 60 J = 1, LL
        IF (J .EQ. 1) READ (1,105) SPECIE(I,J)
        IF (J .NE. 1 .AND. J .NE. LL) READ (1,179) SPECIE(I,J)
        IF (J .EQ. LL) READ(1,178) SPECIE(I,J)
178  FORMAT (A6)
105  FORMAT (///,23X,A6,4X,\)
179  FORMAT (A6,4X,\)
60  CONTINUE
    IF (I .NE. 5) THEN
        DO 61 K = 1, LINES
            READ(1,101) FC
61  CONTINUE
```

```
ENDIF
50 CONTINUE
```

C READ DATA INTO AN ARRAY

```
REWIND 1
DO 52 I = 1,5
  READ (1,132) FC
132 FORMAT (///,A1)
  DO 54 J = 1,LINES
    READ (1,133) DUM
133 FORMAT (13X,F7.2,\)
    LL = 11
    IF (I .EQ. 5) LL = 2
    DO 55 K = 1,LL
      IF (K .NE. LL) READ (1,131) DATA(I,K,J)
      IF (K .EQ. LL) READ (1,171) DATA(I,K,J)
169 FORMAT(1X,A,E9.3)
131 FORMAT (1X,E9.3,\)
171 FORMAT (1X,E9.3)
    55 CONTINUE
  54 CONTINUE
52 CONTINUE
```

C DETERMINE NO_x, NO₂/NO_x AT EACH POINT

C DETERMINE LOCATION OF DESIRED COLUMNS

```
DO 65 I = 1,5
  DO 70 J = 1,11
    IF (SPECIE(I,J) .EQ. 'NO') THEN
      INOR = I
      INOC = J
    ENDIF
    IF (SPECIE(I,J) .EQ. 'NO2') THEN
      INO2R = I
      INO2C = J
    ENDIF
  70 CONTINUE
65 CONTINUE
```

C DETERMINE NO_x & NO₂ PROFILES AND STORE IN ARRAYS

```
DO 100 I = 1,LINES
  NOX(I) = DATA(INOR,INOC,I) + DATA(INO2R,INO2C,I)
  NO2NOX(I) = DATA(INO2R,INO2C,I)/NOX(I)
100 CONTINUE
```

C ASK USER WHAT FILES HE WANTS TO CREATE

C SHOW USER WHAT SPECIES/VARIABLES HE CAN SELECT FROM

```
WRITE(*,*) 'HEY DUDE! THE FOLLOWING IS A LIST OF SPECIES AND VA
+RIABLES THAT'
```

```

WRITE(*,*) 'YOU MAY CHOOSE FROM IN CREATING YOUR FILES: '
WRITE(*,*) ''
WRITE(*,*) 'TIME  NOX  NO2/NOX'
DO 110 I = 1,5
    WRITE(*,203) (SPECIE(I,J) , J=1,11)
203  FORMAT(1X,11(A5,1X))
110 CONTINUE
WRITE(*,*) ''
WRITE(*,*) 'YOU CAN PICK ANY TWO VARIABLES FOR GRAPHING PURPOSES.'

```

C ENTER FILE NAME TO BE CREATED

```

500 WRITE(*,*) ''
    WRITE(*,199) 'ENTER NAME OF FILE TO BE CREATED: '
    READ(*,99) NEWFILE

```

C ENTER SPECIES

```

WRITE(*,*) ''
WRITE(*,199) 'ENTER X AXIS VARIABLE: '
READ (*,181) XVAR
181 FORMAT(A7)
IF (XVAR .NE. 'TIME' .AND. XVAR .NE. 'NO2/NOX') THEN
    WRITE(*,199) 'ENTER DESIRED UNITS - 1 FOR PPM, 2 FOR %, 3 AS IS: '
    + '
        READ(*,*) IDU
        IF (IDU .EQ. 1) DU = 1.0E-6
        IF (IDU .EQ. 2) DU = 0.01
        IF (IDU .EQ. 3) DU = 1.0
    ELSE
        DU = 1.0
    ENDIF

WRITE(*,*) ''
WRITE(*,199) 'ENTER Y AXIS VARIABLE: '
READ(*,181) YVAR
IF (YVAR .NE. 'TIME' .AND. YVAR .NE. 'NO2/NOX') THEN
    WRITE(*,199) 'ENTER DESIRED UNITS - 1 FOR PPM, 2 FOR %, 3 AS IS: '
    + '
        READ(*,*) IDU1
        IF (IDU1 .EQ. 1) DU1 = 1.0E-6
        IF (IDU1 .EQ. 2) DU1 = 0.01
        IF (IDU1 .EQ. 3) DU1 = 1.0
    ELSE
        DU1 = 1.0
    ENDIF

```

C CHECK IF X VARIABLE IS TIME, NO_x, OR NO₂/NO_x - IF NOT, DETERMINE
C LOCATION OF X VARIABLE COLUMN

```

IF (XVAR .EQ. 'TIME') THEN
    DO 120 I = 1,LINES

```

```

        X(I) = TIME(I)/DU
120  CONTINUE
    ELSE IF (XVAR .EQ. 'NOX') THEN
        DO 130 I = 1,LINES
            X(I) = NOX(I)/DU
130  CONTINUE
    ELSE IF (XVAR .EQ. 'NO2/NOX') THEN
        DO 140 I = 1,LINES
            X(I) = NO2NOX(I)/DU
140  CONTINUE
    ELSE
        DO 150 I = 1,5
            DO 160 J = 1,11
                IF (SPECIE(I,J) .EQ. XVAR) THEN
                    XVR = I
                    XVC = J
                ENDIF
160  CONTINUE
150 CONTINUE
        DO 170 I = 1,LINES
            X(I) = DATA (XVR,XVC,I)/DU
170 CONTINUE
    ENDIF

```

C CHECK IF Y VARIABLE IS TIME, NO_x, OR NO₂/NO_x - IF NOT, DETERMINE
C LOCATION OF Y VARIABLE COLUMN

```

    IF (YVAR .EQ. 'TIME') THEN
        DO 180 I = 1,LINES
            Y(I) = TIME(I)/DU1
180  CONTINUE
    ELSE IF (YVAR .EQ. 'NOX') THEN
        DO 190 I = 1,LINES
            Y(I) = NOX(I)/DU1
190  CONTINUE
    ELSE IF (YVAR .EQ. 'NO2/NOX') THEN
        DO 200 I = 1,LINES
            Y(I) = NO2NOX(I)/DU1
200  CONTINUE
    ELSE
        DO 210 I = 1,5
            DO 220 J = 1,11
                IF (SPECIE(I,J) .EQ. YVAR) THEN
                    YVR = I
                    YVC = J
                ENDIF
220  CONTINUE
210 CONTINUE
        DO 230 I = 1, LINES
            Y(I) = DATA(YVR,YVC,I)/DU1
230 CONTINUE

```

ENDIF

C WRITE TO THE FILE

```
OPEN (2, FILE = NEWFILE, STATUS = 'NEW')
WRITE(2,134) (X(I),Y(I) , I = 1,LINES)
134 FORMAT (E10.4,1X,E10.4)

WRITE(*,*) ''
WRITE(*,106) 'THE DATA FILE ', NEWFILE, ' HAS BEEN CREATED.'
106 FORMAT(1X,3A)
WRITE(*,*) ''
```

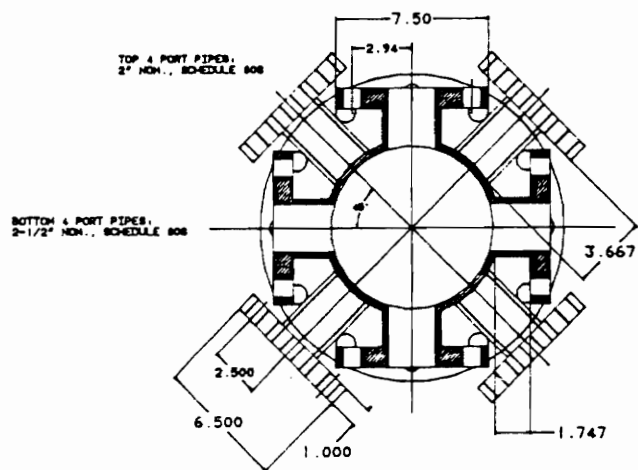
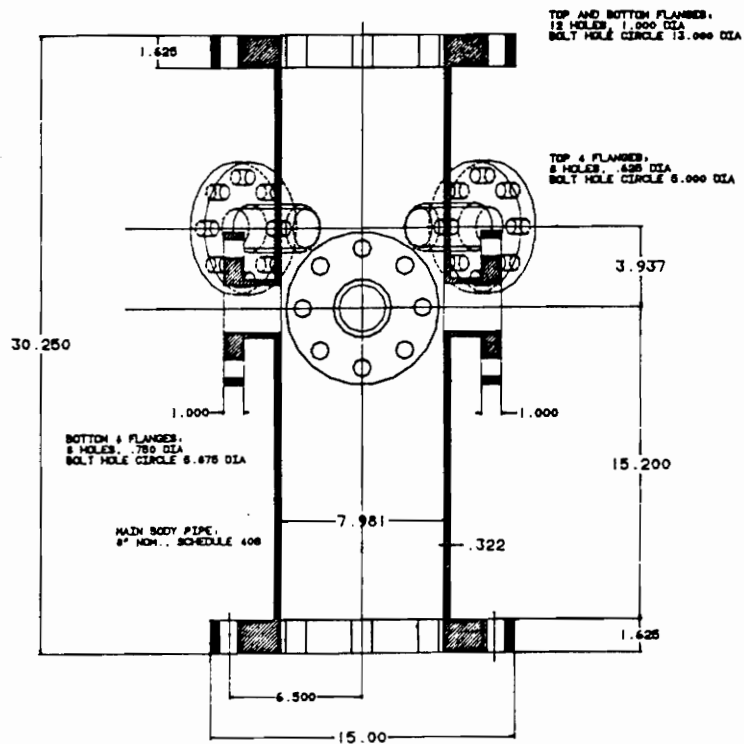
C MAKE ANOTHER FILE?

```
WRITE (*,199) 'DO ANOTHER? '
READ (*,205) YN
205 FORMAT (A1)
IF (YN .NE. 'N') GOTO 500
```

```
CLOSE (2)
CLOSE (1)
```

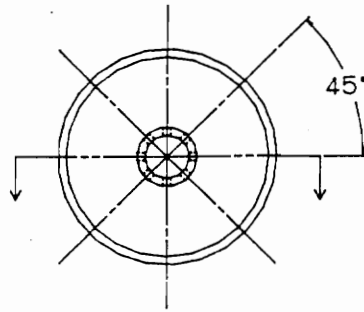
END

APPENDIX D
Shop Drawings



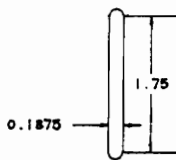
MAT'L: AISI 316L
ALL DIMENSIONS IN INCHES
1/8 SCALE

TITLE: PRESSURE VESSEL
DRAWN BY: J. HUNDERUP
DATE: 7-19-91

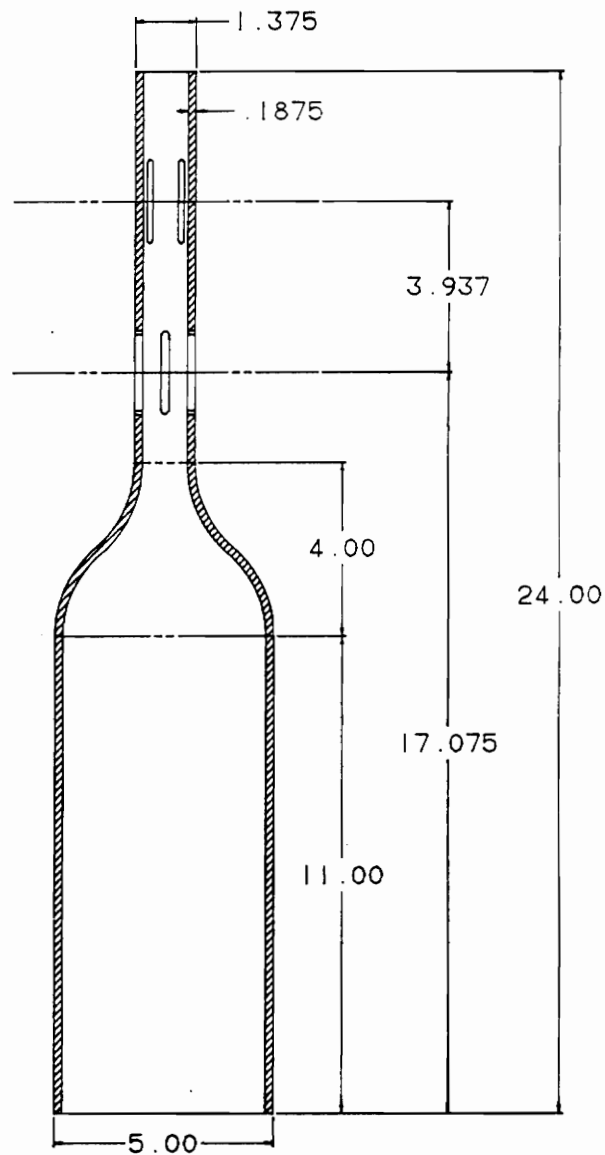


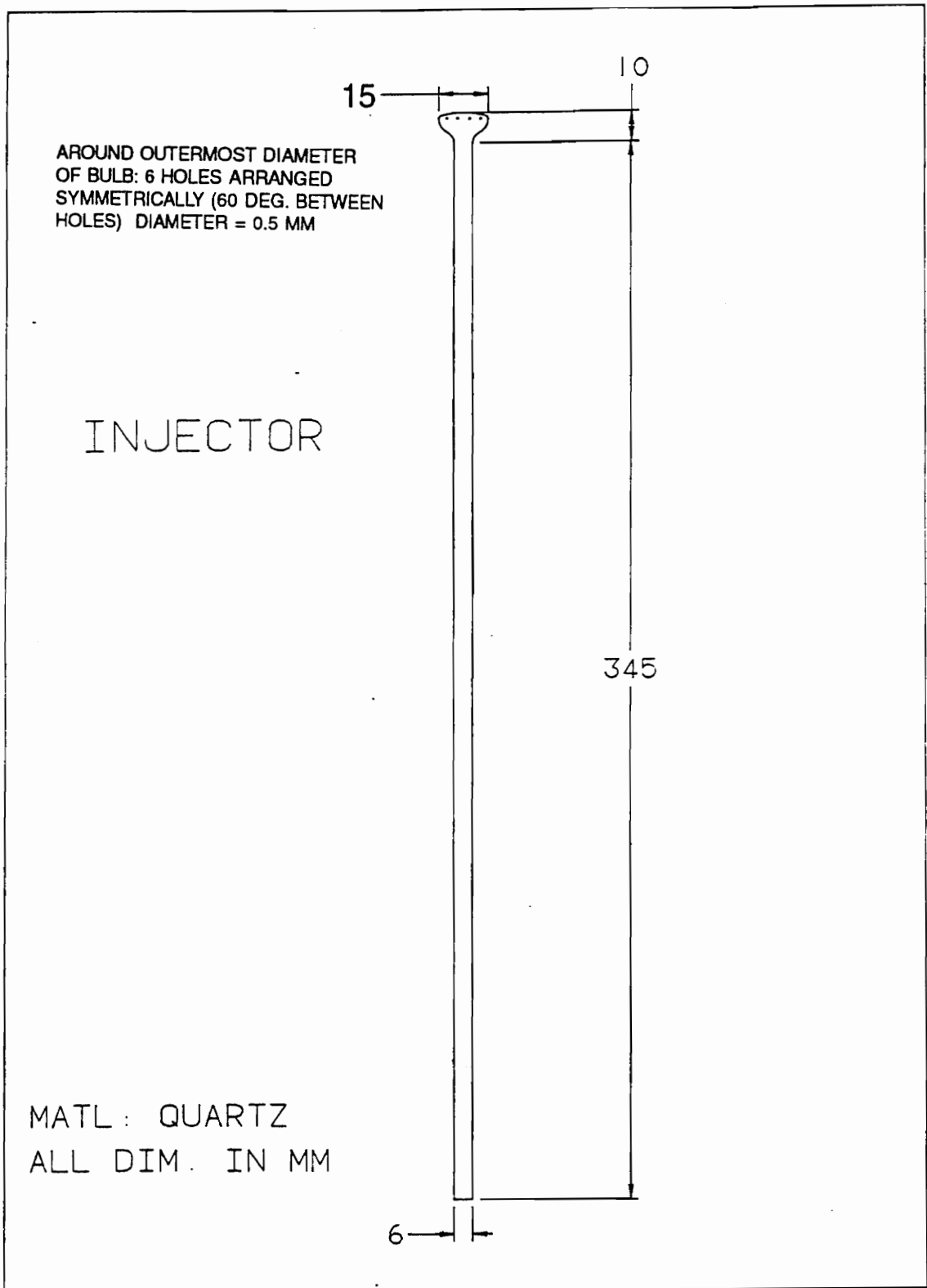
QUARTZ LINER

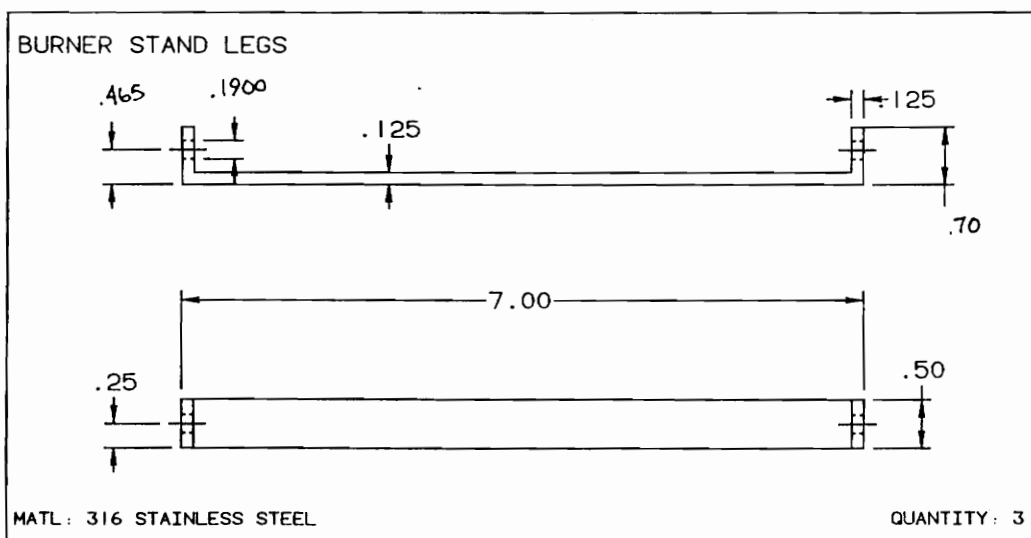
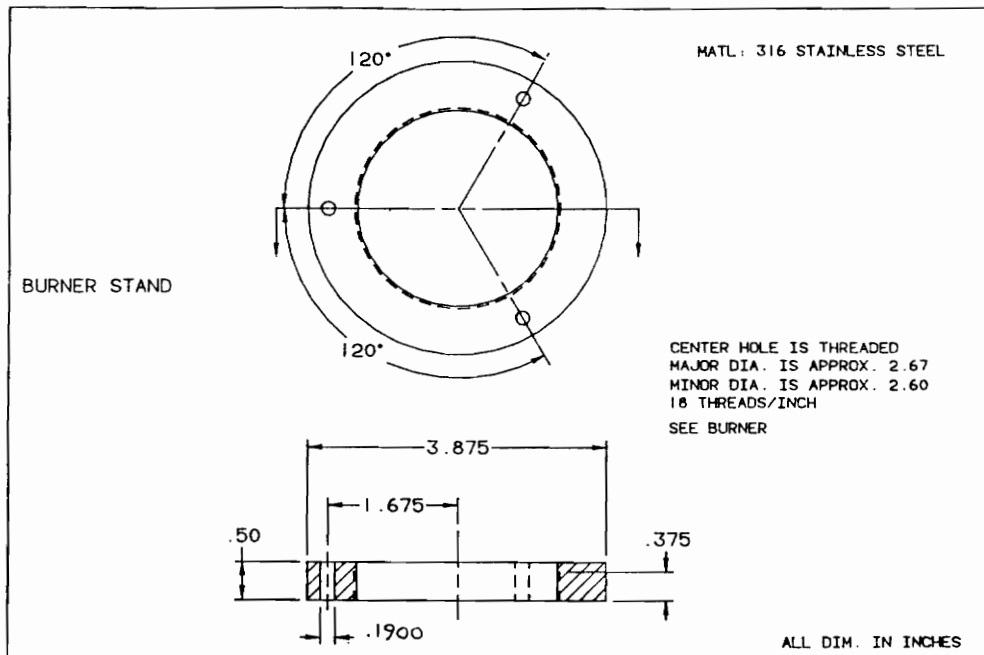
ALL 8 SLOTS ARE
THE SAME DIMENSIONS



ALL DIMENSIONS
IN INCHES



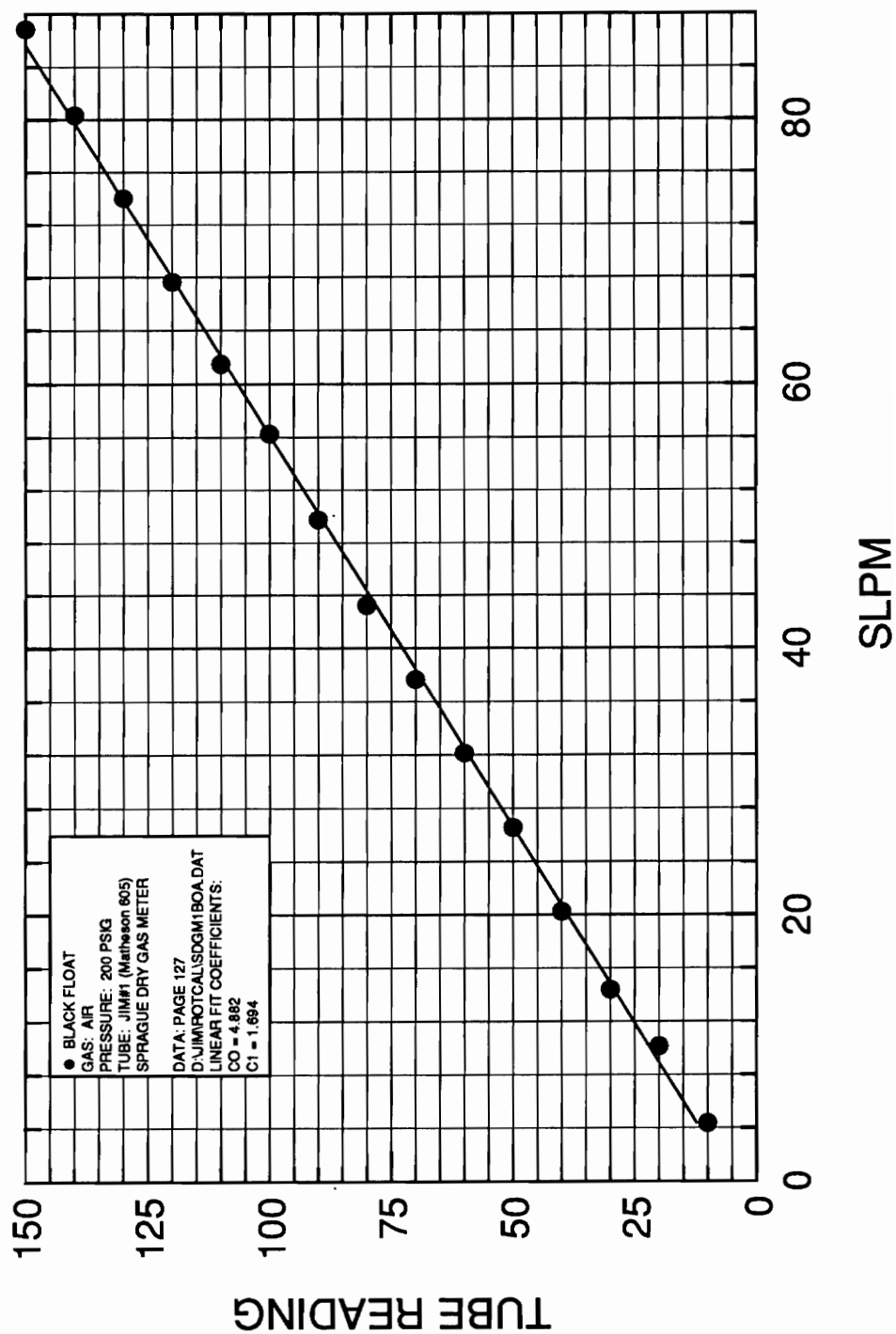




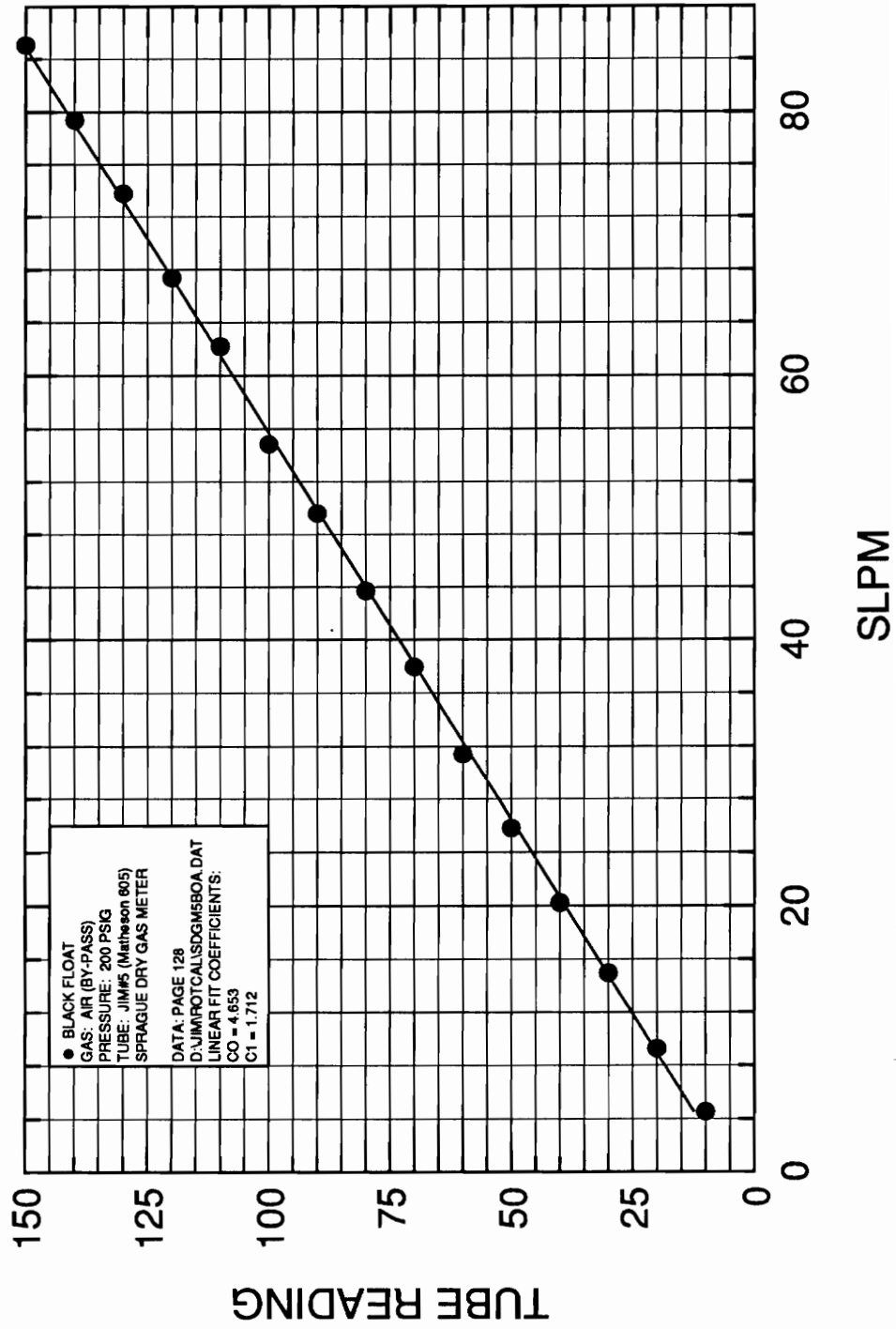
APPENDIX E

Rotameter Calibration Curves

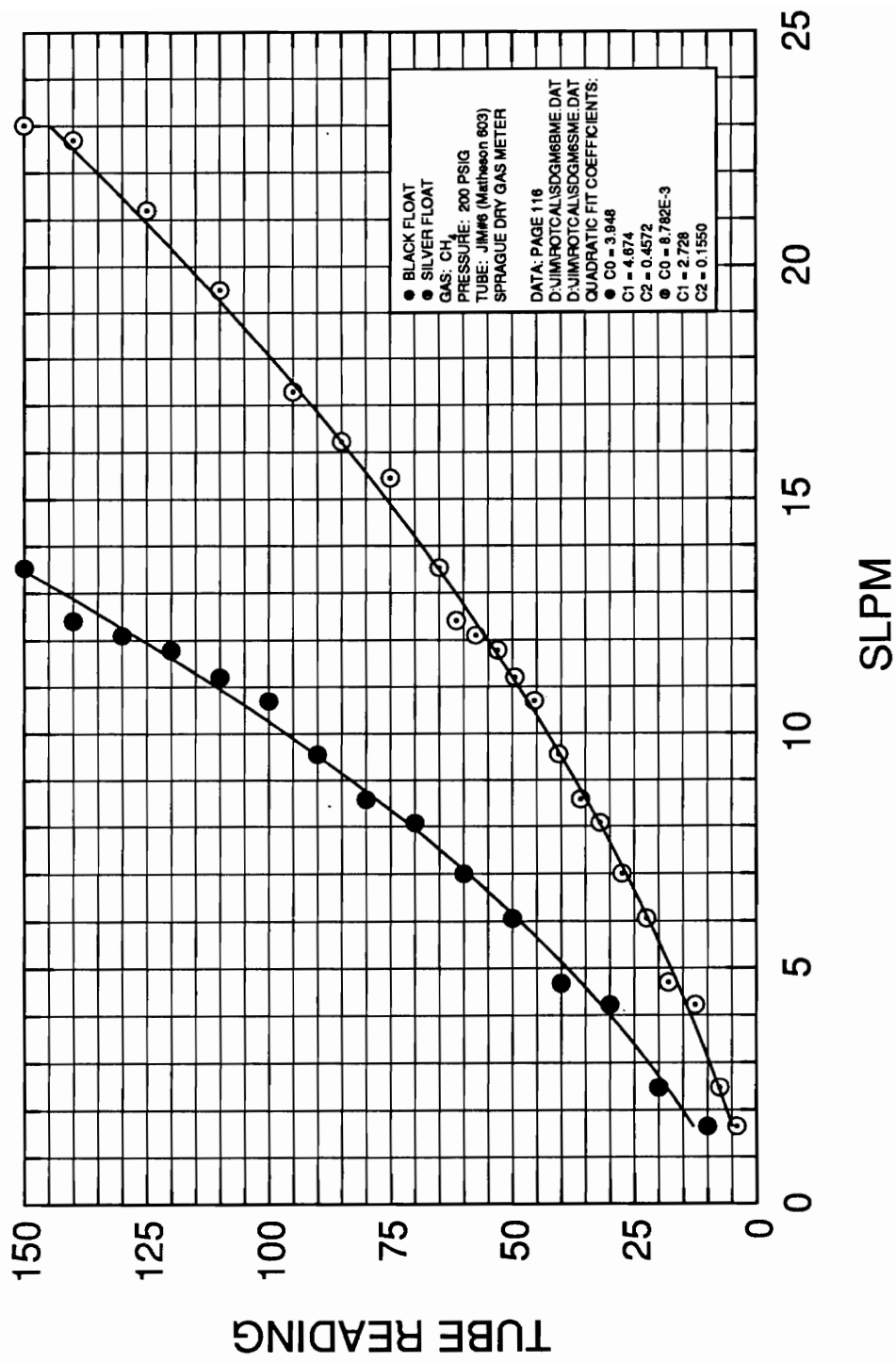
ROTAMETER CALIBRATION



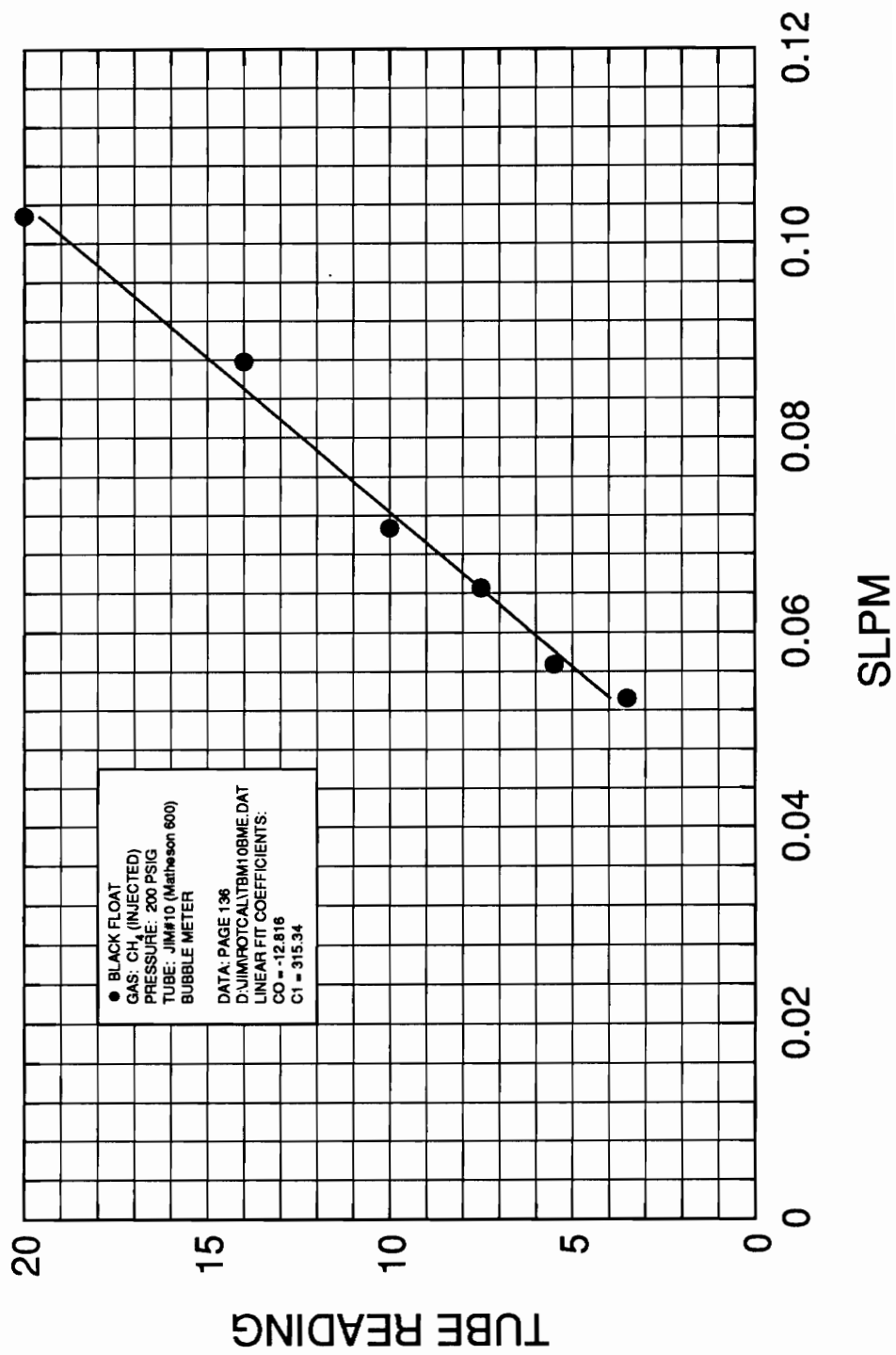
ROTAMETER CALIBRATION



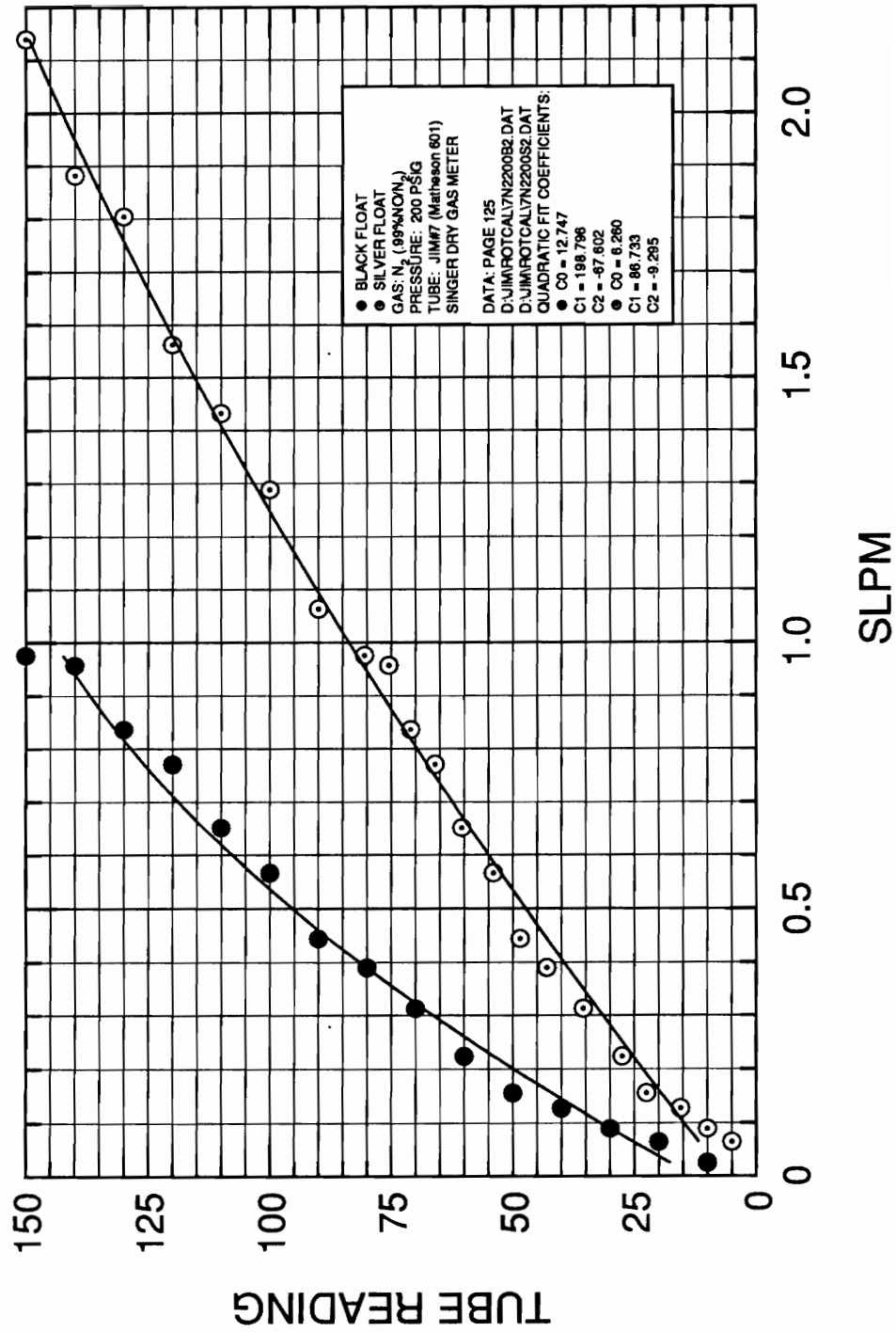
ROTAMETER CALIBRATION



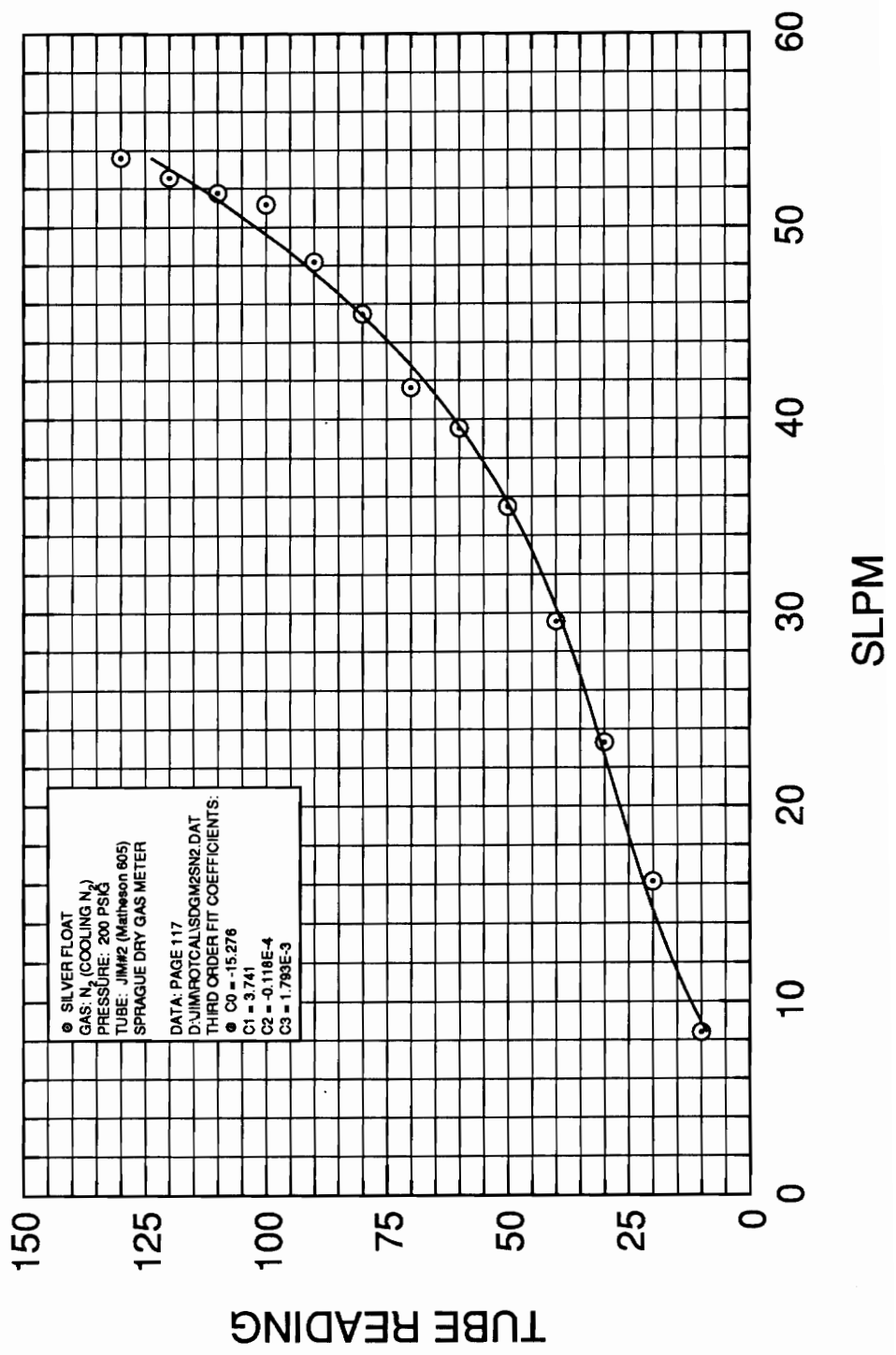
ROTAMETER CALIBRATION



ROTAMETER CALIBRATION



ROTAMETER CALIBRATION



APPENDIX F
Experimental Data Processing Program
DATA.FOR

```
C THIS PROGRAM CRUNCHES EXPERIMENTAL DATA FROM HIGH PRESSURE FLOW  
C REACTOR
```

```
C JIM HUNDERUP      12-28-92
```

```
REAL*8 RCH4,RAIR,RNO,RN2,PA,TA,PV,T,RQF,RQA,RQNO,RQBPA,RQINJ,RQN2,  
$      D,NO,NOX,QF,QA,QNO,QBPA,QINJ,QN2,RHO,PHI,P,MF,MA,MNO,MBPA,  
$      MINJ,MN2,MBURN,MLIN,VEL,RT,NO2,NO2R,QLIN,NOPPM,CH4PPM,PI,  
$      PATM  
INTEGER I,IDUM,K,LINES,IK,INO,INOX,INO2,FLAG  
CHARACTER CDUM*1,DFILE*12,GFILE*12,UNIT*1  
DIMENSION D(100),NO(100),NOX(100),RT(100),NO2(100),NO2R(100)
```

```
C CONSTANTS
```

```
RCH4 = 518.0  
RAIR = 287.0  
RNO = 277.0  
RN2 = 297.0
```

```
PI = 3.141592654
```

```
C INITIALIZE ARRAYS
```

```
68 DO 9 I = 1,100  
    D(I) = 0.0  
    NO(I) = 0.0  
    NOX(I) = 0.0  
    RT(I) = 0.0  
    NO2(I) = 0.0  
    NO2R(I) = 0.0  
9 CONTINUE
```

```
C OUTPUT PROGRAM DESCRIPTION
```

```
WRITE (*,*) 'THIS PROGRAM CRUNCHES EXPERIMENTAL DATA FROM HIGH PRE  
$$SURE'  
WRITE (*,*) 'FLOW REACTOR AND PRODUCES DATA FILES OF RESULTS FOR G  
$RAPHING PURPOSES.'
```

```
C DATA ENTRY
```

```
WRITE (*,*) ''  
WRITE (*,*) 'ENTER THE FOLLOWING DATA:'  
WRITE (*,*) ''  
WRITE (*,105) 'AMBIENT PRESSURE [mm Hg]: '  
105 FORMAT (1X,A,\)  
READ (*,*) PA  
WRITE(*,105) 'AMBIENT TEMPERATURE [K]: '  
READ (*,*) TA
```

```
65 FLAG = 0
```

```

WRITE (*,105) 'ENTER UNITS OF VESSEL PRESSURE (V OR PSIG): '
READ (*,198) UNIT
198 FORMAT (A1)
IF (UNIT .EQ. 'V') FLAG = 1
IF (UNIT .EQ. 'P') FLAG = 2
IF (UNIT .NE. 'V' .AND. UNIT .NE. 'P') GOTO 65
WRITE (*,105) 'ENTER VESSEL PRESSURE: '
READ (*,*) PV
WRITE (*,105) 'POST FLAME GAS TEMPERATURE [K]: '
READ (*,*) T
WRITE (*,*) 'ROTAMETER READINGS FOR: '
WRITE (*,110) 'FUEL: '
110 FORMAT (7X,A,\)
READ (*,*) RQF
WRITE (*,110) 'AIR: '
READ (*,*) RQA
WRITE (*,110) 'NO/N2: '
READ (*,*) RQNO
WRITE (*,110) 'BY-PASS AIR: '
READ (*,*) RQBPA
WRITE (*,110) 'INJECTED CH4: '
READ (*,*) RQINJ
WRITE (*,110) 'COOLING N2: '
READ (*,*) RQN2
WRITE (*,*) ''

```

C OPEN NO/NOX DATA FILE

```

69 WRITE (*,105) 'ENTER THE NAME OF THE DATA FILE: '
READ (*,200) DFILE
200 FORMAT (A12)

OPEN (1, ERR = 69, FILE = DFILE, STATUS = 'OLD')
REWIND 1
WRITE (*,*) ''

```

C DETERMINE NUMBER OF LINES IN FILE

```

K = 0
DO 10 I = 1,100
  READ (1,205) IDUM
205  FORMAT (I3)
  IF (IDUM .NE. 999) THEN
    K = K+1
  ELSE
    LINES = K
    GOTO 12
  ENDIF
10 CONTINUE
12 CONTINUE

```

C READ DATA INTO ARRAYS

```
REWIND (1)
DO 15 I = 1, LINES
  READ (1,*) ID,INO,INOX
  D(I) = REAL(ID)
  NO(I) = REAL(INO)
  NOX(I) = REAL(INOX)
15 CONTINUE
```

C CALCULATE STANDARD FLOW RATES FROM ROTAMETER CALIBRATION CURVES

```
QF = 0.235147 + 0.130507*RQF - 2.91106E-4*RQF*RQF
QA = -2.882071 + 0.5902944*RQA
IF (RQNO .EQ. 0.0) THEN
  QNO = 0.0
ELSE
  QNO = -4.26849E-2 + 9.82282E-3*RQNO + 3.12668E-5*RQNO*RQNO
ENDIF
QBPA = -2.71781 + 0.584054*RQBPA
IF (RQINJ. EQ. 0.0) THEN
  QINJ = 0.0
  GOTO 67
ENDIF
IF (RQINJ .GE. 20.0) THEN
  QINJ = -0.0218568 + 0.00601757*RQINJ
ELSE
  QINJ = 0.040640638 + .00317144*RQINJ
ENDIF
67 QN2 = -0.831049 + 0.971802*RQN2 - 5.82073E-3*RQN2*RQN2 +
$      1.20711E-5*RQN2**3
```

C CALCULATE PRESSURE IN PSIG

```
IF (FLAG .EQ. 1) P = -1.22715 + 100.905*PV
IF (FLAG .EQ. 2) P = PV
PATM = (PA/760.0) + (PV/14.696)
```

C OUTPUT STANDARD FLOW RATES TO SCREEN / OUTPUT PRESSURE TO SCREEN

```
WRITE (*,*) ''
WRITE (*,160) 'VESSEL PRESSURE (ABSOLUTE): ', PATM, ' ATM'
WRITE (*,*) ''
WRITE (*,*) 'STANDARD FLOW RATES OF GASES INTO VESSEL'
WRITE (*,*) ''
WRITE (*,120) 'FUEL: ',QF, ' SLPM'
WRITE (*,120) 'AIR: ',QA, ' SLPM'
WRITE (*,120) 'NO/N2: ',QNO, ' SLPM'
WRITE (*,120) 'BP AIR: ',QBPA, ' SLPM'
WRITE (*,120) 'INJ. CH4: ',QINJ, ' SLPM'
WRITE (*,120) 'N2: ',QN2, ' SLPM'
```

120 FORMAT (1X, A, F6.2, A)

C INPUT POST FLAME GAS DENSITY FROM STANJAN EQUILIBRIUM CALCULATION

```
WRITE (*,*) ''  
WRITE (*,*) ''  
WRITE (*,110) 'ENTER POST FLAME GAS DENSITY (FROM STANJAN): '  
READ (*,*) RHO
```

C CALCULATE EQUIVALENCE RATIO

$$\text{PHI} = (\text{QF}/\text{QA} * (16.04/28.97)) / 0.0580$$

C CALCULATE CONCENTRATIONS OF INJECTED CH4 AND NO

```
QLIN = QF + QA + QNO + QBPA + QINJ  
NOPPM = .0099 * QNO / QLIN * 10**6  
CH4PPM = QINJ / QLIN * 10**6
```

C CALCULATE MASS FLOW RATES OF GASES THROUGH PRESSURE VESSES

C M(GAS) = Q(GAS) * 101325/(RGAS*273) * .001 / 60 ----> [KG/S]

```
MF = QF * 6.1858974E-3/RCH4  
MA = QA * 6.1858974E-3/RAIR  
MNO = .0099*QNO*6.1858974E-3/RNO + .9901*QNO*6.1858974E-3/RN2  
MBPA = QBPA * 6.1858974E-3/RAIR  
MINJ = QINJ * 6.1858974E-3/RCH4  
MN2 = QN2 * 6.1858974E-3/RN2
```

C CALCULATE FLOW THROUGH BURNER / FLOW THROUGH LINER

```
MBURN = MF + MA + MNO  
MLIN = MBURN + MBPA + MINJ
```

C CALCULATE VELOCITY THROUGH LINER

$$\text{VEL} = \text{MLIN} / (\text{RHO} * (\text{PI}/4.0 * .02937 * .02937))$$

C CALCULATE NO2, NO2/NOX, AND RESIDENCE TIME

```
DO 20 I = 1, LINES  
  RT(I) = D(I)/VEL  
  NO2(I) = NOX(I) - NO(I)  
  NO2R(I) = NO2(I)/NOX(I)  
20 CONTINUE
```

C OUTPUT MASS FLOW RATES, RESULTS TO SCREEN

```
WRITE (*,*) ''  
WRITE (*,*) 'MASS FLOW RATES INTO VESSEL'  
WRITE (*,*) ''
```

```

WRITE (*,130) 'FUEL: ',MF,' KG/S'
WRITE (*,130) 'AIR: ',MA,' KG/S'
WRITE (*,130) 'NO/N2: ',MNO,' KG/S'
WRITE (*,130) 'BP AIR: ',MBPA,' KG/S'
WRITE (*,130) 'INJ. CH4: ',MINJ,' KG/S'
WRITE (*,130) 'N2: ',MN2,' KG/S'
130 FORMAT (1P,1X, A, E9.2, A)

```

```

WRITE (*,*) ''
WRITE (*,140) 'EQUIVALENCE RATIO: ', PHI
WRITE (*,130) 'FLOW THROUGH BURNER: ', MBURN, ' KG/S'
WRITE (*,130) 'FLOW THROUGH LINER: ', MLIN, ' KG/S'
WRITE (*,150) 'POST-FLAME GAS DENSITY: ', RHO, ' KG/M^3'
WRITE (*,160) 'VELOCITY THROUGH LINER: ', VEL, ' M/S'
WRITE (*,170) 'INJECTED CH4 CONCENTRATION: ', INT(CH4PPM), ' PPM'
WRITE (*,170) 'NO INJECTED THROUGH FLAME (CALCULATED): ',
$      INT(NOPPM), ' PPM'
140 FORMAT (1X, A, F4.2)
150 FORMAT (1X, A, F7.3, A)
160 FORMAT (1X, A, F5.2, A)
170 FORMAT (1X, A, I4, A)

```

C OUTPUT NOX RESULTS TO FILE

```

WRITE (*,*) ''
WRITE (*,105) 'ENTER NAME OF NOX GRAPHING FILE TO BE CREATED: '
READ (*,200) GFILE

OPEN (2, FILE = GFILE, STATUS = 'NEW')
DO 40 I = 1, LINES
    WRITE (2,180) INT(D(I)), RT(I), INT(NO(I)), INT(NOX(I)),
$      INT(NO2(I)), NO2R(I)
180  FORMAT (1X,I3,3X,F7.2,3X,I3,3X,I3,3X,I3,3X,F5.3)
40 CONTINUE

WRITE (*,*) 'NOX RESULTS HAVE BEEN WRITTEN TO ', GFILE

CLOSE (2)
CLOSE (1)

```

C ANOTHER DATA SET?

```

WRITE (*,*) ''
WRITE (*,105) 'DO YOU WISH TO CRUNCH ANOTHER DATA SET? '
READ (*,201) CDUM
201 FORMAT (A1)
IF (CDUM.EQ. 'Y') GOTO 68

END

```

APPENDIX G

Uncertainty Analysis

UNCERTAINTY ANALYSIS

A brief uncertainty analysis is presented below. It focuses mainly on the uncertainty associated with measurement of oxides of nitrogen, but also addresses uncertainty involved with temperature measurements.

It shall be assumed in this analysis that errors are independent of each other and are normally distributed. Combination of error sources shall be a root mean square method. The following notation shall be used. Per cent error of a measurement, X, shall be denoted by the Greek letter Δ . Therefore, the per cent error associated with the measurement X would be ΔX . The standard error for the measurement X shall be denoted as δX . These two values are related by the expression,

$$\delta X/X = \Delta X.$$

NO and NO_x Measurements

The error associated with NO and NO_x measurements varied quite a lot depending on flow conditions under which a particular data set was taken. Four sources of error were considered in determining the total error for these measurements.

1. Analyzer accuracy

The accuracy of the Thermo Environmental CLA as given in the instruction manual is $\pm 1\%$ of full-scale [24]. Although the configuration of the CLA was significantly changed in order to sample at low pressure, it was assumed that the accuracy remained approximately $\pm 1\%$.

2. Calibration gas

The CLA has a straight line calibration. Both a zero gas ($[\text{NO}] = 0$) and a NO calibration gas must be used to calibrate the instrument. Room air was used as the zero gas. It was assumed that $[\text{NO}] = 0$ for room air, and any error with regard to this was assumed to be negligible.

A concentration of 240 ppm NO in a balance of nitrogen was used to calibrate the CLA. This concentration of NO was accurate to ± 4.8 ppm. This is equivalent to a 2% error.

3. Data spread

Data points for NO and NO_x were determined by "eyeballing" a time averaged value from each specie at each sampling point. Real time NO and NO_x concentrations were recorded using a strip chart recorder. A standard deviation was later estimated from the $[\text{NO}]$ and $[\text{NO}_x]$ real time tracings. These were then translated into per cent errors for each point.

Data spread varied from run to run and even within a given sample range (Sect. 5.1.1). In the mixing region close to the injector, data spread tended to be greater than downstream. Higher Re_D runs also tended to have greater data spread.

4. Calibration correction factor

For experimental tests with pressures greater than 3.0 atm., a correction factor had to be applied to the calibration (Sect. 3.3). To determine this correction factor, flow conditions of data acquisition were recreated by increasing flow of the calibration gas into the CLA until flow into the reaction chamber

matched the experimental flow as judged by a flow meter. The CLA output was then noted, and the correction factor was determined by dividing this by the atmospheric calibration output (240 ppm). The error associated with reading the correction output was estimated to be ± 15 ppm for all cases in which a correction factor was necessary ($P > 3.0$ atm.). This estimated error takes into account both the error associated with reading the scale and any error in recreating the experimental flow conditions into the CLA reaction chamber.

The total error associated with [NO] and [NO_x] measurements is given by the following equation:

$$\Delta NO = ((\Delta NO)_{CLA}^2 + (\Delta NO)_{Cal\ gas}^2 + (\Delta NO)_{Data}^2 + (\Delta NO)_{CCF}^2)^{1/2}$$

$$\Delta NO_x = ((\Delta NO_x)_{CLA}^2 + (\Delta NO_x)_{Cal\ gas}^2 + (\Delta NO_x)_{Data}^2 + (\Delta NO_x)_{CCF}^2)^{1/2}$$

To determine error associated with the calculated values [NO₂] and NO₂/NO_x, the above percent errors were converted to standard errors using the formulas:

$$\delta NO = [NO]\Delta NO$$

$$\delta NO_x = [NO_x]\Delta NO_x.$$

The standard error for the concentration was then determined using the formula:

$$\delta NO_2 = (\delta NO^2 + \delta NO_x^2)^{1/2}.$$

This was converted into a per cent error, and the result was used in conjunction with ΔNO_x to determine the error associated with the calculated value NO₂/NO_x:

$$\Delta(NO_2/NO_x) = (\Delta NO_2^2 + \Delta NO_x^2)^{1/2}.$$

This value was in turn converted to a standard error for plotting purposes. Error bars were included in figures to give the general idea of error trends when appropriate.

It was discovered that the largest source of error in the oxides of nitrogen measurements was a result of data spread and, in cases in which $P > 3$ atm., the calibration correction factor.

Temperature measurements

The major source of error associated with temperature measurements arises from the assumption that the temperature of the post flame gases in the upper portion of the chimney is a constant bulk temperature. It was seen during data acquisition that temperature fluctuated slightly over the course of the period of time during which data was collected. There is probably also some spatial fluctuations in the temperature in the upper chimney. A maximum error was estimated from the experimental run that had the largest temporal change in temperature. This was run 22 which had an estimated standard error of ± 15 K. The maximum standard temperature error, δT_{\max} , is, therefore, ± 15 K. This may be somewhat arbitrary, but probably yields a good idea of the accuracy of the temperature measurements in general.

Another source of temperature measurement error not taken into account is radiation from the thermocouple bead. Several calculations were made using a radiation correction computer program [19] and an assumed temperature of the surroundings. It is difficult to estimate an appropriate surroundings temperature because conditions in the facility outside of the liner were not well known. Even for a worst case scenario

(T_{surr} low), the radiation correction was small (1-2 K). The error due to temperature fluctuation describe above is much greater. Therefore, radiation effects were neglected.

Pressure measurements

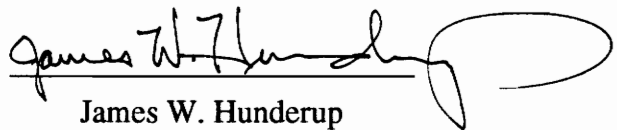
Pressure in the flow reactor was measured for all runs except the first six with a Model K1 Ashcroft pressure transmitter. The first six runs used a Robertshaw pressure gauge. The scale of this gauge could be read to ± 1 psig. This results in an estimated error of 5.6% for these first six runs. Runs 7-26 utilized the Ashcroft transmitter. This was specified as accurate to 1%.

VITA

James W. Hunderup was born April 28, 1968 in Rochester, New York. He was raised outside of Rochester in Webster. He graduated from Webster High School and the Eastman School of Music Preparatory Department in the spring of 1986.

Jim arrived in Blacksburg in the fall of 1986 to pursue an engineering education at Virginia Tech. He has not seemed to have been able to have left Blacksburg since that time. He received his B.S. in Mechanical Engineering and a minor in Spanish from Virginia Tech in the spring of 1990. He spent part of his summer backpacking around Europe then returned to Blacksburg in the fall of 1990 to continue his education.

During his graduate school years, Jim became involved in EMS and decided that an engineering career was not what he desired. Although he values his graduate education in mechanical engineering, after receiving his Master of Science degree, he will attempt to pursue a medical education. If he does not gain acceptance into a medical school, Jim will be a very educated lifeguard and EMS prehospital care provider.


James W. Hunderup